IMPROVING LOAD FORECASTING TECHNIQUES: ADAPTING TO CLIMATE CHANGE

by

Bhagyam Chandrasekharan

A Thesis Submitted to the Faculty of the

DEPARTMENT OF AGRICULTURAL AND RESOURCE ECONOMICS

In Partial Fulfillment of the Requirements

For the Degree of

MASTER OF SCIENCE

In the Graduate College

The University of Arizona

2011

STATEMENT BY AUTHOR

This thesis has been submitted in partial fulfillment of requirements for an advanced degree at the University of Arizona.

Brief quotations from this thesis are allowable without special permission, provided that accurate acknowledgement of source is made. Requests for permissions for extended quotation form or reproduction of this manuscript in whole or in part may be granted by the head of the major department or the Dean of the Graduate College when in his or her judgment the proposed use of the material is in the interest of scholarship. In all other instances, however, permission must be obtained from the author.

SIGNED: Bhagyam

APPROVAL BY THESIS DIRECTOR

This Thesis has been approved on the dates shown below

Bonnie G Colby

Professor Bonnie Colby

Department of Agricultural and Resource Economics

5-6-11

Date

ACKNOWLEDGEMENTS

First and foremost, I would like to thank my advisor, Dr. Bonnie Colby, for giving me the opportunity to work with her during these last two years, and her guidance throughout the planning, research and writing of my thesis. I would also like to express my sincere gratitude to the rest of my thesis committee, Dr. Satheesh Aradhyula and Dr. Gary Thompson, for their encouragement, insightful comments and instruction.

I acknowledge research colleagues with the Climate Assessment for the Southwest program at the University of Arizona. This work was supported by that project through the National Oceanic and Atmospheric Administration's Climate Program Office, grant NA16GP2578. The statements, findings, conclusions, and recommendations are my own and do not necessarily reflect the views of NOAA, US Department of Commerce, or the US Government Climate Program.

I would also like to thank AEPCO (Arizona Electric Power Cooperative), Tucson Electric Power (TEP) and AZMET (Arizona Meteorological Network) for providing the necessary electricity load and weather data.

Moreover, I am grateful for Nancy Smith's (Program Coordinator) sagely advice throughout this endeavor. Finally, I thank my family for their continued love and support.

TABLE OF CONTENTS

LIST OF FIGURES

LIST OF TABLES

ABSTRACT

With the looming threat of climate change, electric utilities need to adapt their current load forecasting techniques so as to generate climate-sensitive load forecasts. This study investigates potential improvements in hourly and monthly load forecasting models by incorporating weather variables. While the hourly models show mixed results across seasons and regions, the monthly model shows marked improvement over a purely autoregressive approach to load forecasting. In light of climate change, electric utilities can avail of economic benefits from minimizing their exposure to the volatile spot market prices and significant losses through inaccuracies in predictions. Moreover, decision-making based on more climate-sensitive forecasts will result in reduction in the carbon footprint of the electric utilities and improvements in their investment strategies for renewable energy technologies for the future.

CHAPTER 1 Introduction

Electricity has been the backbone of economic growth since the 18th century. The energy needs of the growing population and rapid industrialization have been satisfied by the development of electricity supply and generation. With its increasing significance as a key infrastructure, electricity consumption has also increased manifold, fuelling the search for resources to meet this growing demand.

Weather is a major cause of the variation in the demand for electricity for space cooling and heating. The sensitivity of energy demand to weather stems from the fact that that produced electricity must be instantly consumed (Psiloglou et al., 2009). Examination of trends in electricity consumption shows a direct relationship between weather factors such as temperature and precipitation and electricity load. As expected, in the Southwest, space cooling is of a larger concern than heating due to the relative high temperatures experienced during most of the year.

Climate change affects the electricity consumption as well as the quality and quantity of required resources. The increased temperatures and variability in precipitation make climate change a growing challenge for electric utilities. Moreover, the growing scarcity of water supplies will affect both future electricity consumption and production in the Southwest.

Electricity load forecasting is an integral part of the planning and operation of electric utilities since it mitigates costs associated with load switching, overloading, blackouts and equipment failures. Electric load is related with various factors such as the time of day, day of week, season, climatic conditions, and the past usage patterns (Alfares & Nazeeruddin, 2002). Consequently, several methods have been utilized to model these relationships and generate load forecasts.

With the looming threat of climate change, electric utilities need to adapt their current load forecasting techniques to avoid significant losses through inaccuracies in predictions. Climate change enters into forecasting models through variations in weather factors that influence load. These weather variations exhibit a pattern distinct from the past, forming the essence of climate change .Moreover, efficient production by electric utilities, based on improved load forecasts, is likely to reduce their carbon footprint. This is important since only around 11 percent of U.S. electricity is generated from renewable sources (USEIA, 2010).

This study investigates potential improvements in short term and medium term load forecasting models to assist with climate change adaptation by electric utilities. This is achieved by incorporating weather variables in the current models forecasting electricity load. In this research we develop load forecasting models at two distinct time scales, specifically at the hourly and monthly scales. While hourly load forecasting models are critical for operational planning and ensuring supply reliability, load forecasting at the monthly level facilitates decision-making regarding future capital investment and evaluation of energy price contracts.

We develop statistical models for forecasting hourly electricity load for three AEPCO (Arizona Electric Power Cooperative) utilities in the state of Arizona located in Tucson, Mohave and Graham. Moreover, we construct a monthly load forecasting model for the Tucson Metropolitan Statistical Area (MSA) based on load data from the Tucson Electric Power (TEP) utility. We expect that the improved statistical models will perform better than the current models used by the electric utilities, which use only past load data to forecast next-day load profiles. We test this assertion by evaluating the newly generated forecasts using generally accepted measures of forecasting error. We expect that the findings of this investigation will lead to significant cost savings for electric utility managers and efficient investment in future renewable energy projects.

1.1 Electricity Load & Load Forecasting

The term electricity demand is used synonymously with load based on the fact that electric utilities generally supply electricity to specifically meet load demand. While a shortage in electricity supply can lead to brownouts, blackouts or financial losses incurred through purchases in electricity spot markets, overproduction by an electric utility implies wastage of scarce resources, higher production costs and often system overloads. The lack of economically-efficient storage technology for electricity ensures the continuity of this inherent risk in the business of electricity supply. Therefore, foreknowledge of load behavior, through load forecasting, is crucial in planning, analysis and operation of power systems so as to assure an uninterrupted, reliable, secure and economic supply of electricity. Electric load forecasting involves the prediction of both the geographical locations and magnitudes of electric load over the different periods (usually hours) of the planning period (Alfares & Nazeeruddin, 2002).

Electric utilities are mostly concerned with peak load forecasts, i.e., the maximum instantaneous load or the maximum average load over a designated interval of time. Peak load forecasts can be made at the daily, monthly, seasonal or annual level. At the daily level, peak load allows the electric utility to plan its generation and spot-market activity to ensure continuity of electricity supply. Annual and seasonal peak load forecasts are important for planning i.e., for securing adequate generation, transmission and distribution capacities. These medium-term peak load forecasts improve decision-making with regards to capital expenditures and improve the reliability of electric system (Feinberg, 2009).

Traditionally, the electricity industry was characterized by a highly vertically integrated market structure with very little competition. However in the last few decades this has been replaced by competitive markets. With the rise of competition, the costs of over- or under-production and then selling or buying electricity on the spot market have increased substantially. Moreover, since electricity is typically produced by several generating units with different lead times, short-term load forecasts allow each unit to more accurately anticipate its need by the utility, avoiding costs incurred from idle operation. As a result load forecasting has become the central and integral process in the planning and operation of electric utilities, energy suppliers, system operators and other market participants. Since the financial penalties for forecast errors are so high, most research in this field aims at reducing them even by a fraction of a percent (Weron, 2006). There are many modeling techniques used by electric utilities to forecast future loads. These are discussed in greater detail in Chapter 2.

1.2 Impact of Climate Change

The United Nations Framework Convention on Climate Change (UNFCCC) has defined climate change as a change of climate which is attributed directly or indirectly to human activity that alters the composition of the global atmosphere and which is in addition to natural climate variability observed over comparable time periods. This study accepts the premise that climate change is primarily human-induced.

While climate change is a global problem, its effects are felt even at the county level. Global trends observed in recent decades include rising temperatures, increasing heavy downpours, rising sea level, longer growing seasons, reductions in snow and ice, and changes in the amounts and timing of river flows. These trends are projected to continue based on the quantity of heat-trapping gas emissions in the atmosphere. According to a 2009 report by the U.S. Global Change Research Program (USGCRP), in the southwestern U.S., climate change is likely to result in higher temperatures and increased scarcity of water supplies. By the end of the century, average annual temperature is projected to rise approximately 4 degree Fahrenheit to 10 degree Fahrenheit above the historical baseline, averaged over the southwest region. (USGCRP,2009). Dominguez, Cañon and Valdes (2010) showed that the projected future aridity of the region will be characterized by higher temperatures (~0.5°C or 32.9 °F) and lower precipitation (~3 mm/month) than the projected trends from the IPCC climate models. Their improved temperature and precipitation projections for the southwest imply that the region will be 3.52 °C (or 38.33 °F) warmer and 16.25 mm drier by the year 2050.

It must be noted that climate change affects not just the magnitude, but also the variability of temperature and precipitation in the region. This is likely to be further intensified by continuing population shifts to the Southwest.

Moreover, the growing scarcity of water supplies will affect both future electricity consumption and production in the Southwest. This effect is exacerbated by what is generally referred to as the water-energy nexus. The water-energy nexus refers to the interdependency between the water and energy sectors. Due to our focus on load forecasting, it is necessary to highlight the water-energy nexus as it applies to the electricity sector. On the one hand, water is an integral element of energy-resource extraction, refining, processing, transportation and utilization. It is an integral part of electricity generation, where it is used directly in hydroelectric generation and indirectly for cooling and emissions scrubbing. For example, in calendar year 2000, thermoelectric power generation accounted for 39 percent of all freshwater withdrawals in the U.S., roughly equivalent to water withdrawals for irrigated agriculture (Hutson et al., 2004). On the other hand, electricity is used for the treatment, heating and transportation of water. It is predicted that as climate change induced-warming increases competition for water, the energy sector will be strongly affected because power plants require large quantities of water for cooling (USGCRP, 2009).

Moreover, weather is a major cause of the variation in electricity load for space cooling, heating and electric lighting. Examination of trends in electricity consumption shows a direct relationship between weather factors such as temperature and precipitation and electricity consumption. As expected, in the Southwest, space cooling is of a larger concern than heating due to the relative high temperatures experienced during most of the year. It is predicted that climate change induced-warming will decrease demand for heating energy in winter and increase demand for cooling energy in summer. The latter will result in significant increases in electricity use and higher peak loads in most regions (USGCRP, 2009).

Electric utilities have not ignored the repercussions of climate change. In 2005, electric utility company specialists and stakeholders who attended an EPRI workshop titled “Identifying Research to Help Electric Companies Adapt to Climate Change,” unanimously agreed that more applied research on the climate change impacts was necessary, with load forecasting being one of the areas considered for application.

However, most industry-specific climate change reports have emphasized mitigation of green house gas (GHG) emissions. This has resulted in greater investment in mitigation technologies, development of renewable energy sources and the deployment of smart grids and smart meters (Acclimatise, 2009). One such study was conducted by the Electric Power Research Institute (EPRI) to investigate the various options that the U.S. electric utilities might pursue in response to a range of possible climate policy scenarios. It focused predominantly on emissions reduction policies, opportunities and technologies (EPRI, 2003).

While mitigation is integral to an electric company's response to climate change, it is essential for utilities to undertake adaptation. The Carbon Disclosure Project (CDP) undertaken by Acclimatise, highlighted this fact. Under CDP, based on responses of electric companies to a questionnaire, it was reported that electric utilities were responding to climate change by identifying risks and taking actions to manage them. However, while utilities were reporting direct climate impacts (such as those due to extreme climate events), indirect impacts were neglected. Companies also reported investing in climate-resilient materials and designs, such as coastal sea defenses, sustainable drainage systems and dam reservoir overflow management facilities for hydropower. Some companies were also focusing on optimizing their existing assets through improved cooling technologies (Acclimatise, 2009). For supporting climate change adaptation by the electricity sector it is necessary to understand and accurately predict electricity demand in light of climate change. We seek to shed further light on the impact of climate change on the electricity sector by adapting current load forecasting models used by utilities to incorporate climate information.

CHAPTER 2 Literature Review

2.1 Climate and Load Forecasts

While the links between electricity load and weather elements appear to be self-evident, it was necessary for the purposes of this study to review past research to strengthen our understanding of these dynamic relationships. This in turn informed our expectations for the parameters associated with each of the weather variables included in our models.

Given the economic importance of load forecasting and the advent of climate change, the relationships between weather variables and electricity load have been widely investigated and used in short and medium term load forecasting. In one of the earliest works in this field, Joseph Lam (1998) investigated the relationships between residential electricity consumption and economic variables and climatic factors (specifically temperature) for Hong Kong. Among socio-economic factors, he also found that knowledge of temperature, as measured by using cooling degree days, facilitated the estimation of residential electricity use.

Moreover, in their study, Ranjan and Jain (1999) modeled electricity consumption as a function of population and weather sensitive parameters, specifically sunshine hours, temperature, rainfall and relative humidity. It must be noted that they created four different seasonal models to account for the drastic differences in weather conditions from one season to the next, and found that in each of the seasons different weather variables were relevant for explaining electricity consumption. Therefore they highlighted the fact that variability of climatic conditions, whether on a temporal or regional scale, was an essential modeling consideration. This means that, apart from accounting for seasonal variations in weather, electric utilities with service areas in differing climatic regions need to use different approaches for load forecasting for each region. This assertion was supported by Sailor and Muñoz (1997), who developed eight different models, for each of the eight states included in their study, relating electricity consumption to climate parameters.

The experience of many utilities indicates that the weather elements, which influence load demand, consist of temperature, humidity, wind and precipitation.

Temperature has been found to play the most important role in controlling the electricity load (Psiloglou et al., 2009). This is primarily because of the use of electricity for heating and cooling purposes. Past studies have shown that temperature exhibits a non-linear pattern in its relationship with load, often referred to as a 'U-shaped' or 'hockey-stick' curve. Figure 1 illustrates this concept for the three AEPCO electric utilities included in our study. In Figure 1, we observe a bifurcation in the load observations for Graham into two distinct bands. This appears to be due to a discrete shift in load between 1997 and 1998. While information regarding types of customers for Graham will shed further light on this issue and facilitate model fit, the lack of this information precludes such an investigation.

This non-linearity is explained by the Heating and Cooling Effects recently described by Bessec and Fouquau (2008). They argued that in winter, there exists a negative relationship between load and temperature since an increase in temperature diminishes the need for energy resources used for heating purposes. This is referred to as the Heating Effect. On the other hand, in summer an increase in temperature raises the demand for electricity for cooling appliances, lending credence to an evident positive relationship. In literature, this is referred to as the Cooling Effect. Its has also been argued that at a certain temperature level, referred to as the Neutral Temperature, load demand is not sensitive to temperature changes. Tanimoto (2008) calculated that the neutral temperature for the Tucson MSA is around 15 degree Celsius. Most studies have verified and accounted for this non-linearity at the daily and hourly scale. They have utilized degree-day variables (Al-Zayer and Al-Ibrahim, 1996; Sailor, 2001; Pardo et al., 2002; Amato et al., 2005), logistic smooth threshold regression models (Bessec et al., 2008; Moral-Carcedo and Vicéns-Otero, 2005) and semi or non-parametric models (Engle et al., 1986; Henley and Peirson, 1997). In the most recent and well-known study of this relationship, Marie Bessec and Julien Fouquau (2008) used logistic smooth threshold regression (LSTR) model to confirm the non-linearity of this relationship for 15 countries in the EU, using data for a period of 20 years.

Due to its significant influence on load, the effect of temperature has been studied to a much greater extent than the other weather elements. While there is a significant paucity of studies related to the link between humidity and electricity consumption, it is understood that humidity is known to increase the heat-retention capacity of air (Willis, 2002). Consequently high levels of humidity during summer (or winter) months tend to increase the need for cooling (or heating), leading to an increase (or decrease in) in electricity load associated with air-conditioning (Contaxi et al., 2006).

Figure 1: Relationship between Temperature and Electricity Load

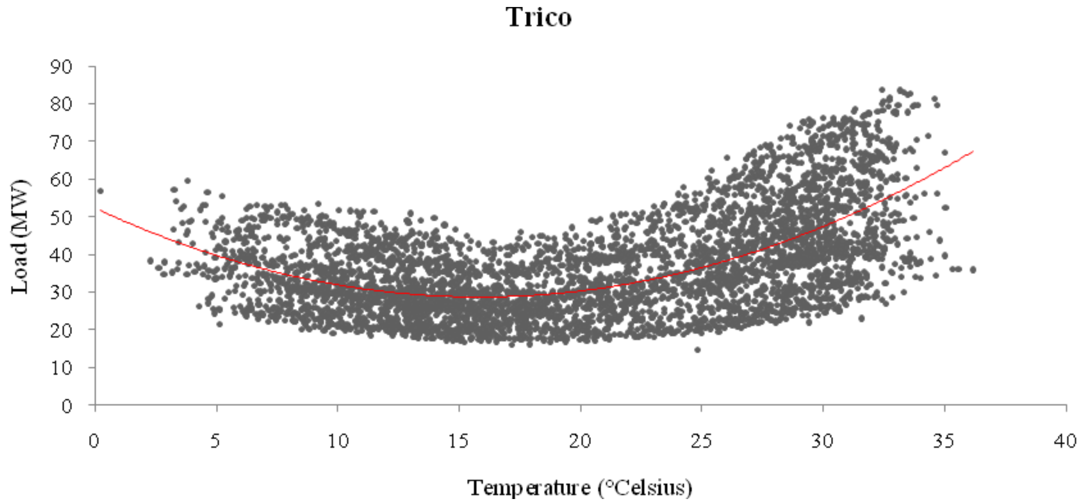

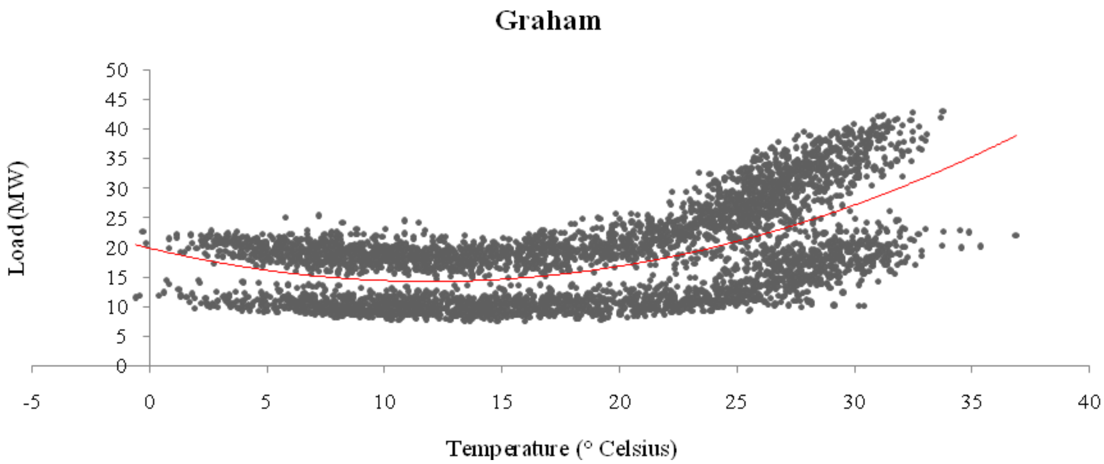

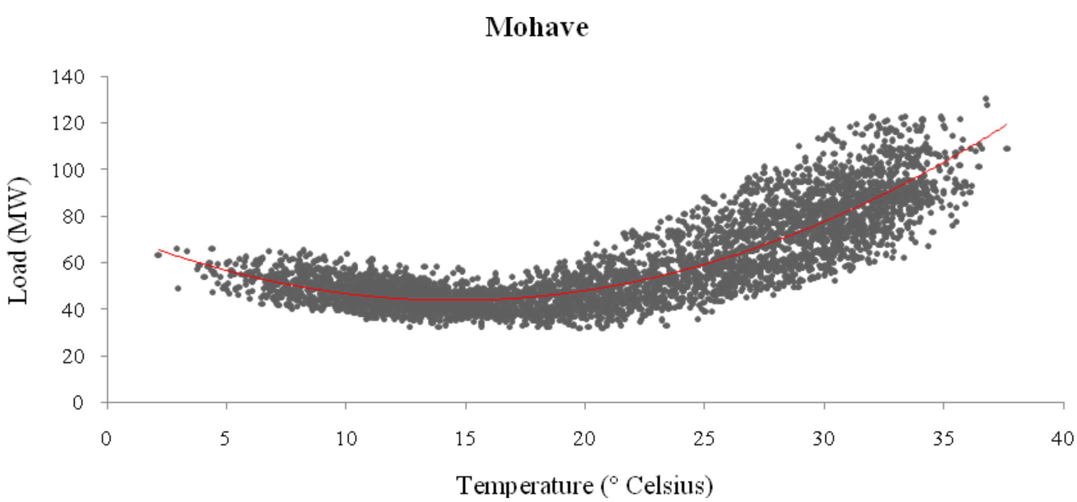

Also, rapid winds are known to generate a chilling sensation, decreasing the need for electric cooling. However, they also augment the need for heating during the winter months.

Precipitation is another significant weather variable which influences electricity demand. An increase in precipitation (specifically rainfall) decreases temperature, which in turn decreases load demand for air-conditioning (Willis, 2002). This implies that load and precipitation should be inversely related. However we must also consider the fact that heavy rainfall can push people indoors, increasing their consumption of electricity (Willis, 2002). Therefore the relationship between precipitation and load is still ambiguous.

Finally, the weather element solar radiation displays the most ambiguity. Higher illumination of surroundings is expected to increase the ambient temperature, thereby increasing the demand for electric cooling (Willis, 2002). However, one can argue that an increase in solar illumination also decreases the use of electric lighting devices.

Therefore, despite a large body of work in this field, there is still significant ambiguity regarding the precise nature of the relationships between weather and electricity demand.

2.2 Load Forecasting Models

After reviewing the relationships between weather and electricity load, it is necessary to examine the various load forecasting modeling techniques currently available.

As the first step, one must consider the two main approaches to load forecasting. Conventional electricity demand models are often applied to forecast the demand at the utility level. These kinds of forecasting methods are commonly employed when there is little or no knowledge about the appliance stocks and other grass-root level consumer details (Paatero and

Lund, 2006). On the other hand, End-use models represent a bottom-up demand modeling approach, the accuracy of which depend on the easy availability of grass-root level consumption details. Due to this limitation of end-use models, the most prevalent approach is the conventional approach to load forecasting. In our study we utilize the conventional approach as opposed to the end-use methodology in light of the significant paucity of household level electricity consumption data.

Next, since electricity load is related with various factors such as the time of day, day of week, season, climatic conditions, and the past usage patterns, several methods have been utilized to model these relationships and generate load forecasts. The different load forecasting modeling techniques can be broadly categorized into the following categories:

1. **Statistical Models:** These models include multiple regressions, exponential smoothing, adaptive load forecasting and time series analysis. They generally involve a mathematical model that represents load as function of different factors such as time, weather, customer class and past values.

2. **Computational Intelligence Techniques:** These techniques are highly sophisticated. At present, they include neural networks, fuzzy logic and genetic algorithms.

3. **Knowledge-based Expert Systems:** Knowledge-based Expert systems are a class of techniques which employ the knowledge and analogical reasoning of experienced human operators. They are designed employing artificial intelligence concepts to emulate human performance.

Third, we must consider the temporal aspect of load forecasting techniques as well. Srinivasan and Lee (1995) classified load forecasting in terms of the planning horizon's duration: up to 1 day for short-term load forecasting (STLF), 1 day to 1 year for medium-term load forecasting (MTLF), and 1 to 10 years for long-term load forecasting (LTLF).

One of the most common STLF techniques utilized by electric utilities is the Similar-day approach. Under this approach, historical data is searched for days within recent years that have similar characteristics (such as weather, day of week, date etc.) to the forecast day. Therefore the load of that similar day is considered as the forecast for a specific day (Feinberg and Genethliou, 2005). Often some adjustments are made to the anticipated load for observable factors, such as holidays, general trend and weather.

The purpose of this study is to demonstrate load forecasting models that incorporate climate information to account for the impact of climate change on electricity load in the future. Keeping this in mind, we conclude that statistical models of load forecasting, due to their accessibility, low-cost and easy interpretation, are best suited for the purpose of this study. Moreover, given the time-series nature of our data, Box-Jenkins models are further scrutinized for their application to our data.

Most popular statistical approaches to load forecasting involve using the Box-Jenkins time series models, specifically the purely autoregressive (AR) and ARMA (Autoregressive Moving Average) or ARIMA (Autoregressive Integrated Moving Average) models, which predict future load based solely on past load data. ARMA models are usually used for stationary processes while ARIMA is an extension of ARMA to non-stationary processes. Hagan and Behr (1987) argued that the Box-Jenkins models are well suited to load forecasting due to the procedures built-in into the models for developing, checking and updating them. These models have been extensively applied to load forecasting (Weron, 2006).

However, the ARMA and ARIMA model forecasts are essentially extrapolations of the previous load history and have problems when there is a sudden change in the weather (Hagan and Behr, 1987). Therefore, since the purpose our study is to aid in the climate change adaptation by electric utilities, we look beyond standard AR and ARMA/ARIMA models, to regression models with autoregressive or ARMA errors that can incorporate climate information. The selection and estimation of our hourly and monthly load forecasting models is detailed in Chapters 3 and 4, respectively.

CHAPTER 3 Hourly Load Forecasting Models

Under this study, we seek to construct load forecasting models for two different temporal scales, specifically at the hourly and the monthly time scales. Selection of the appropriate models for each temporal scale depends on the inherent peculiarities of our datasets. The load and weather data for our research and model selection are further discussed in this chapter (Chapter 3) and the next (Chapter 4) for the hourly and monthly load forecasting models, respectively.

3.1 Data Description

Electric utilities safeguard their electricity system load data due to concerns about the privacy of their clientele. Moreover, given the competitive nature of the electricity market, such data has strategic value. For this research, hourly-level electric load data was provided by the Arizona Electric Power Cooperative (AEPCO). Specific information regarding clients and service region was suppressed for reasons of confidentiality.

AEPCO is a not-for-profit rural electricity cooperative formed in 1961.Since then AEPCO has expanded its membership and undergone significant restructuring, splitting into 3 different organizations, with AEPCO retaining its role in power generation. Currently, AEPCO and its members serve customers in nine Arizona counties (Cochise, Coconino, Graham, Greenlee, Mohave, Pima, Pinal, Santa Cruz and Yavapai), one county in California (Riverside) and two counties in New Mexico (Hidalgo and Grant).

We were provided with hourly load data for three of its members, Graham County Electric Cooperative (GCEC), Mohave Electric Cooperative (MEC) and Trico Electric Cooperative

(Trico). For the reader's convenience, from here on we will refer to them as Graham, Mohave and Trico, respectively. Graham and Mohave serve the Safford and Bullhead City regions of Arizona and Trico serves to some parts of Marana and the Tucson Metropolitan Statistical Area (MSA). The period covered starts in January 1993 and ends in December 2004.

As detailed in Chapter 2, electricity demand or load is sensitive to changes in weather conditions. In order to effectively incorporate weather information in our hourly load forecasting models we obtained hourly weather data from the Arizona Meteorological Network (AZMET). AZMET is a University of Arizona Cooperative Extension project which collects of meteorological data from a network of 28 automated weather stations located in central and southern Arizona. Temperature, precipitation, relative humidity, solar radiation and wind speed data, measured at the hourly level, were obtained from this source for the time period of the AEPCO load data. The three specific weather stations used for Trico, Graham and Mohave were Marana, Safford and Mohave, respectively. Issues regarding duplicate and missing observations in the AZMET dataset were corrected through deletion and averaging.

Table 1 provides the summary statistics for the load and weather variables used in this study for each of the three cooperatives. All three regions display weather characteristics consistent with the general climatic conditions in central and southern Arizona. This is evident from the fact that all three service areas exhibit almost equivalent average relative humidity levels. Also, they each experience maximum precipitation in July and August, during the monsoon season. While all of them experience generally very high variation in temperature, Mohave, due to its location in the Mohave Desert region experiences the highest maximum temperature of 48.5 degree Celsius. Mohave also experiences the fastest blowing winds. The service area of Graham is on average cooler than that of Trico and Mohave. The service area of the three AEPCO cooperatives is represented in Appendix G.

Table 1: Summary Statistics for Hourly Load Forecasting Models

Variable	Units	Mohave				Graham				Trico			
		Max	Min	Std Dev	Mean	Max	Min	Std Dev	Mean	Max	Min	Std Dev	Mean
Hourly Load	MW	175.33	8.90	24.07	59.51	57.27	0.69	8.76	18.54	112.45	10.40	15.96	36.54
Temp	° F	48.50	-6.30	10.42	21.01	45.60	-8.70	10.44	18.15	45.80	-7.80	10.02	20.17
RH	%	100.00	0.00	22.58	43.32	100.00	2.20	24.77	42.25	100.00	2.50	25.23	43.25
SolRad	MJ/m^2	59.00	0.00	1.15	0.85	4.41	0.00	1.15	0.85	4.29	0.00	1.15	0.86
Precip	mm	20.40	0.00	0.21	0.01	37.00	0.00	0.33	0.02	33.00	0.00	0.38	0.03
Windspd	m/s	16.50	0.00	2.11	2.33	14.70	0.20	1.69	2.51	12.90	0.20	1.46	2.46

T=105,192

3.2 Model Selection

The complete dataset for all three cooperatives, Trico, Graham and Mohave, comprised of time series data on electricity load and weather variables for the time period starting January 1993 to December 2004. Keeping this in mind, we reviewed literature on time series models in order to gain a better understanding of the construct of a successful model.

While the presence of heteroskedasticity and autocorrelation in time series data violate significant assumptions of the linear regression models, purely Autoregressive (AR), Moving Average (MA) or even standard Autoregressive Moving Average (ARMA) models involve only univariate time series analysis. In order to account for the possibility of non-stationarity of our load data, as well as allow for the inclusion of weather factors as explanatory variables, the basic construct of the dynamic regression models was selected.

Standard ARMA and ARIMA (Autoregressive Integrated Moving Average) models use only time and past load values as input variables. However, from Chapter 2 it is evident that electricity load also depends on weather variables. The dynamic regression models also known as ARIMAX or Transfer Function models, permit input time series which offer the potential for improved load forecasting. In their most basic form, these models involve a multivariate regression, with the errors (or 'noise') exhibiting both autoregressive and moving average components.

For example, consider the following model, where the noise series is assumed to be an ARMA (1,1) process:

$$Y_t = \mu + \omega_1 X_{1t} + \omega_2 X_{2t} + \frac{(1-\theta_1 Y_{t-1})}{(1-\emptyset_1 Y_{t-1})}\, \varepsilon_t \qquad (3.2)$$

Here, t indexes time, μ is the mean term, X_{1t} and X_{2t} are the input series and ε_t is the random error term, also referred to as white noise.

Once the basic model construct was selected, it was necessary to study the nature and behavior of the variables to be included in the model and modify the basic construct accordingly.

3.3 Model Variables

Dependent Variable: For our Hourly load forecasting models, we utilized electricity load data (Load), collected at the hourly intervals, as our dependent variable. As a time series, this variable was fraught with concerns regarding stationarity and seasonality. Figure 2 shows the plots of average daily load over the time period of the study for the three AEPCO cooperatives. It is evident from these plots that average load exhibits an overall increasing trend (except for Graham) and seasonality. As mentioned earlier, average load for Graham exhibits a shift from 1997 to 1998. However, in the absence of customer-related information, we cannot further pursue this line of study.

A time series is said to be stationary if its statistical properties, specifically its mean, variance and autocorrelation structures do not change over time (Weron, 2006). It is necessary for a time series to be stationary to ensure that the variance is not explosive and that the predictions are reliable.

For the purposes of our study we were concerned with the stationarity of the fitted residuals from the regression of hourly load on weather variables. In the absence of the input series, the response series (or the hourly load) and the 'noise' series are the same. However, by including the input series, we are imposing the restriction of stationarity on the residuals after the effect of the inputs is removed. From here on we will refer to these residuals as the residual series, to distinguish them from the white noise series introduced later in this section.

We utilize the Augmented Dickey- Fuller (ADF) test as a formal test of stationarity for the residual series. The ADF test statistic is given by the following formula:

$$ADF_T = \frac{\hat{\gamma}-1}{S.E.(\hat{\gamma})} \tag{3.3}$$

The basic idea behind this test is to ascertain if the coefficients of the autoregressive part of an ARMA model fitted on the residual series are not equal to one, i.e., that none of the characteristic roots equal one. If all the characteristic roots are less than 1 in absolute value, then the residual series is stationary.

Figure 2 shows that the load data for Trico, Graham and Mohave display increasing variation over time. In order to correct for this, we transformed the load variables by taking their natural logarithm.

Box and Jenkins (2008) suggested that the first property that can indicate departure from stationarity is that the series, when graphed over time, does not appear to have a constant mean. Keeping this in mind, we see from Figure 2 that the hourly load series is non-stationary for all three AEPCO cooperatives. Therefore, to make the logged hourly load series was detrended by taking the first difference.

After these transformations and differencing, we use the Augmented Dickey Fuller (ADF) test of stationarity on the residual series to determine the need for additional filtering. The results of the ADF test are shown by Table 2. It is evident from the associated p-values that we fail to reject the null hypothesis of a unit root. Therefore we conclude that the residual series for all three cooperatives were not stationary. Considering the daily seasonality involved in load data, we further differenced the logged hourly load by 24 hours to make the resulting residual series stationary. Therefore our final dependent variable, after filtering, is the logged hourly load differenced twice, first by one and then by 24. This pattern of load differencing is similar to one utilized by Thompson and Cathers (2005).

Figure 2: Average Daily Load for Trico, Graham and Mohave (1993-2004)

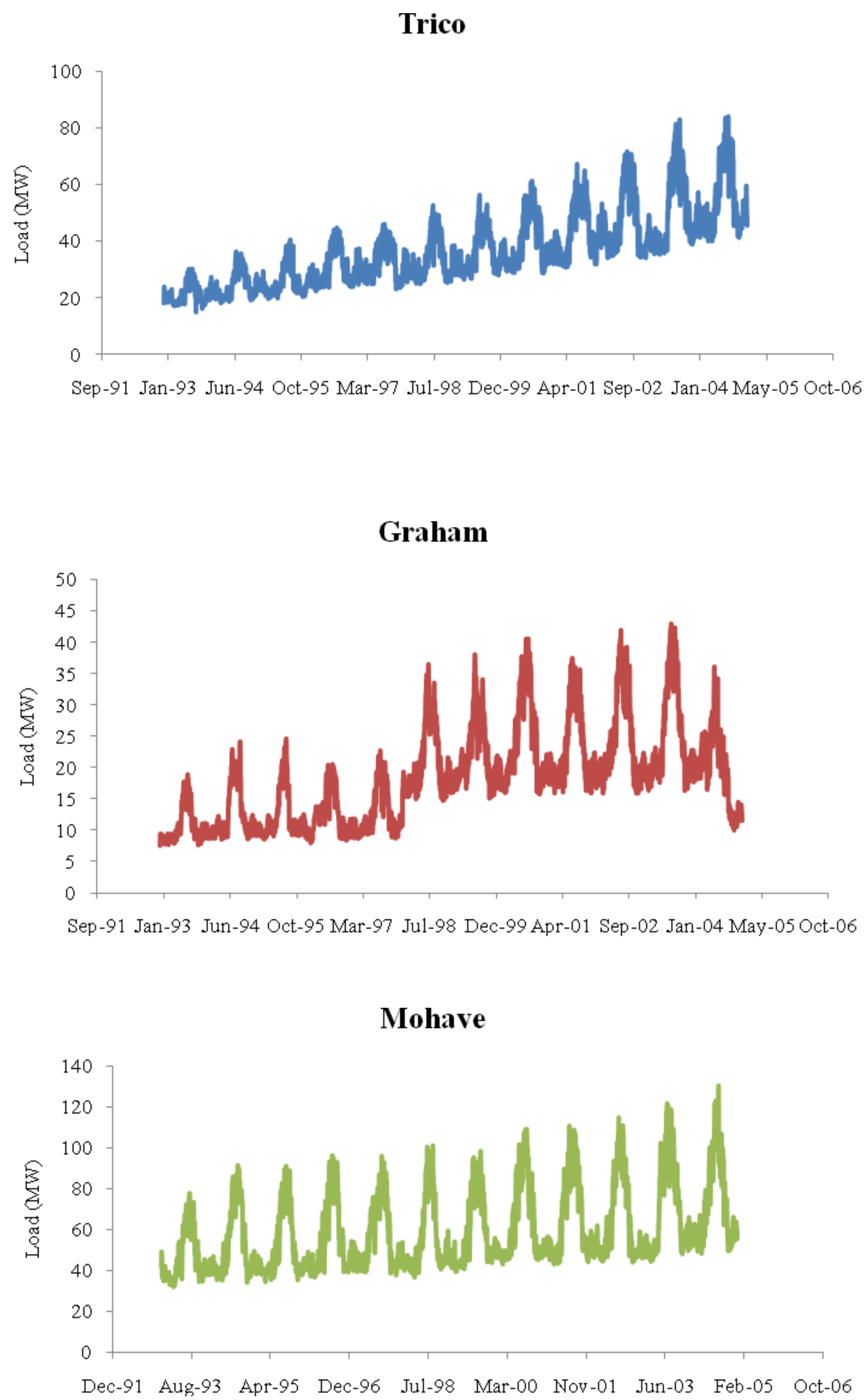

Table 2: Augmented Dickey-Fuller Test for log(Load) differenced by 1

Type	Lags	Trico		Graham		Mohave	
		Rho	Pr < Rho	Rho	Pr < Rho	Rho	Pr < Rho
Zero Mean	1	-59,536.50	0.0001	-47,544.20	0.0001	-42,319.50	0.0001
	2	-60,505.00	0.0001	-54,591.10	0.0001	-46,677.30	0.0001
	3	-97,023.80	0.0001	-77,362.10	0.0001	-64,967.40	0.0001
	4	-498,137.00	0.0001	-149,247.00	0.0001	-129,147.00	0.0001
	12	49,402.04	0.9999	424,767.20	0.9999	44,648.53	0.9999
	24	-1,721.75	0.0001	-1,311.09	0.0001	-1,901.66	0.0001
	168	-587.51	0.0001	-402.50	0.0001	-644.06	0.0001
Single Mean	1	-59,536.50	0.0001	-47,544.20	0.0001	-42,319.50	0.0001
	2	-60,505.00	0.0001	-54,591.10	0.0001	-46,677.30	0.0001
	3	-97,023.80	0.0001	-77,362.10	0.0001	-64,967.40	0.0001
	4	-498,137.00	0.0001	-149,247.00	0.0001	-129,147.00	0.0001
	12	49,402.04	0.9999	424,767.10	0.9999	44,648.53	0.9999
	24	-1,721.75	0.0001	-1,311.09	0.0001	-1,901.66	0.0001
	168	-587.51	0.0001	-402.50	0.0001	-644.09	0.0001
Trend	1	-59,546.10	0.0001	-47,544.20	0.0001	-42,322.30	0.0001
	2	-60,520.40	0.0001	-54,591.20	0.0001	-46,681.80	0.0001
	3	-97,069.40	0.0001	-77,362.20	0.0001	-64,977.20	0.0001
	4	-499,421.00	0.0001	-149,248.00	0.0001	-129,188.00	0.0001
	12	49,320.32	0.9999	424,723.60	0.9999	44,627.73	0.9999
	24	-1,729.79	0.0001	-1,311.10	0.0001	-1,904.56	0.0001
	168	-593.34	0.0001	-402.50	0.0001	-647.27	0.0001

T= 152,192

Explanatory Variables: When a time series exhibits periodic fluctuations, it is said to display seasonality. From visual inspection of the pattern displayed by average loads plotted against time, it is evident that electric load data displays seasonality at the daily, weekly and annual time scale.

- **Hourly Variability of Load:** Figure 3 shows the variation of electric load throughout a day. For this study we define the time period of the five seasons experienced in Arizona as below:

1. Winter: December and January
2. Spring: February, March and April
3. Dry Summer: May and June
4. Monsoon Summer: July and August
5. Fall: September, October and November

While a bimodal distribution of load is evident during wintertime, during the rest of the year the distribution is unimodal, with daily peak load occurring around. From both these cases it is evident that the hours from 8 am to 8 pm behave differently from the rest of the day. Therefore we can designate this time period as peak hours of the day. The coefficient associated with the dummy variable for this peak period (Peakhr) is expected to have a positive sign since demand for electricity appears to be at a higher magnitude during the peak hours relatively to the rest of the day.

Figure 3: Monthly Averaged Load for 2004

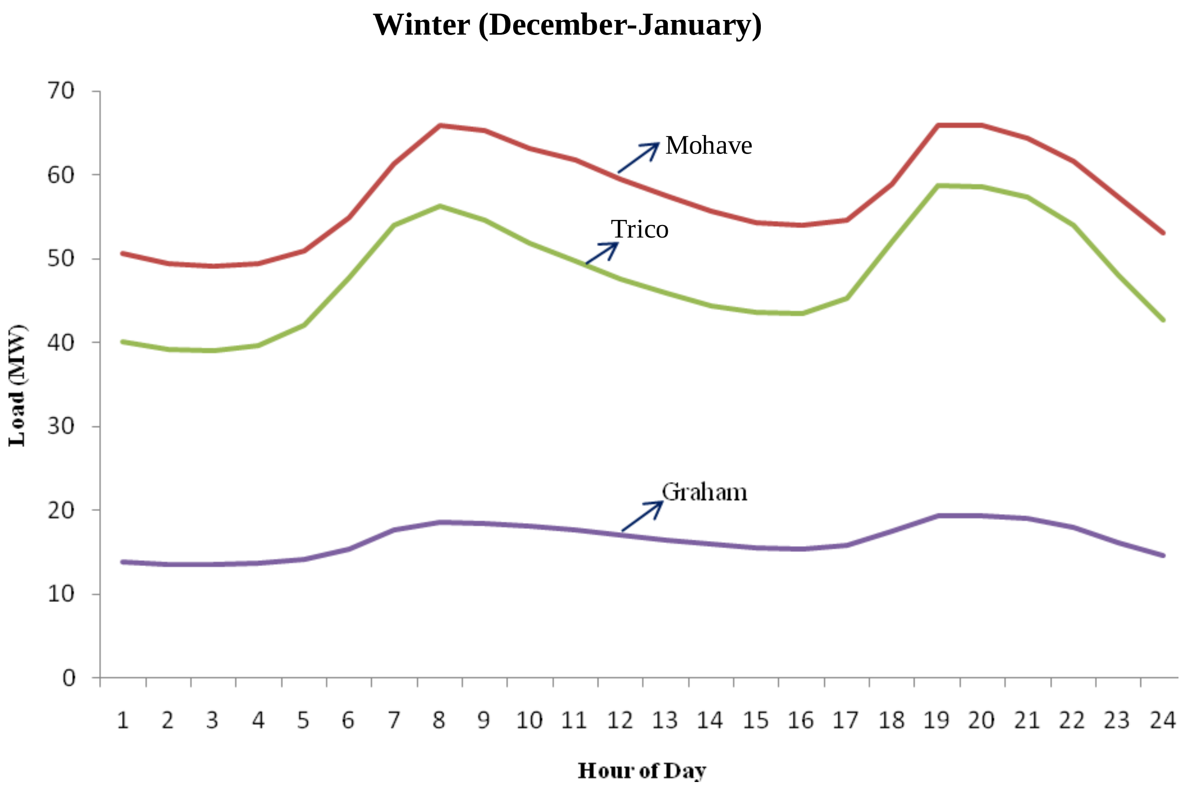

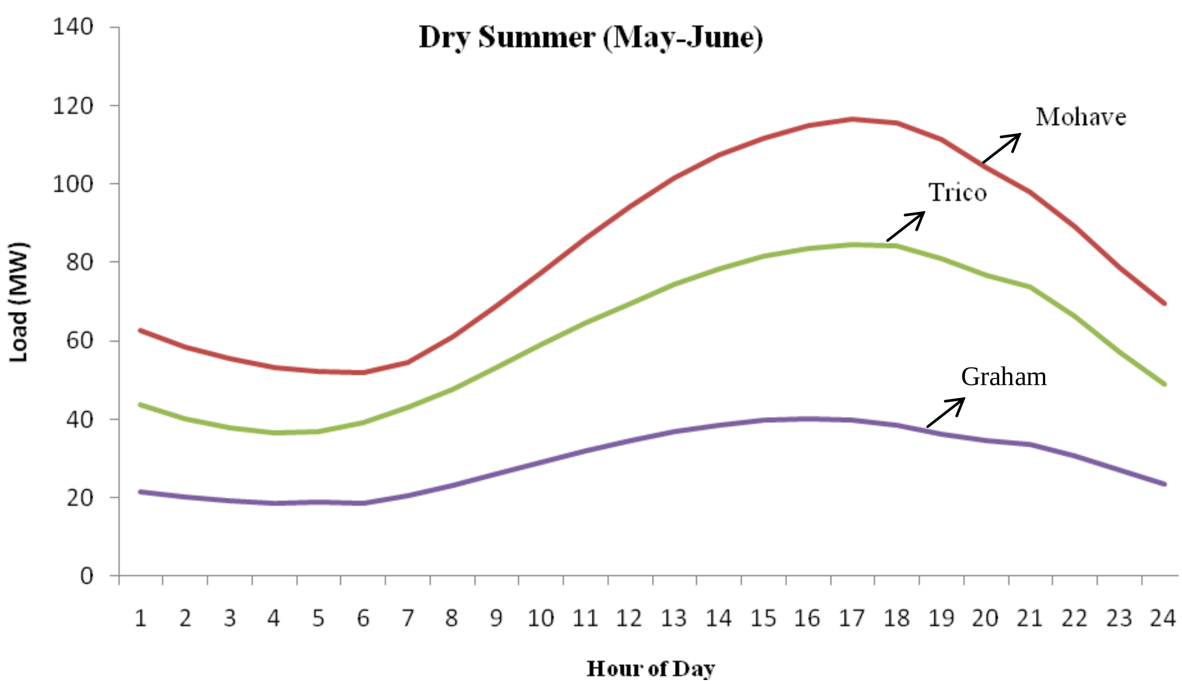

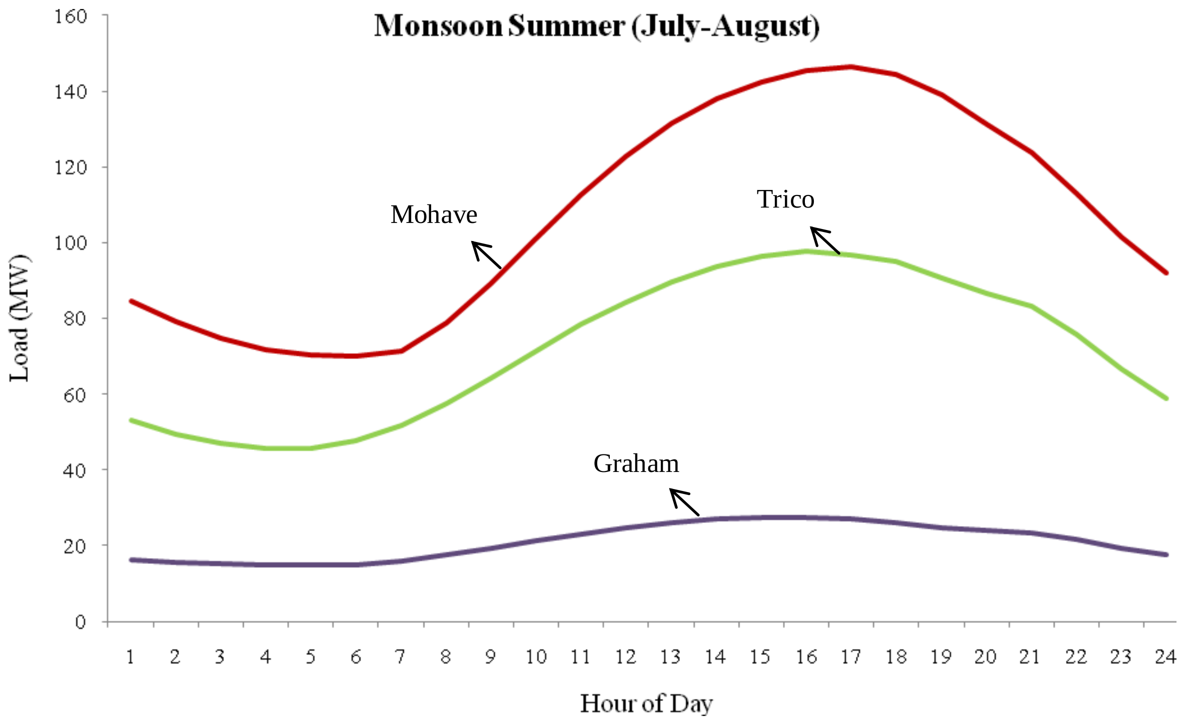
Monsoon Summer (July-August)
Load (MW)
Hour of Day
Mohave
Trico
Graham
0
20
40
60
80
100
120
140
160
1 2 3 4 5 6 7 8 9 10 11 12 13 14 15 16 17 18 19 20 21 22 23 24

- **Day-of-Week Variability of Load:** By plotting average electric load against weekdays, we observe a unique pattern (Figure 4) for all three of the AEPCO cooperatives. Sunday has the least average load in a week, followed by Saturday and then Friday. Therefore we can incorporate a dummy variable for weekends to model this phenomenon. We expect that the coefficients associated with this dummy variable will have a negative coefficient.

Figure 4: Average Load by Day of Week

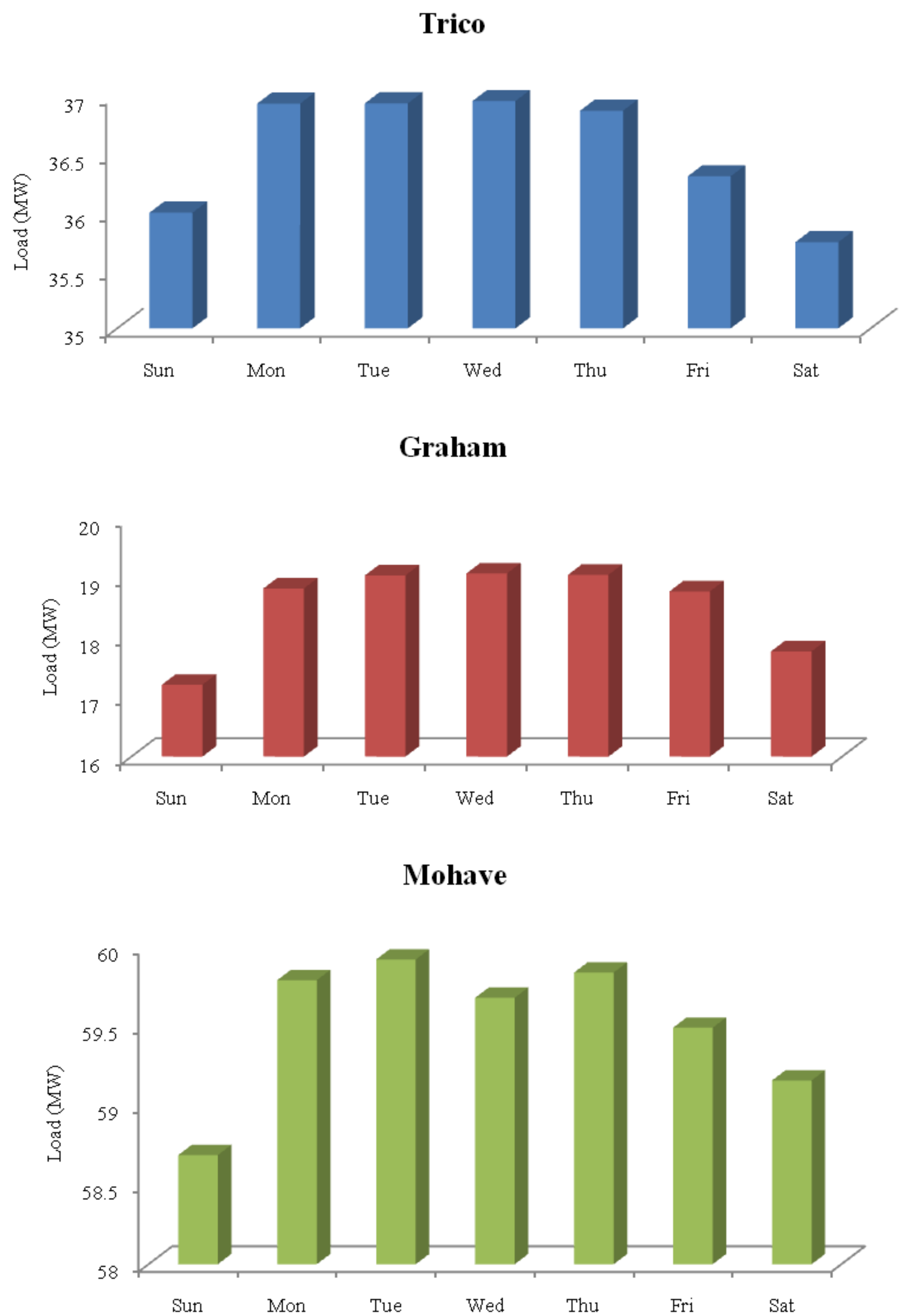

- **Monthly Seasonality:** It is evident from Figure 5 below that the annual average load curves for Trico, and Mohave peak during the monsoon season i.e., during the month of July or August. This is consistent with the fact that high humidity during this period, by raising the heat retentive capacity of air, raises the overall ambient temperature. It is also important to note the use of swamp coolers and air conditioners in the study regions. Due to high levels of humidity and temperature during the monsoon season, people shift from evaporative cooling to air conditioners. Since air conditioners use more electricity than swamp coolers, this could explain the incidence of annual peak loads during the monsoon seasons. Average load is lowest during the winter months, gradually rising over spring, and then rapidly increasing during the dry summer season, starting from beginning of May to the end of June. For our study regions, this can be explained by the blended use of natural gas and electricity for household heating and cooling. Shifting from natural gas-powered heating in winter to electricity-based cooling in summer can explain the higher load over the two summer seasons. Therefore, load appears to vary over seasons, which can be modeled using dummy variables. We expect that the coefficient associated with the monsoon dummy variable to be positive.

Figure 5: Average of Monthly Load

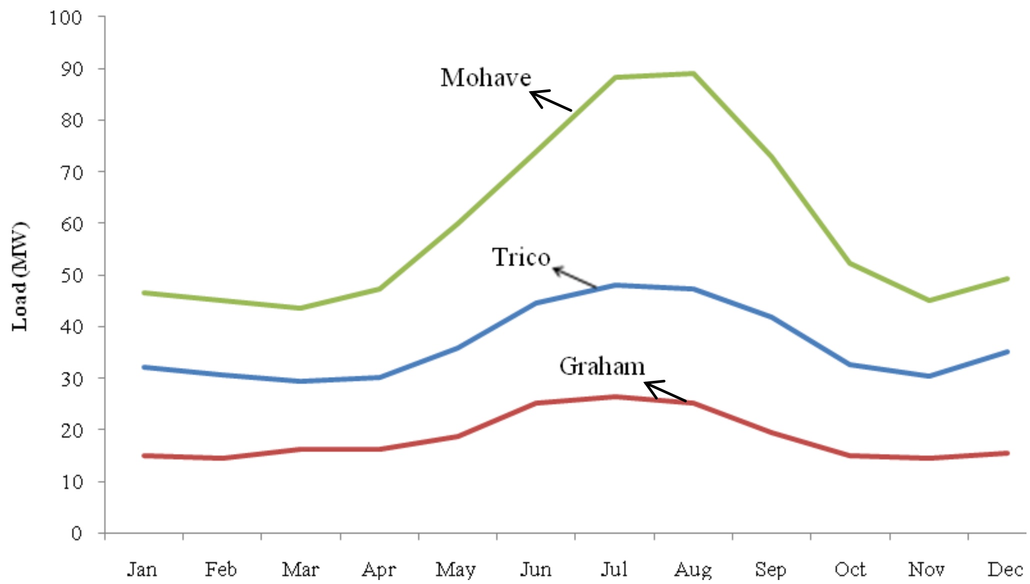

In order to deal with these different levels of seasonality, we utilized dummy variables for weekdays (keeping Monday as baseline), the peak hours during a day and for four of the five seasons in Arizona (with the winter season as baseline).

Holidays (Hol): It is commonly understood that on holidays consumers indulge in modified consumption and demand behavior. We assume that this applies to the electricity demand as well by including a dummy variable for holidays that do not fall on weekends (Hol). However, the expected coefficient on this variable is ambiguous. This is because while some holidays encourage higher demand for electricity, others may lead to a reduction in electric load. For example, Christmas Day is well known to be a holiday where people tend to congregate and utilize decorative lighting. Therefore load demand is likely to be higher on Christmas. However, it is unclear whether load is likely to increase or decrease on significant travel holidays, such as Thanksgiving, given that the destinations are often unclear and varied.

Hourly weather data from AZMET included temperature, precipitation, relative humidity, solar radiation and wind speed.

- **Temperature (Temp) :** Given the non-linear relationship between temperature and electricity load (discussed in Chapter 2), we modeled this relationship in a quadratic manner by including a linear term, a squared term and interaction terms for temperature with relative humidity (int1) and temperature with wind speed (int2). Despite the availability of more sophisticated techniques, due to the inherent simplicity and convenience of this approach, a quadratic function was selected. While we expect the coefficient associated with the linear term to be positive, we expect that the squared term to have a positive coefficient in order to satisfy the non-linear relationship between load and temperature.

- **Precipitation (Precip):** Precipitation lowers the ambient temperature, thereby lowering load demand. Therefore we expect the coefficient associated with precipitation to have a negative sign. It should be noted that for all three of the study regions, Tucson, Graham and Mohave, a lack of precipitation for most of the year implies that the variable Precip has many values (approximately 98 percent of observations) close to zero. Since we cannot ignore the role of precipitation in our study regions, we created a precipitation dummy variable (Precipdum) to be included instead. The same rationale applies regarding our expectation of the associated model coefficient. Moreover, due to the cooling effect of precipitation, we expect precipitation to interact with temperature and affect electric load inversely. Therefore, we also include an interaction term of precipitation with temperature (int3) in our hourly load forecasting models.

- **Relative humidity (RH):** As mentioned earlier in Chapter 2, at higher levels, humidity is known to increase the heat-retention capacity of air (Willis, 2002), leading us to expect a positive coefficient associated with the interaction term between temperature and humidity. However, due to the extremely dry weather in the study regions, one can also consider that an increase in relative humidity may provide relief and make weather conditions more pleasant, decreasing the demand for electric cooling. This would imply a negative coefficient associated with a linear humidity term.

- **Solar radiation (Solrad):** Higher illumination of surroundings is expected to increase the ambient temperature, thereby increasing the demand for electric cooling (Willis, 2002). However, many argue that an increase in solar illumination also decreases the use of electric lighting devices. In Arizona, the former effect is more likely due to the predominantly sunny weather of the region. Therefore, it is expected that a linear solar radiation term will have a positive coefficient.

- **Wind speed (Windspd):** Rapid winds are known to generate a chilling sensation, decreasing the need for electric cooling. However, they also augment the need for heating during the winter months. Therefore, it is expected that in the model the coefficient of the interaction term with temperature is negative. In Tucson, fast blowing winds are unobstructed due to the predominantly flat landscape, giving rise to dust storms. Since people are forced indoors, it is expected that the increased electricity consumption on windy (and hence dusty) days implies a positive coefficient for the wind speed linear term.

Table 3 summarizes this discussion by clearly stating the input series variables used in our three hourly load forecasting models, and our expectation regarding the signs of the associated model coefficients. Further detail regarding the values of dummy variables is given in Appendix F.

Table 3: Expected Signs of Hourly Model Coefficients

Variable	Description	Expected Sign
Temp	Temperature	Negative
SqTemp	$Temperature^2$	Positive
RH	Relative humidity	Negative
Solrad	Solar radiation	Positive
Windspd	Wind speed	Positive
Int1	Temp*Humidity	Positive
Int2	Temp*Windspeed	Negative
Int3	Temp* Precipitation	Negative
Precipdum	Precipitation dummy	Negative
Weekend	Weekend dummy	Negative
Hol	Holiday dummy	Positive
Peakhr	Peak load hours dummy	Positive
Spring	Seasonal dummies	Negative
Drysummer		Positive
Monssummer		Positive
Fall		Negative

T=105,192

3.4 Model Estimation

In the previous sections of this chapter, we selected a dynamic regression model as our basic model construct and identified the relevant weather and seasonal model variables. We also transformed our dependent variable, hourly load, by taking its natural log and differencing it twice to make the residual series stationary. From here on we will refer to this new dependent variable as the transformed load.

Using the construct of a dynamic regression model, our hourly load forecasting models consist of two key components:

1. The Transfer function which consists of the input variables, i.e., the weather variables and seasonal dummies.
2. The ARMA model fitted to the residual series obtained after regressing the transformed load on the input variables.

Fitting an ARMA model to the residual series is a crucial step. We use the following steps to fit an appropriate ARMA model for the residual series:

1. First we need to obtain the residual series and confirm stationarity using the Augmented Dickey Fuller test. This was already achieved through the creation of the transformed load variable.

2. Next we test for the presence of white noise in the residual series using the Ljung-Box test. The test statistic for this model is a Chi-Square given by the following formula:

$$Q = n\,(n+2)\sum_{k=1}^{h}\frac{\hat{\rho}_k^2}{n-k} \qquad (3.4.1)$$

where $\hat{\rho}_k^2$ is the sample autocorrelation at lag *k*, n is the sample size and *h* is the number of lags being tested. The null hypothesis of this test is that all of the autocorrelations up to the stated lag are jointly zero i.e., the residual series is white noise. The results of our Ljung-Box test on the residual series are shown by Table 4. The extremely large and highly significant Chi-square values imply that we reject the null hypothesis. Consequently, the residual series are not white noise and a model can be fit to the residual series.

Table 4: Results of Ljung-Box Test for White Noise on residual series

To Lag	Trico			Graham			Mohave		
	Chi-Square	DF	Pr > ChiSq	Chi-Square	DF	Pr > ChiSq	Chi-Square	DF	Pr > ChiSq
6	9999.99	6	<.0001	1264.17	6	<.0001	9999.99	6	<.0001
12	9999.99	12	<.0001	1489.48	12	<.0001	9999.99	12	<.0001
18	9999.99	18	<.0001	1549.4	18	<.0001	9999.99	18	<.0001
24	9999.99	24	<.0001	9999.99	24	<.0001	9999.99	24	<.0001
30	9999.99	30	<.0001	9999.99	30	<.0001	9999.99	30	<.0001
36	9999.99	36	<.0001	9999.99	36	<.0001	9999.99	36	<.0001
42	9999.99	42	<.0001	9999.99	42	<.0001	9999.99	42	<.0001
48	9999.99	48	<.0001	9999.99	48	<.0001	9999.99	48	<.0001

3. Third, we use the associated Autocorrelation function (ACF), Partial autocorrelation function (PACF) and the Inverse autocorrelation function (IACF) plots to determine order of autoregressive (p) and moving average terms (q). However, no clear patterns are evident for all three cooperatives.

4. Therefore, next we utilize the Extended Sample Autocorrelation Function (ESACF) and the Minimum Information Criterion (MINIC) procedures in SAS's PROC ARIMA to tentatively identify potential p and q values. While the ESACF method can tentatively identify the orders of an ARMA process based on iterated least squares estimates of the autoregressive parameters, the MINIC method is based on selecting an autoregressive order that minimizes the Akaike information criterion (AIC). AIC is calculated by the following formula:

$$AIC = n\ln(MSE) + 2k \tag{3.4.2}$$

where MSE is the Mean Squared Error, n is the model sample size and k is the number of parameters. However ARMA models fit to the residual series based on outputs from these procedures fail to pass the test for white noise. This means that the error terms generated after fitting an ARMA model to the residual series are autocorrelated. In simpler terms this implies that since these errors still hold explanatory power, the fit of the ARMA model is poor. We observe that the values of the Ljung-Box Chi-square statistics remain very large and highly significant (with p values <0.0001). Results from the Godfrey-Lagrange multiplier test for serial autocorrelation (Appendix B) further support these findings. Leamer (1978) argues that this may be due to the large sample size of our study. He states that the null hypothesis is more frequently rejected in large samples than in small because as the sample size increases, discrepancies in estimates, that were undetectable in smaller samples, get magnified in larger ones. Therefore it is possible that we may be rejecting the null hypothesis of the white noise test when in reality the error series are white noise. However, since we repeatedly reject the null hypothesis, we must look towards models that can at least significantly diminish autocorrelations between the errors.

5. Keeping this discussion in mind, we select an alternative modeling technique for the residual series which can account for the remaining seasonality from the hourly load data. We utilize the following multiplicative seasonal ARIMA model presented by Hagan and Behr (1987):

$$(1 - a_1 L^1 - a_2 L^2)(1 - a_{168} L^{168})\, r_t = (1 + b_{24} L^{24} + b_{48} L^{48})\varepsilon_t \qquad (3.4.3)$$

Here r_t is the residual series, ε_t is the random error and L^t refers to the lag operator such that $L^p r_t = r_{t-p}$. a_1, a_2, a_{168} , b_{24} and b_{48} are parameters to be estimated. This model was selected because it reduces the Ljung-Box Chi-square statistics and the associated residual series autocorrelations (shown by Table 5, 6 and 7). This is due to the rich interaction pattern between the autoregressive and moving average terms, which is captured with a small number of coefficients. The major limitation of such a model is that since the estimates of the AR and MA coefficients are interrelated, we can expect a larger error sum of squares than if the coefficient restrictions were not applied (Enders, 2004).

Table 5: Ljung-Box Test Results for Trico with multiplicative seasonal ARIMA residuals

To Lag	Chi-Square	DF	Pr > ChiSq	Autocorrelations					
6	1314.76	1	<.0001	-0.007	0.039	-0.065	-0.015	-0.055	-0.059
12	2795.6	7	<.0001	-0.078	-0.074	-0.028	-0.037	-0.012	-0.018
18	3489	13	<.0001	-0.022	-0.036	-0.048	-0.023	-0.042	-0.013
24	5086.44	19	<.0001	-0.001	0.004	0.022	0.012	0.120	0.009
30	7107.89	25	<.0001	0.133	-0.011	0.011	-0.023	0.000	-0.029
36	7309.55	31	<.0001	-0.021	-0.029	-0.015	0.002	-0.018	-0.008
42	7714.81	37	<.0001	-0.027	-0.023	-0.042	-0.027	-0.011	-0.004
48	8154.69	43	<.0001	0.012	0.005	0.039	0.036	0.011	0.034

Table 6: Ljung-Box Test Results for Graham with multiplicative seasonal ARIMA residuals

To Lag	Chi-Square	DF	Pr > ChiSq	Autocorrelations					
6	426.98	1	<.0001	0.000	-0.002	-0.014	-0.032	-0.036	-0.040
12	1601.71	7	<.0001	-0.055	-0.056	-0.041	-0.043	-0.030	-0.025
18	2340.81	13	<.0001	-0.037	-0.035	-0.041	-0.040	-0.030	-0.014
24	3568.11	19	<.0001	0.003	0.012	0.025	0.044	0.094	0.001
30	4455.58	25	<.0001	0.078	0.028	0.001	-0.010	-0.022	-0.031
36	4657.55	31	<.0001	-0.030	-0.024	-0.016	-0.009	-0.007	-0.008
42	4790.96	37	<.0001	-0.017	-0.021	-0.018	-0.013	-0.005	0.004
48	4970.91	43	<.0001	0.007	0.015	0.021	0.027	0.017	0.003

Table 7: Ljung-Box Test Results for Mohave with multiplicative seasonal ARIMA residuals

To Lag	Chi-Square	DF	Pr > ChiSq	Autocorrelations					
6	491.56	1	<.0001	-0.002	0.010	-0.024	0.016	-0.034	-0.051
12	2356.84	7	<.0001	-0.081	-0.048	-0.053	-0.048	-0.047	-0.039
18	3393.04	13	<.0001	-0.047	-0.057	-0.046	-0.039	-0.025	-0.011
24	5144.85	19	<.0001	0.012	0.022	0.047	0.048	0.107	0.005
30	6269.64	25	<.0001	0.093	0.026	0.016	-0.001	-0.014	-0.030
36	6604.03	31	<.0001	-0.030	-0.028	-0.014	-0.022	-0.022	-0.018
42	6987.63	37	<.0001	-0.022	-0.032	-0.039	-0.021	-0.012	-0.003
48	7519.18	43	<.0001	0.005	0.018	0.033	0.045	0.031	0.024

Therefore, our final model for hourly load forecasting is given by the following equation:

$$\Delta^1 \Delta^{24} \ln(Load_t) = \sum_{i=1}^{j} \beta_t X_{it} + r_t \qquad (3.4.5)$$

where the residual series is modeled as $r_t = \frac{(1+b_{24}L^{24}+b_{48}L^{48})}{(1-a_1L^1-a_2L^2)(1-a_{168}L^{168})}\varepsilon_t$, j refers to number of input series variables and X_{it} refers to weather and seasonal dummy variables in the transfer function.

CHAPTER 4 Monthly Load Forecasting Model

4.1 Data Description

This component of our study involves creating a medium-term time series model for predicting monthly electricity load in the Tucson MSA. The load data consisted of hourly measurements of total electricity provided by the Tucson Electric Power (TEP) company for the time period of 10 years, starting January 2000 and ending December 2009. It was converted to monthly averages for the purposes of this model. Similar confidentiality restrictions applies to the TEP load data as in case of the AEPCO load data used for the short-term models.

The Tucson Electric Power Company (TEP) is a publicly held utility engaged in the generation, purchase, transmission, distribution, and sale of electricity to customers in Tucson, Arizona, and the surrounding area. Its service area roughly covers most of the Tucson MSA, including some of the operating copper mines in the region. It must be noted that for the monthly load forecasting model, we used Tucson MSA data and Pima County data interchangeably since Tucson MSA geographically coincides with Pima County.

To control for seasonality we used both weather and socio-economic explanatory variables. Monthly average measurements for temperature, precipitation, relative humidity, solar radiation and wind speed data were available from the Arizona Meteorological Network (AZMET). Socio-economic data was acquired from a variety of sources. While U.S. Census annual population estimates were used, they were supplemented with 1999 estimates from the Arizona Department of Economic Security. Monthly population estimates were constructed using traffic count data from the Pima County Department of Transportation. Copper mine production data was obtained from the Arizona Department of Mines and Mineral Resources (AZDMMR) and from the U.S. Geological Survey (USGS) .Finally, annual per capita income data was sourced from the U.S. Department of Commerce and the University of Arizona Economic and Business Research Center. Table 8 shows the summary statistics for the different key variables included in our model.

Table 8: Summary Statistics for the Monthly Load Forecasting Model

Variable	Units	Mean	Std Dev	Minimum	Maximum
Load	MW	1,099.68	213.66	818.47	1,593.08
Temp	° F	68.23	13.86	46.00	89.00
Precip	mm	0.03	0.04	0.00	0.18
RH	%	40.61	13.12	16.00	69.00
Windspd	m/s	4.11	0.65	2.50	5.50
SolRad	MJ/m^2	482.39	143.99	247.00	754.00
Cuprod	Metric ton	12,005.58	2,880.45	7,640.32	17,913.83
PCY	$/person	29,708.63	3,494.60	24,885.50	34,058.00
Popnch	Change in number of Persons	1,095.28	1,538.53	-3,570.76	2,297.63

T=120

4.2 Model Variables

4.2.1 Dependent Variable

The dependent variable for our model is average monthly measurements of TEP electricity load for the Tucson MSA region, obtained from averaging load values measured at the hourly level for each month. In effect the dependent variable is a representative value of the average hourly load during a particular month of a specific year. This variable behaves in a manner consistent with our rationale used in the short-term load forecasting models. Figure 6 shows that average monthly load exhibits considerable seasonality and has a gradually increasing trend. As explained in Chapter 3, the seasonality at the monthly level is explained by the close relationship between electricity load and seasonal weather conditions. As shown previously for the AEPCO data, TEP load data shows similar peaks during the monsoon months of July and August, and relative troughs during the rest of the year.

Figure 6: Average Monthly Load for TEP (2000-2009)

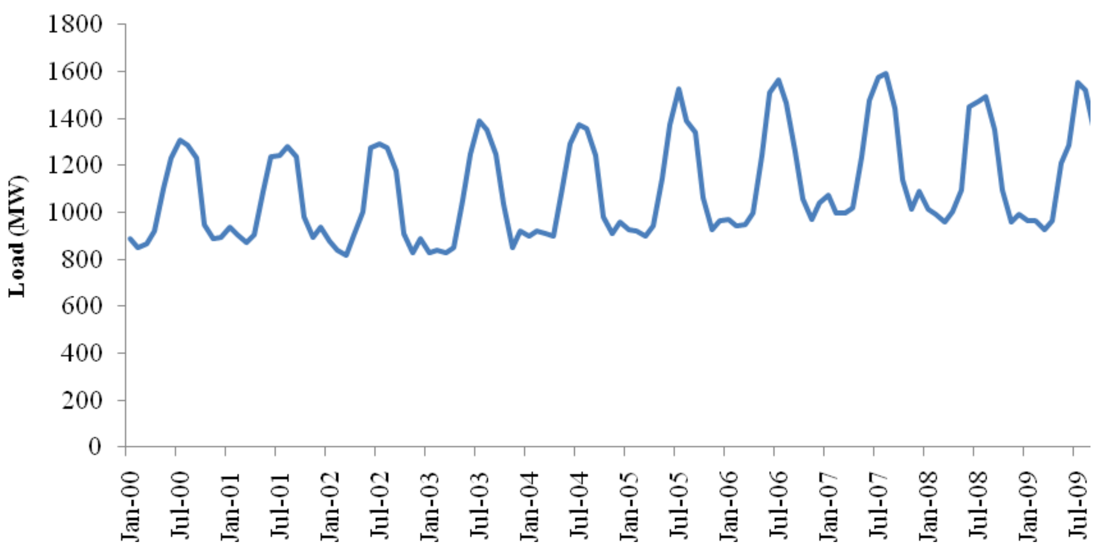

4.2.2 Explanatory Variables:

In order to adapt medium-term load forecasting models to climate change, we needed to include weather data as some of our explanatory variables. Therefore similar to the short-term load forecasting models, our medium-term model included the following weather variables:

- **Temperature (Temp):** To model non-linearity of the relationship between load and temperature, we included a linear term (Temp), a squared term (Sqtemp) and interaction variable with wind speed (Int2).
- **Precipitation (Precip):** Unlike the hourly measurements of precipitation, which suffered from very minute magnitudes, monthly average precipitation measurements were found to be more substantial.
- **Relative humidity (RH)**
- **Solar radiation (Solrad)**
- **Wind speed (Windspd)**

Based on our previous analysis of the impact of weather on electric load, we had similar expectations for the signs associated with each of weather variable coefficients. To account for the seasonality displayed by monthly load, we include the following socio-economic variables in our analysis:

- **Change in monthly population (Popnch):** Since population increases are generally associated with increase in electricity consumption by households, associated businesses and infrastructure, we expect the monthly population variable to have a positive coefficient. In Tucson, monthly population shows significant variation over the calendar year due to the departure of college students in the summer and the arrival of vacationers during the mild winter months. However, the annual U.S. Census estimates were unable to capture this phenomenon adequately. Therefore, as part of this study, a monthly population estimate was created utilizing traffic count data for Pima County. The underlying assumption of this new monthly estimate is that variations in traffic count are directly related to changes in the population, i.e., an increase in traffic count implies an increase in population.

The U.S. Census provides a snapshot of the population at a particular point of time, indicated as July 1st of the respective year. This date is selected for the convenience of governmental agencies and congressional activities. However, for the purposes of this study we assume that the annual population estimates provided by the U.S. Census, are beginning-of-year estimates, thereby reflecting total change over a calendar year. This assumption was necessary due to the significant lack of reliable beginning-of-year population estimates and mathematical convenience in constructing the estimates.

Average monthly traffic count data for six critical traffic intersections was selected based on geographical location and data availability (Refer to Appendix C). These traffic count values had been adjusted for the number of days in each month through averaging. The following formula was utilized to estimate population for month j in year t:

$$Popn_i = Popn_{i-1} + \left[\frac{TC_{j,t}}{\sum_{j=1}^{12} TC_{j,t}} \times (CenPopn_{t+1} - CenPopn_t)\right] \qquad (4.2.2)$$

where j = 1, 2,….12 refers to months of the year t = 1,2,…..10 refers to years starting 2000 to 2009

i = 1, 2,….120 refers to the total number of sample observation multiplying, given by i = j x t

TCj = Average Traffic Count for month j

$CenPopn_t$ = Annual Census Population estimate for year t

- **Per Capita Income (PCY):** It is expected that an increase in per capita income leads to increased purchase and utilization of a varied range of power-consuming appliances. Therefore, the coefficient associated with a linear term is expected to be positive. Annual per capita income data was obtained from the US Census. This data was scaled down to the monthly level, assuming equal incremental increases in per capita income from month to month.

- **Copper Mine production (Cuprod):** Due to confidentiality issues, the actual composition of the TEP load data was not disclosed. However based on general information regarding TEP's clientele, it was evident that TEP provides electricity to three major copper mines in the region, namely, Mission Complex, Sierrita and Silver Bell mines. Therefore, in lieu of specific data on electricity used by each mine, this study included total copper mine production data from the Arizona Department of Mines and Mineral Resources (AZDMMR) for these three mines. Since this data was annual, monthly data was obtained through extrapolation based on newspaper reports related to strikes and shutdowns at each of the mines. This allowed for sufficient month to month variation in this variable. It is expected that the associated coefficient displays a positive coefficient.

Table 9 shows the expected signs of coefficients associated with the model variables.

Table 9: Expected Signs of Coefficients for Monthly model

Variable	Description	Expected Sign
Temp	Temperature	Negative
$Temp^2$	$Temperature^2$	Positive
RH	Relative humidity	Negative
Solrad	Solar radiation	Positive
Precip	Precipitation	Negative
Windspd	Wind speed	Positive
PCY	Per capita income	Positive
Popnch	Population change	Positive
Cuprod	Copper mine production	Positive
Int2	Temp*Windspd	Negative

T=120

4.3 Model Estimation

In order to estimate the monthly load forecasting model using Ordinary Least Squares (OLS), it was necessary to confirm that the errors were spherical, i.e., errors were homoskedastic and are not correlated with each other. Therefore, next the data was tested for heteroskedasticity and autocorrelation.

The data was analyzed for heteroskedasticity using the White's test. It was evident from this test statistic that we failed to reject the null hypothesis of homoskedasticity (Refer to Table 10). These findings were further supported by the Breusch-Pagan test. This implies that there was no heteroskedasticity.

Table 10: Tests of Heteroskedasticity

Test	Test Statistic	DF	Pr > ChiSq
White's Test	74.53	62	0.1322
Breusch-Pagan	13.91	11	0.1769

However, based on the highly significant Durbin-Watson test statistic of 0.8947 (Refer to Table 11); it was evident that the errors exhibited autocorrelation since the null hypothesis of no autocorrelation was rejected. These findings were further supported by the Godfrey-Lagrange multiplier test (Refer to Table 12) where the null hypothesis of uncorrelated residuals was rejected. This was anticipated not only because the model is based on a time series, but also because weather variables are expected to be highly correlated with each other.

Table 11: Durbin Watson Test for Autocorrelation

Order	Durbin-Watson	Pr < DW	Pr > DW
1	0.8947	<.0001	1

Table 12: Godfrey-Lagrange Multiplier Test for Autocorrelation

Equation	Alternative	LM	Pr > LM
Load	1	35.50	<.0001
	2	35.50	<.0001
	3	38.24	<.0001
	4	38.24	<.0001

Due to the presence of autocorrelation, OLS could no longer be utilized for estimating this model. This is because the calculated OLS estimates would have been inefficient. Therefore we utilized Feasible Generalized Least Squares (FGLS), as opposed to OLS, for estimating a monthly load forecasting model with autoregressive terms.

CHAPTER 5 Analysis of Results

The purpose of our study is to construct hourly and monthly load forecasting models which generate improved load forecasts as compared to the load forecasting techniques commonly used by electric utilities. As explained in the previous chapters, we attempt to specifically examine the effects of incorporating weather variables and seasonality indicators in the generally used purely autoregressive and ARIMA models.

In this chapter, we first describe the criteria used to evaluate the performance of the new load forecasting models, followed by results related to the specific models and a brief discussion on the significance of the coefficient estimates in each of the models. Finally, we generate forecasts for the next model year based on two theoretical climate change scenarios.

5.1 Criteria for Evaluating Load Forecasting Models

Murphy (1993) recognized three 3 types of "goodness" of forecasts, namely, consistency, quality and economic value.

- **Consistency:** A forecast is said to be consistent if it corresponds to the forecaster's best judgment derived from his/her knowledge base (Murphy, 1993). In this study we achieve this through an in-depth literature review to inform our expectations regarding the signs of our model coefficients. We check the consistency of our load forecasts by determining if the estimated coefficients of our load forecasting models were consistent with our expectations stated in Chapter 4. Models conforming to our expectations are considered more consistent.

- **Quality:** If the forecast corresponds closely to the observed values at (or during) the valid time of the forecast, it is generally considered to be of superior quality. This has been the primary focus of most forecasting studies, often calculated using measures of mean absolute error, the mean-square error and various skill scores. Keeping in mind the key parties involved in load forecasting, the electricity industry and the forecasters, we utilize two familiar measures of forecast quality, Mean Absolute Percentage Error (MAPE) for the former and Root Mean Squared Error (RMSE) for the latter. MAPE is given by the following formula:

$$MAPE = \frac{1}{T}\sum_{t=1}^{T}\left|\frac{A_t - F_t}{A_t}\right| \tag{5.1.1}$$

where A_t is the actual value, F_t is the forecast and T is the size of forecasting sample. This measure of error is comparable across different models since it is unitless. It also assigns equal weights, in absolute terms, to both positive and negative errors. It must be noted that MAPE will be undefined when the actual value is zero. However, this is not a significant concern since electricity load data in our study does not include zero values.

Another relevant measure of error is the Root Mean Squared Error (RMSE). It is calculated by the following formula:

$$RMSE = \sqrt{\frac{1}{T}\sum_{t=1}^{T}(A_t - F_t)^2} \tag{5.1.2}$$

Since errors are squared, giving greater weight to large errors, the RMSE is very sensitive to the presence of large magnitudes of errors. Another key difference between MAPE and RMSE is the fact that RMSE across models can only be compared if they are measured in the same units.

Both MAPE and RMSE are well-known single measures of predictive power which move in tandem i.e. a ‘good’ (or ‘bad’) model will perform well (or ‘poorly’) in terms of both MAPE and RMSE.

In addition to MAPE and RMSE, we also report the Peak Load Error as a percentage. This measure further illustrates the quality of forecasts generated by our models. in term of its accuracy in predicting the peak load during the given forecasting time period. It is calculated by the following formula:

$$Peak\ Load\ Error\ \% = \left(\frac{Actual\ Peak\ Load - Forecasted\ Peak\ Load}{Actual\ Peak\ Load}\right) \times 100 \tag{5.1.3}$$

- **Economic Value:** Forecasts are said to have economic value is there are incremental economic and/or other benefits realized by decision makers through the use of the forecasts. Electric utilities experience cost savings through the use of more accurate forecasts, by avoiding scenarios of over and underproduction. Using International Energy Agency (IEA) estimates of costs of production under different generation technologies, we are able to provide reasonable estimates of these cost savings. Other benefits from using forecasts which perform better on the last two criteria include improved capacity planning and operational efficiency. While there are other policy implications and social benefits of using ‘good’ forecasts, we discuss them further in the next chapter.

Therefore, we use these three approaches to evaluate the overall performance of our load forecasting models.

Due to the absence of additional load data for evaluating forecasts, accuracy of our model forecasts was tested through the use of 'hold-out' samples. With this technique, the time period of the load data used to fit the models ends before the end of the data series. The remainder of the load data is retained as a period of evaluation. Therefore, with respect to the 'fit'period, the hold-out sample is a period in the future, used to compare the forecasting accuracy of the models fit to past data. This 'hold-out' sample approach can be further illustrated using an example. For instance, for the Trico hourly model we first determine the peak load days during the dry-summer and the monsoon seasons of 2004. Next, we estimate our model parameters by fitting the model only to the available data up till the midnight of the day before the peak load day of the respective season. Finally, using these model parameters and actual weather data for the peak load days, we forecast load for the entire 24 hours of the peak load day. Therefore we forecast out-of-sample for a single day i.e., the peak load day that occurs during the dry-summer season (from May to June 2004) and for another peak load day in the monsoon season (from July to August 2004) of 2004.

As shown in the previous chapter, our study regions display their annual peak loads during the dry-summer and monsoon seasons. Given the importance of annual peak loads for capital investment and supply reliability, electric utilities are particularly interested in forecasting the summer peak load values. Consequently we focus on forecasting 24 hour load values for the peak load days of the two summer seasons of 2004. .

For the monthly model, we utilize the hold-out sample approach by keeping the year 2009 as our hold-out sample, and fitting our forecasting model to data up till December 2008.

We acknowledge that the use of actual weather data, as opposed to daily or seasonal weather forecasts, may overestimate the accuracy of our models. The hold-out sample approach described above assumes perfect knowledge of weather events. In reality, next-day or next-month weather forecasts are utilized by electric utilities. Therefore, the quality of weather forecasts utilized in forecasting is also an issue to be taken into consideration. However, for the purposes of this study we use actual weather data as opposed to forecasts. Future work based on this study can investigate the use of weather forecasts in load forecasting.

In order to study the implications of the load forecasts in light of the changing climate, we generate forecasts for a year based on two theoretical climate scenarios:

1. **Simple Change Scenario:** In this scenario, following up on the most likely impact of climate change in the Southwest (Dominguez et. al.,2010) temperature is increased at the rate of 3.52 ° C (or 6.33 °F) per month as compared to the identical month in the previous year. However, precipitation is diminished by 10 percent every month as compared to the previous year.

2. **More Intense Summer Shift (MISS) Scenario:** This scenario assumes a 50 percent decline in monsoon precipitation and warmer temperatures during the summer months from May to August (specifically an increase of 4 ° C or 7.2 °F) and a general increase in temperature by 2.5° C (or 4.5 °F) for the rest of the year.

It must be noted that in both the scenarios, all other factors are held constant.

5.2 Hourly Load Forecasting Models

As shown in Chapter 3, we estimate three hourly load forecasting models using dynamic regression model with seasonal multiplicative ARMA errors. We evaluate the forecasting performance of each of our models, referred to as ‘Full’ models, with the forecasting performance of the ‘No Weather’ models. As the name suggests, the latter models do not include any weather variables, including only autoregressive and moving average terms along with dummies for the work hours of the day (peakhr), weekend, seasons (drysummer, monssummer, fall and spring) and holidays (hol).

Table 13, Table 14 and Table 15 show the hourly model coefficient estimates with their associated standard deviations for the three AEPCO cooperatives, Trico, Graham and Mohave, respectively. It must be noted that since the dependent variable is the log of hourly load, the coefficient and standard errors cannot be easily interpreted with regard to their magnitude.

While both temperature coefficients are statistically significant, they have the opposite signs from what was expected. This means that the temperature coefficient has a negative coefficient and the squared temperature coefficient has a positive coefficient. This is a puzzling phenomenon which merits further investigation regarding the nature of hourly temperature for these three regions in Arizona.

The humidity coefficients are also significant. The linear term has a positive coefficient, while the coefficient of the interaction term with temperature (int1) is negative. Therefore the signs of these coefficients also do not match our expectations.

Solar radiation is significant at the 0.001 level and displays a positive coefficient. This implies that the theory that solar radiation is affects electricity consumption by raising the ambient temperature holds for all three service regions of Trico, Graham and Mohave.

The dummy variable for precipitation (precipdum) is not significant for all three regions. It must be noted that this might be due to the large number of zero values for this variable.

Wind speed is significant at the 0.01 level only for the Tucson MSA region. It has a negative coefficient, which does not meet our expectations. Its interaction term with temperature is highly significant and has the expected negative sign for Mohave alone. Mohave, in general, experiences the fastest blowing winds of all the three regions included in our study. This may serve to increase the impact of wind speed on electricity load for only the Mohave service area.

Except for Mohave, Trico and Graham have highly significant and negative coefficients for the interaction term between precipitation and temperature (int3). This may imply that for these two regions the cooling effect of precipitation is significant enough to inversely affect electric load.

The peak hours of the day dummy (peakhr) is only significant for Mohave, and has an unexpected negative sign. This implies that from 8 am to 8 pm in a day, consumers in the Mohave service region use less electricity than during the early mornings and late nights. This is highly counter-intuitive, and therefore merits further study. One possible explanation of this result is the presence of a major electricity user in Mohave who primarily utilizes electricity during the night. However since we do not have information regarding specific AEPCO customers in this region, at present this claim cannot be verified.

The weekend dummy is significant at the 0.001 level for Trico and Mohave alone. It also exhibits the expected negative sign, implying that consumers in these regions consume less electricity during the weekends, as compared to the rest of the week.

We also included dummy variables for the five seasons in the state of Arizona, taking winter as the baseline. None of these seasonal dummies were significant throughout the sample. This may imply that they might have failed to capture the impact of seasonal changes on electricity load.

The dummy variable for holidays is also not significant for all three of the AEPCO service areas. Therefore it is still unclear whether the incidence of holidays increases or decreases electricity load.

Table 13: Trico Hourly Model Maximum Likelihood Estimates

	Full Model		No Weather Model	
Parameter	Estimate	Std. Error	Estimate	Std. Error
Intercept	-0.0001165	0.0003015	0.0004322***	0.0001224
MA(24)	0.67438***	0.0030698	0.67446***	0.0030696
MA(48)	0.20304***	0.0030372	0.20202***	0.003035
AR(1)	0.50786***	0.0031047	0.50894***	0.0031041
AR(2)	-0.08274***	0.0031147	-0.08302***	0.0031137
AR(168)	0.32566***	0.0030539	0.32563***	0.0030536
Temp	0.00007757***	0.00002002		
Sqtemp	-0.00000137***	3.55E-07		
RH	0.00001258***	3.18E-06		
SolRad	0.0001585***	0.00002651		
Precipdum	0.00079	0.0004302		
Windspd	-0.0002008**	0.00006829		
Int1	-0.000000742***	1.75E-07		
Int2	0.00000102	2.83E-06		
Int3	-0.0000285***	5.46E-06		
Peakhr	-0.000045	0.00004642	-7.3481E-08	3.444E-05
Weekend	-0.0015027***	0.0003779	-0.0015044***	0.0003784
Spring	-0.0000202	0.00007474	3.03713E-06	0.0000697
Drysummer	-0.0000539	0.0001019	3.23715E-06	7.429E-05
Monssummer	0.0001695	0.0001311	-4.3518E-06	7.397E-05
Fall	0.00000885	0.00008618	0.00001283	6.873E-05
Hol	-0.0005587	0.0006193	-0.0004829	0.0006154

Significance Levels *=0.05 **=0.01 ***=0.001

Table 14: Graham Hourly Model Maximum Likelihood Estimates

	Full Model		No Weather Model	
Parameter	Estimate	Std Error	Estimate	Std Error
Intercept	-0.0001492	0.0001873	0.0001149	8.4E-05
MA(24)	0.79004***	0.0030917	0.79081***	0.00309
MA(48)	0.09507***	0.0030855	0.09398***	0.00308
AR(1)	0.0094457**	0.003103	0.01094***	0.0031
AR(2)	-0.06222***	0.0030837	-0.06224***	0.00308
AR(168)	0.15757***	0.0031478	0.15707***	0.00315
Temp	0.00003905**	0.0000124		
Sqtemp	-0.00000060292**	2.42E-07		
RH	0.00000696252***	2.08E-06		
SolRad	0.00009296***	0.00001962		
Precipdum	0.0008743	0.0005767		
Windspd	-0.0000863	0.00005399		
Int1	-0.00000037312**	1.31E-07		
Int2	-6.285E-07	2.29E-06		
Int3	-0.0000865***	9.23E-06		
Peakhr	-0.0000456	0.00004683	-3.7861E-06	2.7E-05
Weekend	-0.0004277	0.0002579	-0.0004171	0.00026
Spring	-2.807E-06	0.00005454	8.57337E-06	4.8E-05
Drysummer	-0.0000432	0.00007987	6.86651E-06	5E-05
Monssummer	0.00003952	0.0001004	-6.7969E-06	0.00005
Fall	-0.000045	0.00006439	0.00001512	4.7E-05
Hol	-0.0001768	0.000512	0.00002949	0.0005

Significance Levels *=0.05 **=0.01 ***=0.001

Table 15: Mohave Hourly Model Maximum Likelihood Estimates

	Full Model		No Weather Model	
Parameter	Estimate	Std Error	Estimate	Std Error
Intercept	-0.0006131*	0.0002794	0.0003319***	8.67E-05
MA(24)	0.67324***	0.0030782	0.67336***	0.003077
MA(48)	0.15382***	0.0030633	0.15389***	0.003062
AR(1)	0.47516***	0.00309	0.47616***	0.00309
AR(2)	-0.0812***	0.0030858	-0.08101***	0.003085
AR(168)	0.14763***	0.0031273	0.14741***	0.003128
Temp	0.00009776***	0.00001886		
Sqtemp	-0.000001225***	2.85E-07		
RH	0.00001589***	3.41E-06		
SolRad	0.0001921***	0.00002625		
Precipdum	-0.0003892	0.0004525		
Windspd	0.00002981	0.00005315		
Int1	-0.0000011435***	1.84E-07		
Int2	-0.0000073768**	2.37E-06		
Int3	-9.0233E-06	8.75E-06		
Peakhr	-0.0000997*	0.00004423	1.18839E-06	3.28E-05
Weekend	-0.0011562***	0.0002405	-0.0011483***	0.000241
Spring	-0.0000668	0.00007245	4.19253E-07	6.37E-05
Drysummer	-0.0000791	0.00009871	4.11565E-06	6.82E-05
Monssummer	0.0001969	0.0001221	-0.000014	6.79E-05
Fall	-0.0000287	0.00008167	7.86876E-06	6.28E-05
Hol	-0.0005779	0.0005534	-0.0003758	0.00055

Significance Levels *=0.05 **=0.01 ***=0.001

The signs of the coefficients explain only part of the relationship between the dependent variable (i.e., hourly load) and the explanatory variables (specifically the weather variables) included the model. In order to fully comprehend the impact of the weather variables on hourly load, we need to study their marginal effects. In our study, marginal effects measure the expected instantaneous change in hourly load as a function of a change in a particular weather variable, holding all the other explanatory variables constant.

Marginal effects were calculated for each of the hourly models, but only for those weather variables which were found to be significant. Due to inherent complexity of the hourly models, marginal effects were estimated using the following steps:

1. First, we estimated the long term value of the dependent variable, i.e., the twice differenced natural log of hourly load (Z_t), using the following formula:

$$Long\ Term\ Value\ of\ Z_t\ =\left(\frac{\hat{\mu}+\sum_{i=1}^{16}\hat{\beta}_i\bar{X}_i}{1-\bar{\emptyset}_1-\bar{\emptyset}_2-\bar{\emptyset}_{168}}\right)$$

where i = 1, 2 ….16 is the number of explanatory variables and t= -168, -11,.., 0,..,1, 2, ,400 refers to a specific hour in a total time period of 569 hours. This time period occurred in January 2004, which was selected arbitrarily since the date selected is inconsequential in the calculation of marginal effects. $\widehat{\mu}$ is the intercept term estimate from the model results. $\widetilde{\emptyset_1}$, $\widetilde{\emptyset_2}$ and, $\widetilde{\emptyset_{168}}$ are estimated model coefficients for the AR (1), AR (2) and AR (168) terms, and $\hat{\beta}_i$ refers to model coefficient for explanatory variable X_i.

2. Next, we assume that the estimated value of the dependent variable ($\hat{Z}_t$) for the first 168 hours is equal to the long term value calculated in the previous step. The estimated value of the dependent variable for the remaining time periods (i.e., from t=0 to t=400) is calculated by the following formula at the mean values for the explanatory variables ($\bar{X}_i$):

$$\hat{Z}_t = \hat{\mu} + \widehat{\emptyset_1}\hat{Z}_{t-1} + \widehat{\emptyset_2}\hat{Z}_{t-2} + +\widehat{\emptyset_2}\hat{Z}_{t-168} + \sum_{i=1}^{16} \hat{\beta}_i(\bar{X}_i + S_{i,t})$$

where $S_{i,t}$ is the shock to significant explanatory variable X_i in time period t

3. In the above formula, we introduce a unit change (or unit shock) by increasing the initial value of the shock term($S_{i,0}$) by one (from zero) for variable X_i, whose marginal effect we are trying to estimate, holding all other variables constant at their respective means. The resulting $\widehat{Z}_t$ is recorded. Similarly a sustained shock is introduced by increasing all the shock values for an explanatory variable X_j by one, holding all other variables constant at their respective means. The $\widehat{Z}_t$calculated based on the sustained shock is also recorded.

4. Since we are interested in the marginal effect of the explanatory weather variables on hourly load (which is not our dependent variable), we use the following equation to obtain our estimated hourly load ($\widehat{Load_t}$) from $\widehat{Z}_t$ values under both the initial and sustained shock scenarios:

$$\widehat{Load}_t = e^{(\widehat{Z}_t + \ln(\widehat{Load})_{t-1} + \ln(\widehat{Load})_{t-24} - \ln(\widehat{Load})_{t-25})}$$

We do not adjust our estimation of estimated hourly load from the log values by using standard deviation values because the next step makes such an adjustment irrelevant. The $\ln(\widehat{Load})_{t-1}$, $\ln(\widehat{Load})_{t-24}$ and $\ln(\widehat{Load})_{t-25}$ values are estimated as the average of the logged values of hourly load for the first 168 hours (from t=-168 to t=-1) and using the following formula for the remaining time period (from t=0 to t=400):

$$\ln(\widehat{Load})_t = \widehat{Z}_t + \ln(\widehat{Load})_{t-1} + \ln(\widehat{Load})_{t-24} - \ln(\widehat{Load})_{t-25}$$

5. Finally, marginal effect of an explanatory variable on the hourly load is calculated as the difference between $\widehat{Load}_t$ after the introduction of the shock and $\widehat{Load}_t$ in the absence of shock. These are calculated for both scenarios i.e., one scenario where only the initial shock is introduced, and another scenario where the variable of interest suffers a sustained shock.

The estimated marginal effects of the relevant significant weather variables for Trico, Graham and Mohave are illustrated by Figures 7, 8 and 9, respectively. These figures show marginal effects for the entire selected time period of 400 hours. The tabulated results for all three AEPCO utilities are presented in Appendix I. It must be noted that while we have estimated marginal effects for the entire selected time period (i.e., 400 hours), for sake of brevity, we present our tabulated results only for the first 48 hours of our total time period.

Figure 7: Marginal Effects for Trico

(a) Temperature

Initial Shock

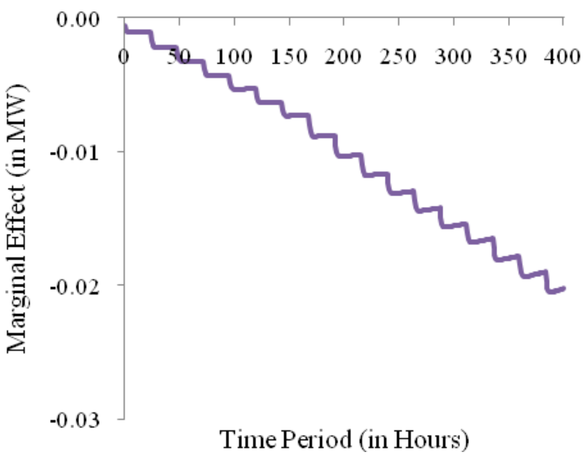

Sustained Shock

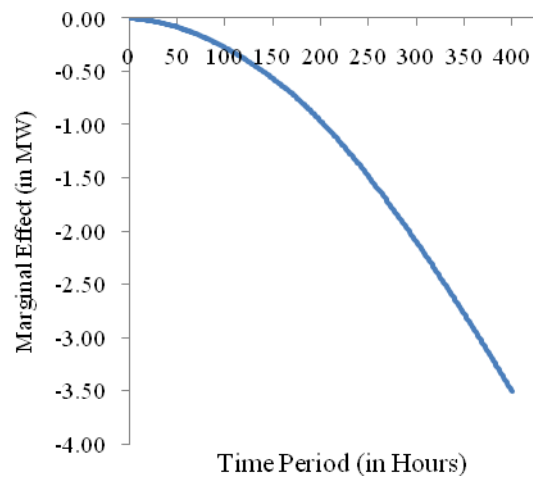

(b) Wind Speed

Initial Shock

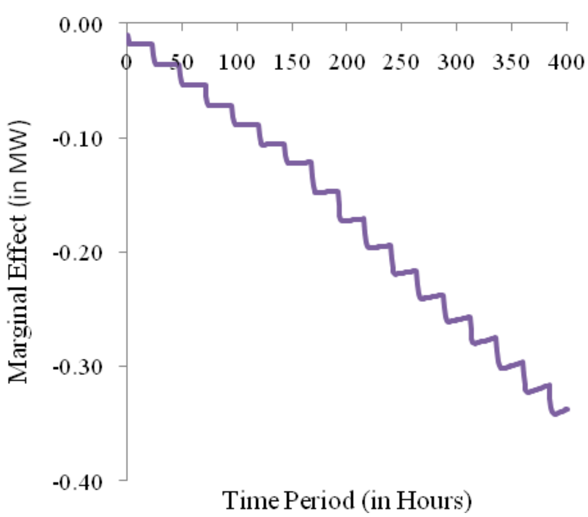

Sustained Shock

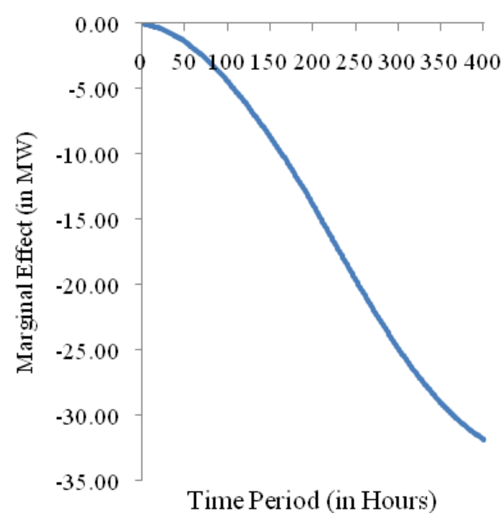

(c) Relative Humidity

Initial Shock

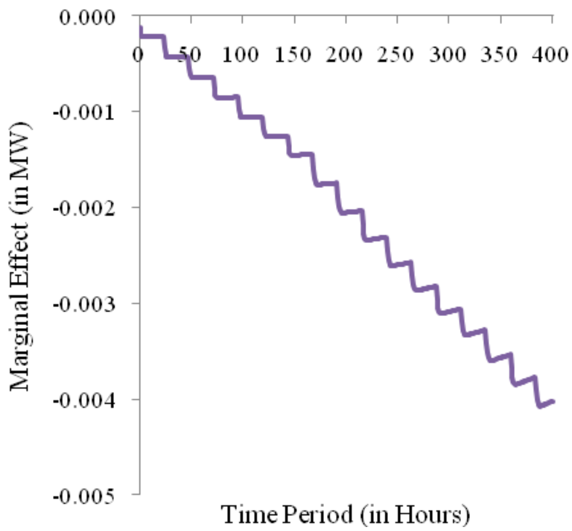

Sustained Shock

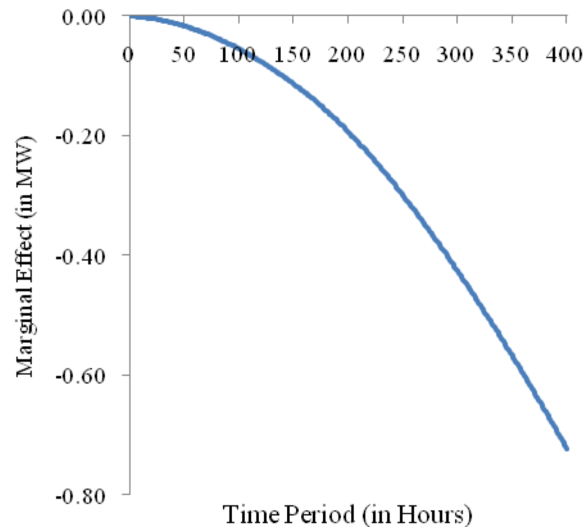

(d) Solar Radiation

Initial Shock

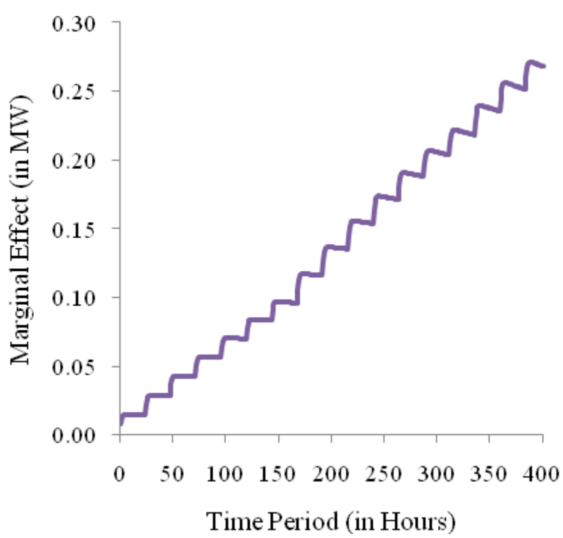

Sustained Shock

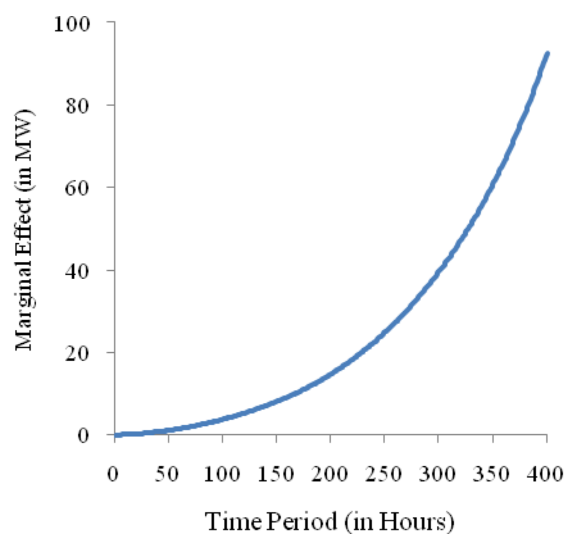

Figure 8: Marginal Effects for Graham

(a) Temperature

Initial Shock

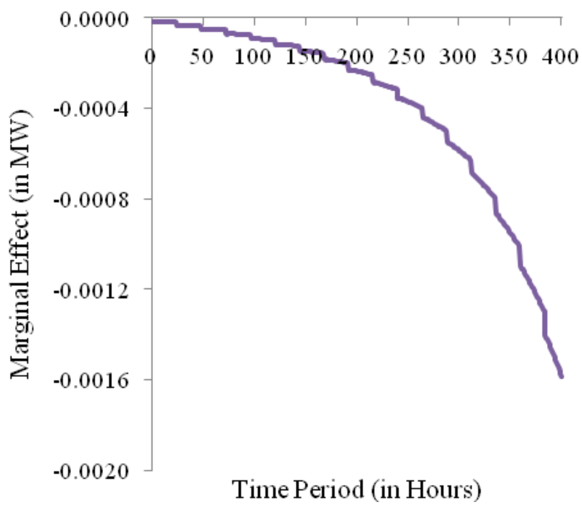

Sustained Shock

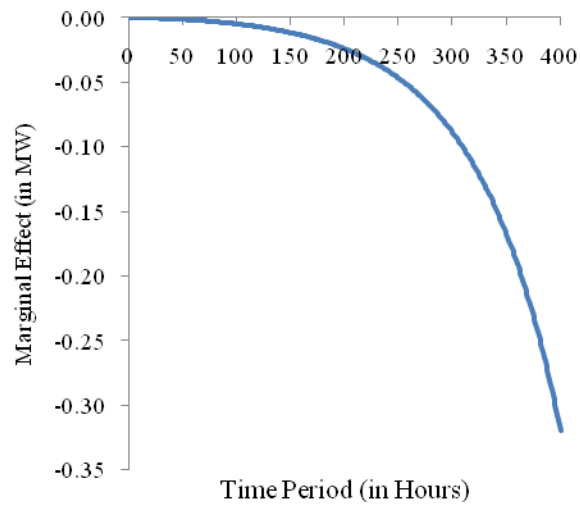

(b) Relative Humidity

Initial Shock

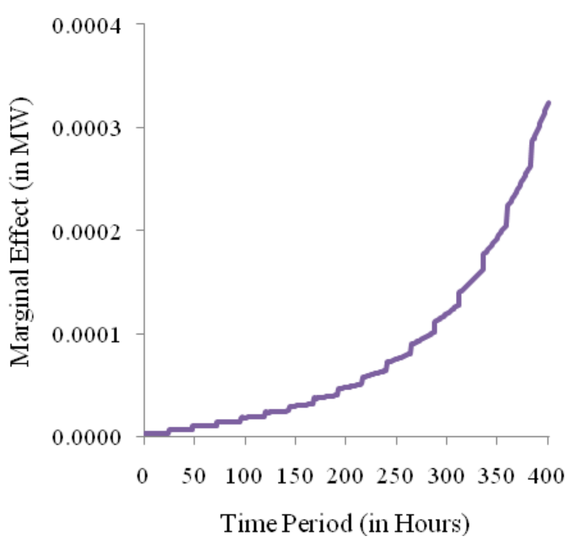

Sustained Shock

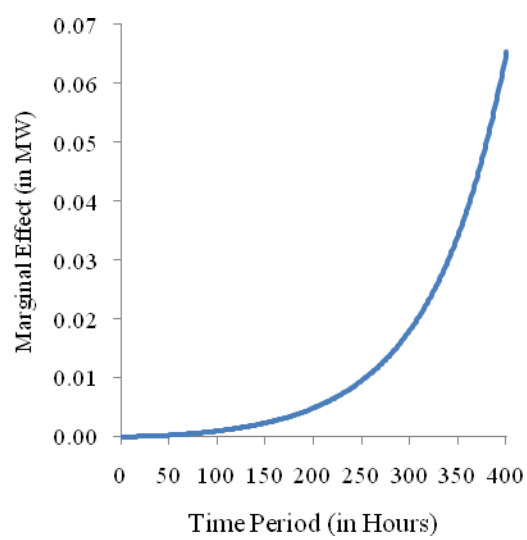

(c) Solar Radiation

Initial Shock

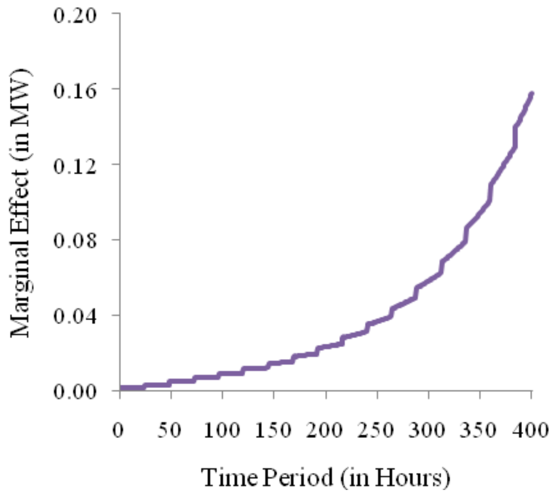

Sustained Shock

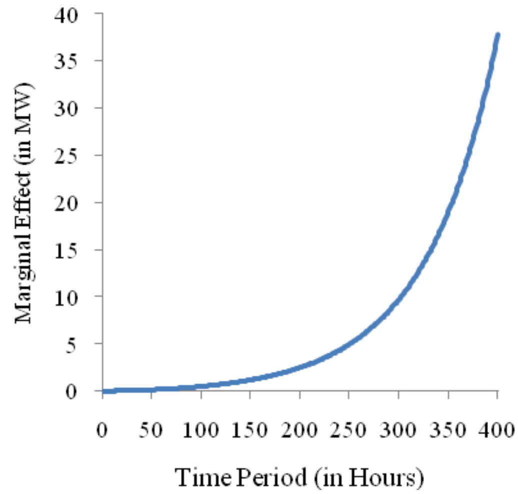

Figure 9: Marginal Effects for Mohave

(a) Temperature

Initial Shock

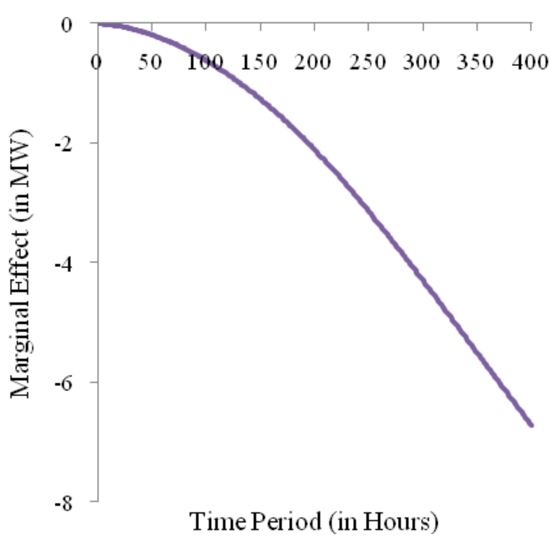

Sustained Shock

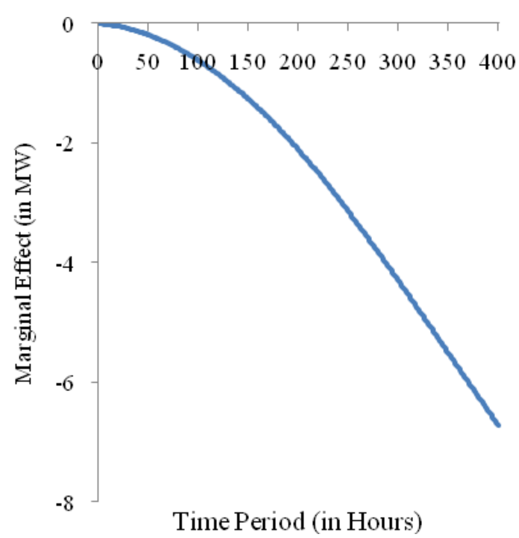

(b) Relative Humidity

Initial Shock

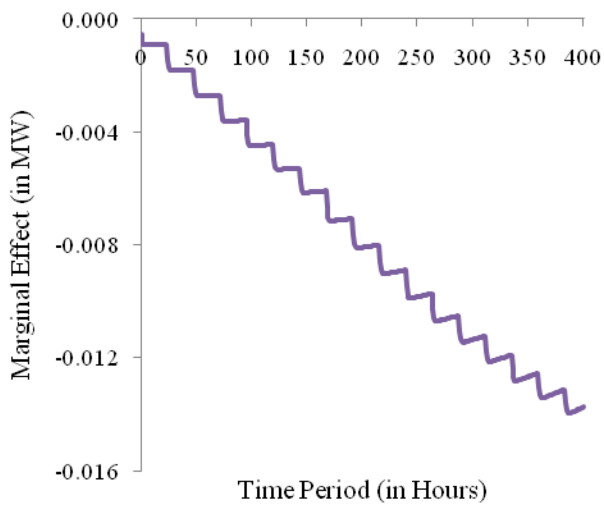

Sustained Shock

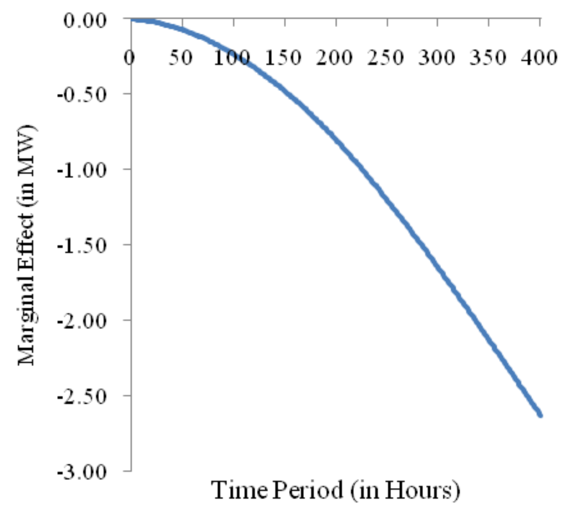

(c) Solar Radiation

Initial Shock

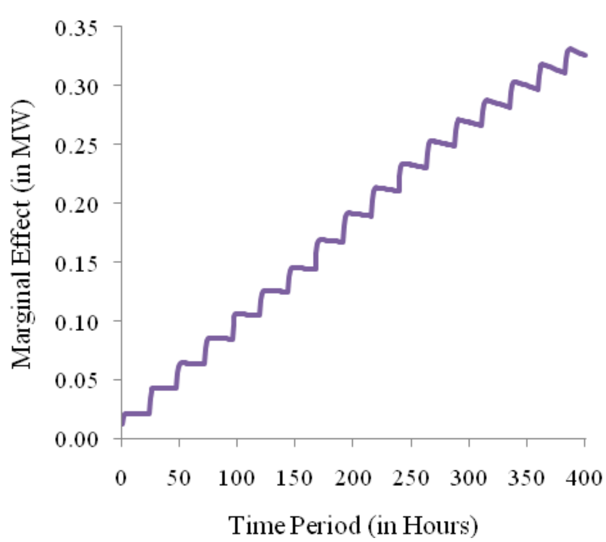

Sustained Shock

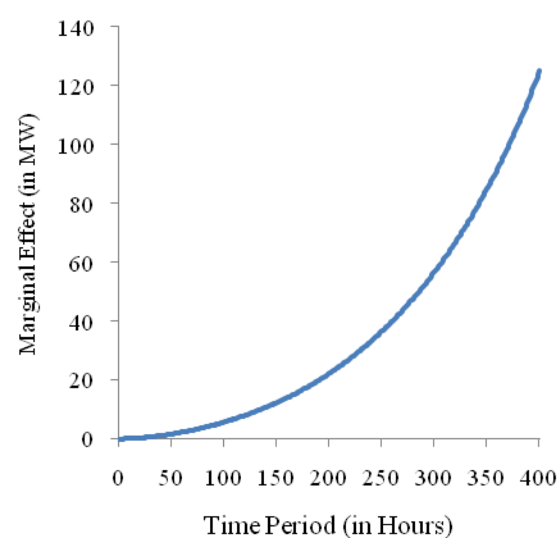

The marginal effects for all three AEPCO utilities reflect the non-stationarity of the original hourly load data. This is evident from the fact that neither of the marginal effects shows dampening over time. For example, for Trico, Graham and Mohave the marginal impact of a 1 °Fahrenheit increase in temperature decreases hourly load at an increasing rate over time, both in case of an initial shock or a sustained shock to temperature. As mentioned earlier, this counter-intuitive relationship between temperature and hourly load is puzzling and merits further investigation

Relative Humidity shows varied marginal effects for the three regions. For Trico and Mohave, a single percentage increase in relative humidity decreases hourly load consumption. However, for Graham, such an increase results in a positive change in hourly load.

Moreover, for Trico, an increase in wind speed, through its consequent chilling effect, brings about a decrease in hourly load. The marginal effects of solar radiation show that by increasing the ambient temperature, a unit increase in solar radiation has a positive impact on the hourly load for all three AEPCO service regions.

As mentioned in previous section of this chapter, in order to evaluate forecasting performance of the hourly load models, we compare the accuracy of our model forecasts (Full Model) with those of the so-called ‘No Weather’ models, which do not include the weather variables. We use the last year in our dataset, 2004, and forecast 24-hour load profiles for the following two days of the year:

1. Peak load day occurring in the dry summer season, i.e., during the time period from May to June 2004.

2. Peak load day occurring in the monsoon season i.e., during the time period from July to August 2004.

The results of this evaluation are shown for all three AEPCO utilities in Table 16.

Table 16: Evaluating Hourly Load Forecast Models

		Dry Summer		Monsoon	
		Full Model	No Weather Model	Full Model	No Weather Model
Trico	MAPE	6.027	5.876	3.932	3.934
	RMSE	3.391	3.269	4.603	4.648
	Peak Load Error%	-6.701	-6.256	-3.211	-2.490
Graham	MAPE	2.595	2.970	1.781	1.799
	RMSE	1.026	1.252	0.589	0.589
	Peak Load Error%	3.935	5.118	-1.203	0.120
Mohave	MAPE	3.180	3.176	8.295	7.746
	RMSE	4.457	4.551	14.456	13.765
	Peak Load Error%	4.249	4.608	-6.495	-5.254

From Table 16 it is evident that our hourly load models have varied performance across the seasons and regions. Our hourly model (Full model) performs well for both the dry summer and monsoon seasons of Graham, showing improvement of around 0.5 percent and 00.018 percent over the Basic model. According to MAPE, the Full model performs better than the No Weather model in the monsoon season for Graham. However, peak load percentage error shows that the Full model over-predicts by a greater percentage than the No Weather model under-predicts. For Trico, the Full model shows improvement over the Basic No Weather model only for the monsoon season, with an improvement of 0.002 percent than the No Weather model. This improvement is also reflected in the RMSE. However, for Trico in the monsoon season, the No Weather model appears to forecast the peak load better than the Full model. In the dry-summer season, the No Weather model performs better than the Full model according to all three measures of error. Mohave shows a reverse trend, with an improved forecasting performance in the dry summer season, but a poor performance in the monsoon season due to under-prediction.

Generally lower performance in the monsoon season can be explained by the erratic weather conditions experienced during this season. For example, sudden rainfall often brings about a precipitous drop on temperature, bringing about sudden changes in electricity consumption. These effects are exacerbated at the hourly time scale, introducing further difficulties in predicting hourly load. Therefore we obtain mixed results from evaluating the performance of our hourly load forecasting models. These findings are further illustrated by forecast plots for the evaluation time periods given in Appendix D.

5.3 Monthly Load Forecasting Model

Table 17 shows the monthly model coefficient estimates with their associated standard deviations. In our monthly load forecasting model, except for solar radiation and relative humidity, the coefficients of all other variable are significant either at less than 0.001 level or at less than 0.05 level of significance. Therefore we cannot clearly establish the relationship between these weather elements and electricity load.

Moreover, save relative humidity and precipitation, all other variables show the expected signs. This implies that the generally assumed cooling effect of precipitation is not valid for the Tucson MSA region. In fact, the positive coefficient on precipitation lends credence to the theory that rainfall in Tucson pushes people indoors, increasing their consumption of electricity.

Per capita income and change in population coefficients are clearly positive and significant, implying that load demand increases with population and per capita income. The positive and highly significant coefficient associated with copper mine production is consistent with the fact that the three mines in the region (Sierrita, Mission Complex and Silver Bell) are significant TEP customers and contributors to the load demand.

The highly significant autoregressive lags of order 1, 3 and 12 were included in the monthly model to account for autocorrelation. This can be interpreted as stating that the load in the current month is also determined by load in the previous month, in the previous season and the previous year. The coefficients associated with these terms indicate that while load in the current month is directly related to the load in the previous season, electric load in the previous month and the previous year have a negative impact on the current monthly load. This is an unexpected result which merits deeper investigation through future studies.

From Table 17 we can clearly see that the Full model i.e. the hourly model which uses weather and socio-economic variables, performs better in terms of RMSE and MAPE of 2009 load forecasts than the purely autoregressive model (referred to as the Basic model) used by electric utilities. In other words, on average the Full model forecasts are 4.73 percent more accurate than the forecasts from the Basic model.

The marginal effects for the monthly load forecasting model were also calculated at the mean values for those explanatory variables which were found to be significant (Refer to Appendix J for details).

Based on per unit generation cost estimates provided in the 2008 study, “Powering Arizona” (Considine & McLaren, 2008) , Table 18 shows that cost savings from utilizing the Full model as opposed to the Basic model are substantial. This shows the economic value of improved load forecasts by incorporating weather information. We consider the following two situations in the electricity spot market:

CASE A: Penalty for purchasing electricity in the spot market is equal to the cost of generating a unit of electricity.

CASE B: Penalty for purchasing electricity in the spot market is equal to twice the cost of generating units of electricity, i.e., losses are asymmetrical.

For calculations please refer to Appendix E. Here the ‘penalty’ in the spot market actually refers to the spot market price for electricity. Due to absence of reliable data for our relevant region and cooperatives, we assume the above two situations. While these two cases provide a simple explanation of the monetary value of improved forecasts, future work can further study the impact of asymmetry of losses in the electricity spot market on the economic value of forecasts.

Table 17: Monthly Model Yule –Walker Estimates

Variable	Full Model	Basic Model
Intercept	1797***	1099***
	(121.323)	(23.0153)
Temp	-62.907***	
	(2.864)	
Sqtemp	0.601***	
	(0.024)	
RH	0.729	
	(0.374)	
SolRad	0.002	
	(0.053)	
Precip	184.390*	
	(75.140)	
Windspd	75.384**	
	(24.488)	
Int2	-1.294**	
	(0.355)	
PCY	0.022***	
	(0.001)	
Popnch	0.007**	
	(0.002)	
Cuprod	0.004**	
	(0.001)	
Lag1	-0.456**	-0.585**
	(0.085)	(0.06)
Lag3	0.188**	0.262**
	(0.083)	(0.042)
Lag12	-0.236**	-0.446**
	(0.083)	(0.055)
AIC	1,077.22	1,364.44
SBC	1,116.13	1,375.59
Forecasts for 2009		
RMSE	34.80	94.24
MAPE	2.80	7.33

Significance Levels *=0.05 **=0.01 ***=0.001

Table 18: Annual Cost Savings from Improved Monthly Forecasts for 2009

Technology	Average Cost of Generation* ($ /MWh)	Spot Market Penalty** ($/MWh)	CASE A: Annual Cost Savings ($)	CASE B: Annual Cost Savings ($)
Scrubbed Coal	51.5	103	23,802,647.86	42,249,940.55
Conventional Gas	106	212	48,991,857.74	86,961,042.68

*2008: Powering Arizona by Timothy Considine

** Spot Market Penalty= 2 x Average Cost of Generation

Next, Figure 10 illustrates load demand response under the Simple Change scenario (temperature increased by 6.336 °F per month and precipitation diminished by 10 percent per month).We observe that the forecasted peak load is approximately 300 MW higher than the previous 2009 year level. There is also a clearly discernable spike in load in the month of January. However, on the whole, monthly load appears to follow a similar seasonal pattern. It increases as the average load increases, and declines when the average monthly load curve declines.

In Figure 11, monthly load forecasts in case of the More Intense Summer Shift (MISS) scenario show the expected load response when temperatures and precipitation change dramatically. Under this scenario, we assume a 50 percent decline in monsoon precipitation and warmer temperatures during the summer months from May to August (specifically an increase of 4 ° C or 7.2 °F) and a general increase in temperature by 2.5° C (or 4.5 °F) for the rest of the year. We observe that the annual peak load, while still occurring in July, is more pronounced and is greater than the load under the Simple Change scenario in the same month in 2009. It must be noted that the seasonal patterns remain intact in either of the scenarios. Moreover, in both scenarios load demand at the beginning of the year shows an unexpected spike. However, in MISS the load curve appears to be more highly peaked in July, as compared to the simple change scenario.

Figure 10: Simple Change Scenario for Monthly Model

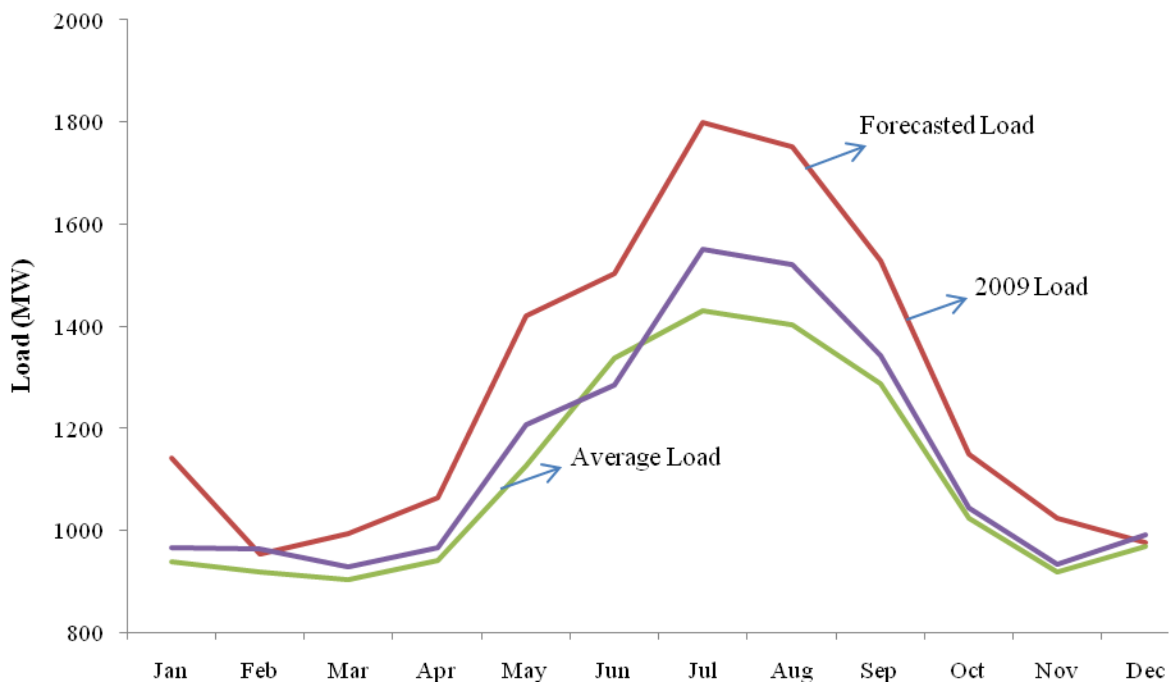

Figure 11: More Intense Summer Shift Scenario for Monthly Model

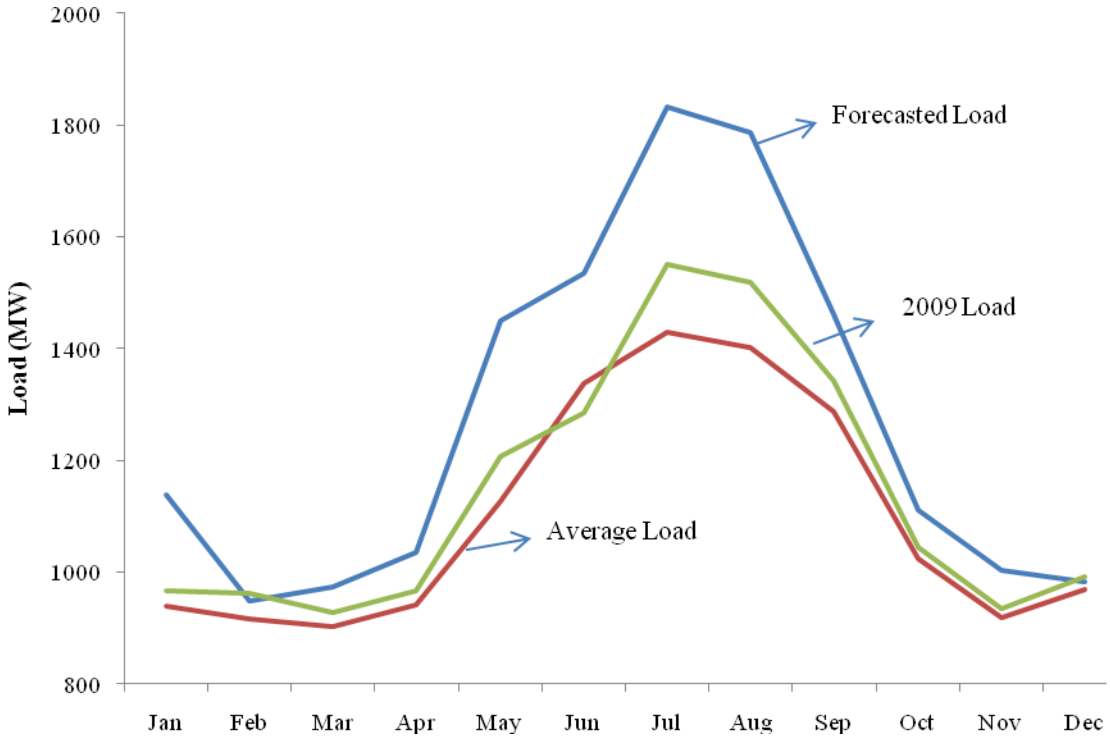

The economic and policy implications of the more pronounced seasonal effects are further discussed in the final Chapter.

The marginal effects for the monthly load forecasting model were calculated at the mean values ($\bar{X}_i$) for those explanatory variables which were found to be significant. Since the coefficients associated with relative humidity and solar radiation were not significant, their marginal effects were not calculated. Due to the presence of autoregressive terms at lags 1, 3 and 12, we utilized an approach similar to that used for estimating the marginal effects for the hourly load forecasting models. Therefore, the marginal effects of the significant explanatory variables in the monthly model were estimated using the following steps:

1. First, we estimated the long term value of the dependent variable, average hourly load

in a specific month (Z_t), using the following formula:

$$Long\ Term\ Value\ of\ Z_t\ =\left(\frac{\hat{\mu}+\ \sum_{i=1}^{10}\hat{\beta}_i\bar{X}_i}{1-\bar{\hat{\emptyset}}_1-\bar{\hat{\emptyset}}_3-\bar{\hat{\emptyset}}_{12}}\right)$$

where i = 1, 2 ….10 is the number of explanatory variables and t= -12, -11,.., 0,..,1, 2, ,107 refers to a specific month in time period of 120 months. $\hat{\mu}$ is the intercept term estimate from the model results and $\bar{\hat{\emptyset}}_1$, $\bar{\hat{\emptyset}}_3$ and , $\bar{\hat{\emptyset}}_{12}$ are estimated model coefficients for the AR(1), AR(3) and AR(12) terms. $\hat{\beta}_i$ refers to model coefficient for explanatory variable X_i

2. Next, we assume that the estimated value of the dependent variable ($\hat{Z}_t$) for the first 12 time periods (i.e., first 12 months) is equal to the long term value calculated in the previous step. The estimated value of the dependent variable for the remaining time periods (i.e., from t=0 to t=107) is calculated by the following formula at the mean values for the explanatory variables ($\bar{X}_i$):

$$\hat{Z}_t=\ \hat{\mu}+\ \bar{\hat{\emptyset}}_1\hat{Z}_{t-1}+\bar{\hat{\emptyset}}_2\hat{Z}_{t-3}++\bar{\hat{\emptyset}}_2\hat{Z}_{t-12}+\sum_{i=1}^{10}\hat{\beta}_i(\bar{X}_i+S_{i,t})$$

where $S_{i,t}$ is the shock to significant explanatory variable X_i in time period t

3. In the above formula, we introduce a unit change (or unit shock) by increasing the initial value of the shock term($S_{i,0}$) by one (from zero) for variable X_i, whose marginal effect we are trying to estimate, holding all other variables constant at their

respective means. The resulting $\hat{Z}_t$ is recorded.

4. Similarly a sustained shock is introduced by increasing all the shock values for an explanatory variable X_j by one, holding all other variables constant at their respective means. The $\hat{Z}_t$ calculated based on the sustained shock is also recorded.

5. Marginal effects are calculated as the difference between $\hat{Z}_t$ after the introduction of the shock and $\hat{Z}_t$ in the absence of shock. These are calculated for both scenarios i.e., one scenario where only the initial shock is introduced, and another scenario where the variable of interest suffers a sustained shock.

The estimated marginal effects for the monthly model are illustrated by Figure 12 for the time period of 60 months (i.e., from t=0 to t=60). For sake of brevity, the marginal effects results for only 48 months (i.e., from t=0 to t=48) are tabulated in Appendix J.

Figure 12: Marginal Effects for Monthly Model

(a) Temperature

Initial Shock

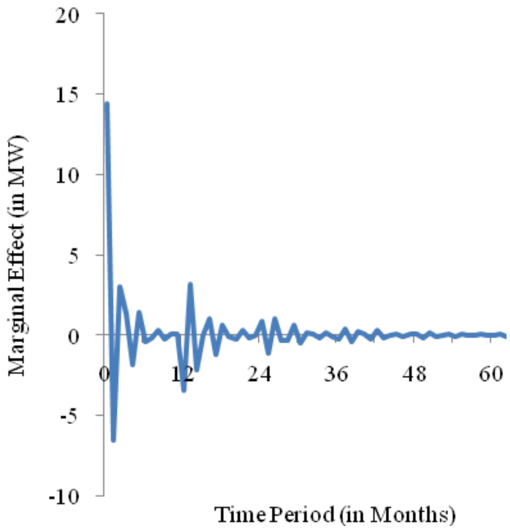

Sustained Shock

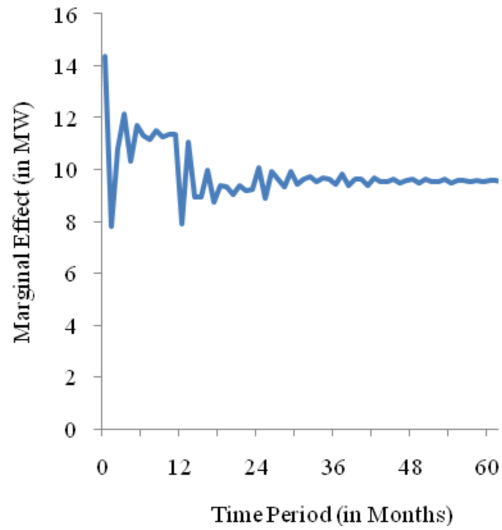

(b) Precipitation

Initial Shock

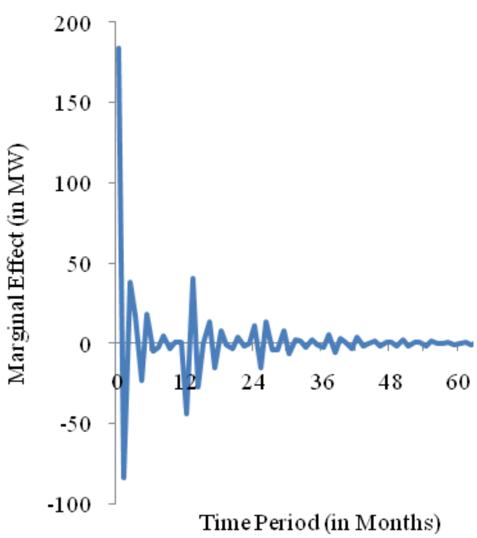

Sustained Shock

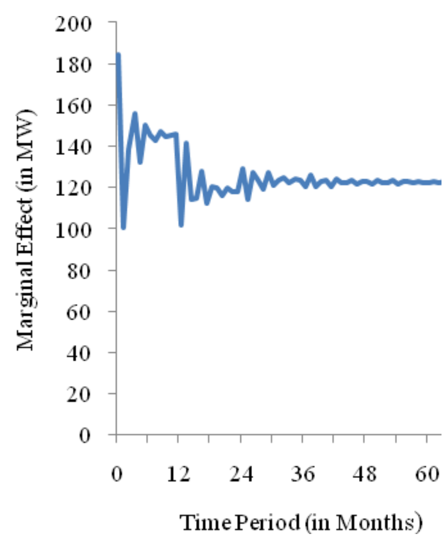

(c) Wind Speed

Initial Shock **Sustained Shock**

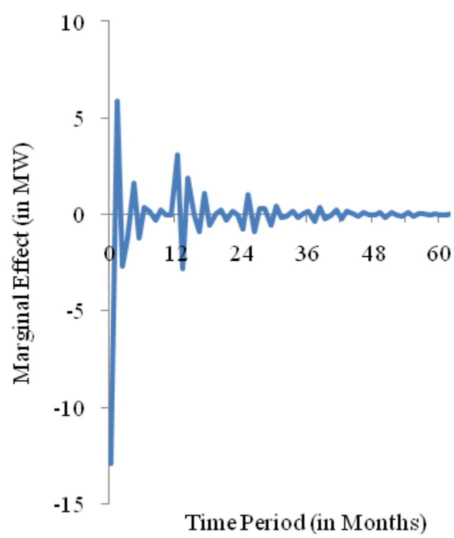

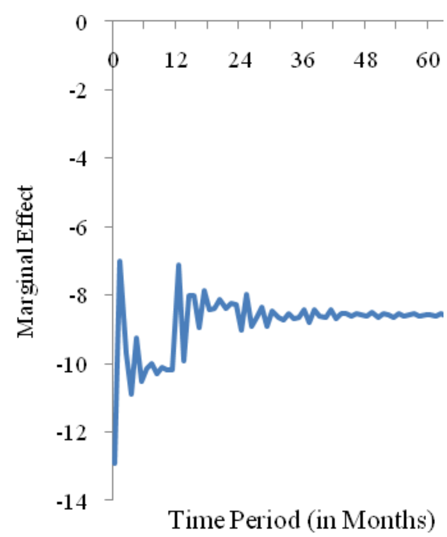

(d) Per Capita Income

Initial Shock **Sustained Shock**

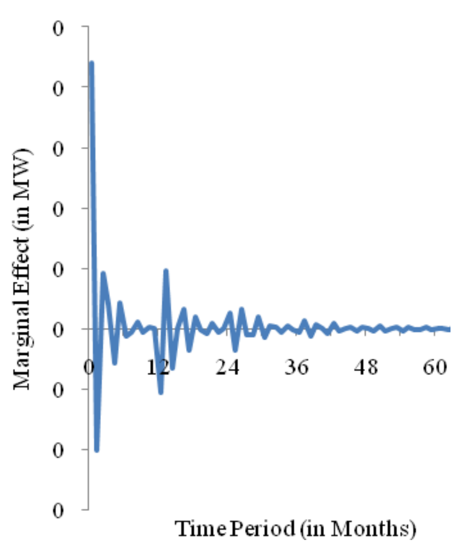

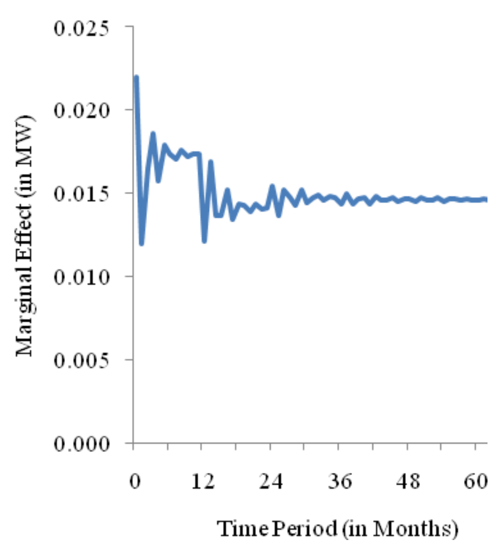

(e) Change in Population

Initial Shock

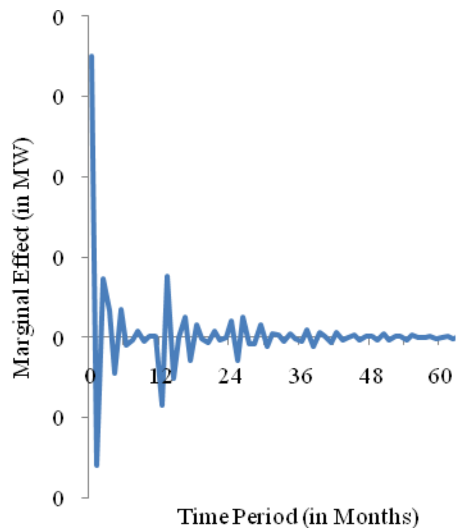

Sustained Shock

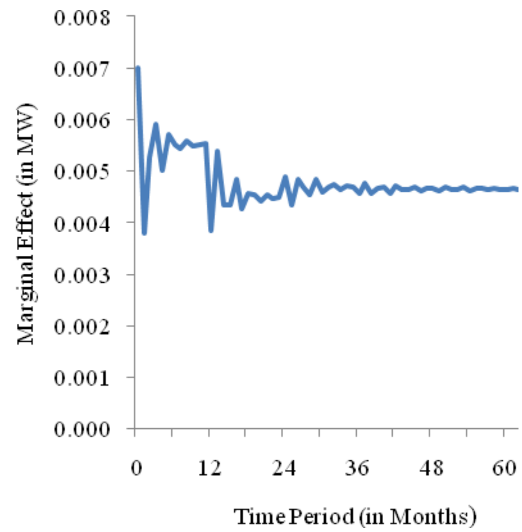

(f) Copper Mine Production

Initial Shock

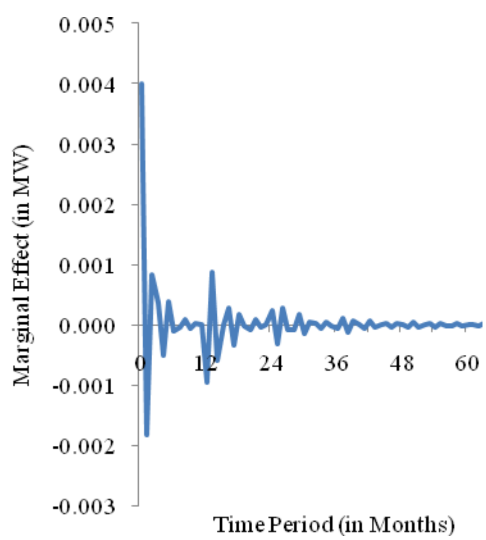

Sustained Shock

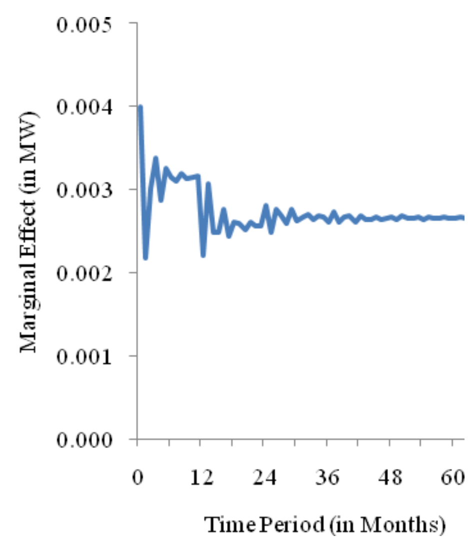

The marginal effects indicate that when temperature rises by 1 °Fahrenheit from the mean, the average hourly load in a specific month at increases in the first period, by approximately 14 MW, and then decreases precipitously in the next by around 6 MW, following a pattern of rise and fall in alternate periods until the marginal effect due to an initial shock to temperature damps out by the 60th month in the future. A sustained shock to temperature by 1 °Fahrenheit increases the average hourly load in a month such that the new long term mean is also increased to a higher level by approximately 9 MW.

Precipitation, per capita income, population change and copper mine production displays a similar trend. A sustained unit shock has a positive long term impact on average hourly load in a month. However, a unit increase in wind speed brings about a chilling effect, reducing the average hourly load in a specific month by almost 13 MW in the first period. In the next period, this initial shock results in an increase of 6 MW, followed by another crest-trough pattern, in dampening manner. It must be noted that a unit sustained shock to wind speed negatively impacts the long term value of average hourly load in a month by around 9 MW.

CHAPTER 6 Conclusion

6.1 Significant Findings

As is evident from the increased incidence of extreme weather events worldwide, climate change is already underway globally. Most global climate models (GCMs) predict hotter and drier weather for the southwestern United States. Despite the variety of load forecasting tools available, electric utilities tend to utilize the simplest approach of using past load data to predict future load profiles. In light of climate change, electric utilities need to adapt their current load forecasting techniques to avoid significant losses through inaccuracies in predictions.

In this study we investigate the potential for adapting the current load forecasting techniques to climate change by incorporating weather variables into the current models used by electric utilities. We constructed three hourly load forecasting models for three AEPCO cooperatives (Trico, Graham and Mohave) and one monthly load forecasting model for the TEP utility in the Tucson MSA.

The hourly load forecasting model followed the basic construct of a transfer function with seasonal multiplicative ARMA errors. Our results suggest that the new hourly load forecasting models have varied performance across regions and seasons. For the Graham electric cooperative our hourly model showed improvement over the Basic model (model without weather variables and seasonal dummies) for both the monsoon as well as the dry summer peak day evaluation periods. Our hourly models for Trico and Mohave performed well in the dry summer season, but showed a higher forecast error percentage in case of the monsoon season. This hints at the possibility that our hourly models failed to capture some aspects of seasonality and weather variations. Moreover, the highly erratic weather conditions during the monsoon season further complicated the process of generating accurate load forecasts for the study regions

Our monthly load forecasting model for TEP involved a regression with autoregressive terms. It showed modest improvement in terms of forecast accuracy (approximately 5 percent improvement) over the purely autoregressive model.

6.2 Policy Implications and Future Research

We recognize the potential for improving the performance of our hourly load forecasting models by going beyond the use of seasonal dummies and utilizing more sophisticated techniques to model the complex seasonality which exists at the hourly time scale. Future research in this field can explore the use of complex sinusoidal functions or polynomials, such as those discussed by Tanimoto (2008). Also, in order to further improve forecasting ability, additional information regarding load attributable to various customer class types will be very valuable and particularly helpful for modeling seasonality. This is because each customer class responds in a different manner to changes in weather, seasons, time of day, day of week etc. For example, household consumption of electricity on weekends is higher than that of commercial customers. However, information regarding individual customer class load was suppressed due to confidentiality reasons in our current load data.

While our models have assumed static seasons, i.e. we assume seasonal time periods to have remained static over the period of our study; we recognize the impact of climate change on the time period and severity of the seasons. This is a growing concern among the scientific community, as is reflected in the increased interest in the changing patterns in the growing seasons of crops (Backlund, 2008). As shown by the results of our monthly model, the annual peak load occurs during the monsoon season. Therefore, the monsoon season is of critical importance for the electricity industry. We recommend the utilization of dew point readings as opposed to fixed dates for the beginning and the end of the monsoon season. Future research can focus on the creation of such seasonal shift indicators to further adapt load forecasting models to climate change.

Furthermore, we acknowledge that the use of actual weather data in out-of-sample prediction (based on the hold-out sampling approach) assumes perfect knowledge of weather events. Since electric utilities use weather forecasts in reality, the quality of weather forecasts used is a crucial consideration in assessing forecasting performance. Future work can involve assessing the forecasting performance of our models based on daily and seasonal weather forecasts.

Despite these shortcomings, improved forecasts from our monthly models exhibit potential for applications in a variety of areas. For example, the load forecasting models presented in this study can also be used to predict the hour of the day as well as the day of the year when the annual peak load is likely to occur. While this has not been shown explicitly in this study, further research can explore this aspect of our models.

The most evident benefit from more accurate load forecasts is the economic value due to minimizing exposure to the volatile spot markets. As we have already mentioned, electric load demand exhibits seasonal fluctuations due to changing climatic conditions. Since the supply side is also vulnerable to these changes, this translates into seasonal behavior of spot market prices as well. Moreover, spot electricity prices exhibit infrequent, but large jumps. This is the consequence of the fact that electricity to be delivered at a specific hour cannot be substituted for electricity available shortly after or before, since it has to be consumed at the same time as it is produced. Any severe fluctuations in demand or even small increments in demand when the demand level is high, causes huge price spikes (Weron, 2006). Keeping these factors in mind we may assume that, in response to climate change, the future spot market conditions will grow increasingly volatile. Therefore, more accurate load forecasting models that incorporate the changing climate information will minimize a utility's need for engaging in the volatile electricity spot markets.

Moreover, electric utilities are likely to reap economic benefits from using improved load forecasts in contract evaluations and evaluations of various sophisticated financial products on energy pricing offered by the market.

More accurate load forecasts can also aid in reducing the carbon footprint of electric utilities by ensuring efficient utilization of resources and reduced GHG emissions.

For obtaining a more comprehensive picture of the impact of climate change on the electricity industry, future work can focus on using dynamically downscaled GCM data to predict future load profiles in light of different climate change scenarios. These predicted load profiles can then influence discussions on the economic and environmental viability of investment in generation technologies. For example, in Arizona, the Renewable Energy Portfolio Standard (RPS) requires electricity providers to supply 15 percent of their electricity from renewable sources by the year 2025. For this region, solar energy is considered a natural alternative to current generating technologies. However, the inhibiting factor for the installation of large solar thermal power plants is their high water demand (Pasqualetti, 2010). .Moreover, since 2007, Georgia, Idaho, Arizona, and Montana have denied permits for conventional power plants because there was not enough water to run them (Glennon 2009). Using improved climate-sensitive load forecasts and water-use estimates for alternative generation technologies, one can study the water-use implications of solar energy prospects in the water-scarce Arizona under various climate change scenarios.

APPENDIX A List of Abbreviations

ACF	Autocorrelation function
ADF	Augmented Dickey Fuller
AEPCO	Arizona Power Cooperative
ARIMA	Autoregressive Integrated Moving Average
ARMA	Autoregressive Moving Average
AZDMMR	Arizona Department of Mines and Mineral Resources
AZMET	Arizona Meteorological Network
CDC	Carbon Disclosure Project
EPRI	Electric Power Research Institute
ESACF	Extended Sample Autocorrelation Function
GCEC	Graham County Electric Cooperative
GCM	Global Climate Model
GHG	Green House Gas
IACF	Inverse autocorrelation function
IPCC	Intergovernmental Panel on Climate Change
LTLF	Long-term load forecasting
MAPE	Mean Absolute Percentage Error
MEC	Mohave Electric Cooperative
MINIC	Minimum Information Criterion
MISS	More Intense Summer Shift
MSA	Metropolitan Statistical Area
MTLF	Medium-term load forecasting
PACF	Partial Autocorrelation function
RMSE	Root Mean Squared Error
RPS	Renewable Energy Portfolio Standard

STLF	Short-term load forecasting
TEP	Tucson Electric Power
UNFCCC	United Nations Framework Convention on Climate Change
USGCRP	U.S. Global Change Research Program
USGS	U.S. Geological Survey

APPENDIX B Godfrey Lagrange Multiplier Test for Serial Autocorrelation

	Trico		Graham		Mohave	
Alternative	LM	Pr>LM	LM	Pr > LM	LM	Pr > LM
1	161.6	<.0001	0.3	0.586	10.73	0.0011
2	167.6	<.0001	0.48	0.7884	11.34	0.0034
3	606.4	<.0001	21.64	<.0001	69.46	<.0001
4	638.2	<.0001	126.6	<.0001	95.03	<.0001
5	903.6	<.0001	263.5	<.0001	217.1	<.0001
6	1318	<.0001	432.3	<.0001	499.6	<.0001
7	1954	<.0001	761.5	<.0001	1166	<.0001
8	2605	<.0001	1128	<.0001	1428	<.0001
9	2733	<.0001	1349	<.0001	1743	<.0001
10	2994	<.0001	1614	<.0001	2033	<.0001
11	3106	<.0001	1793	<.0001	2323	<.0001
12	3253	<.0001	1953	<.0001	2593	<.0001
13	3509	<.0001	2259	<.0001	3011	<.0001
14	3933	<.0001	2575	<.0001	3668	<.0001
15	4587	<.0001	3005	<.0001	4208	<.0001
16	4895	<.0001	3465	<.0001	4736	<.0001
17	5488	<.0001	3848	<.0001	5139	<.0001
18	5793	<.0001	4082	<.0001	5419	<.0001
19	5962	<.0001	4201	<.0001	5532	<.0001
20	6167	<.0001	4275	<.0001	5605	<.0001
21	6247	<.0001	4297	<.0001	5606	<.0001
22	6400	<.0001	4300	<.0001	5606	<.0001
23	6949	<.0001	4681	<.0001	6034	<.0001
24	7013	<.0001	4755	<.0001	6120	<.0001
25	7964	<.0001	5081	<.0001	6536	<.0001
26	7980	<.0001	5109	<.0001	6552	<.0001
27	7986	<.0001	5110	<.0001	6553	<.0001
28	7993	<.0001	5122	<.0001	6555	<.0001
29	7994	<.0001	5151	<.0001	6564	<.0001
30	8004	<.0001	5206	<.0001	6588	<.0001
31	8006	<.0001	5259	<.0001	6618	<.0001
32	8024	<.0001	5294	<.0001	6624	<.0001
33	8024	<.0001	5303	<.0001	6626	<.0001
34	8027	<.0001	5305	<.0001	6626	<.0001
35	8041	<.0001	5307	<.0001	6626	<.0001

36	8045	<.0001	5308	<.0001	6627	<.0001
37	8085	<.0001	5330	<.0001	6629	<.0001
38	8117	<.0001	5361	<.0001	6665	<.0001
39	8266	<.0001	5390	<.0001	6753	<.0001
40	8320	<.0001	5411	<.0001	6787	<.0001
41	8351	<.0001	5422	<.0001	6816	<.0001
42	8374	<.0001	5425	<.0001	6839	<.0001
43	8381	<.0001	5430	<.0001	6856	<.0001
44	8420	<.0001	5432	<.0001	6867	<.0001
45	8432	<.0001	5434	<.0001	6867	<.0001
46	8433	<.0001	5434	<.0001	6874	<.0001
47	8456	<.0001	5434	<.0001	6876	<.0001
48	8462	<.0001	5491	<.0001	6890	<.0001

APPENDIX C Traffic Count-based Monthly Population Estimate

Step 1: Selection of Permanent Traffic Counter based on region: Table C1 lists the Permanent Traffic Counter ID numbers designated for each region of the Pima County. For every year, one from each region was selected to ensure that the total traffic count from all counters were representative of the whole county.

Table C1: Pima County Traffic Counter ID Numbers by Region

North (n=1)	South (n=2)	Southeast (n=3)	Southwest (n=4)	Northwest (n=5)	Northeast (n=6)
1	28	21	4	25	26
10	13	22	5	19	8
6	31	9	30	33	23
24	22			20	3
35	27				3
12					

Step 2: Calculate Average Monthly Traffic Count for each month: The Average monthly traffic count ($TC_{j,t}$) for each month of the year was calculated by the following formula:

$$TC_{j,t} = \frac{\left[\sum_{n=1}^{6} tc_n\right]_{j,t}}{6}$$

where tc_n= Traffic count from the selected regional Pima County Traffic Counter in region 'n'

j = 1, 2,….12 refers to months of the year

t = 1,2,…..10 refers to years starting 2000 to 2009

n = 1,2,…..6 refers to the region of Pima County

Approximately 12 percent of the traffic count values (88 out of 720 values) were missing. These missing values were filled in using averages, and are italicized in Tables C2 to C11. .

Step 3: Calculate monthly population estimate using $TC_{j,t}$ and census population estimates: The following formula was utilized to estimate population for month j in year t:

$$Popn_i = Popn_{i-1} + \left[\frac{TC_{j,t}}{\sum_{j=1}^{12} TC_{j,t}} \times (CenPopn_{t+1} - CenPopn_t)\right]$$

where i = 1, 2,….120 refers to the total number of sample observations

$CenPopn_t$ = Annual Census Population estimate for year t

Table C2: Pima County Traffic Count Values for Year 2000

Traffic Intersection	Region	Jan	Feb	Mar	Apr	May	Jun	Jul	Aug	Sep	Oct	Nov	Dec	Total
Alvernon S of Irvington	S	19561	20535	20279	19584	19140	18297	18029	19028	18085	18693	18432	18569	228232
Ina RD E of La Canada	N	35437	37672	37259	37047	36079	35805	34347	35374	34982	36236	36790	38523	435551
Kolb Rd S of Valencia	SE	10836	11690	11392	10865	9854	9470	9216	9487	9531	10624	10321	10349	123635
Mission RD S of Wyoming Strt	SW	20935	22206	22315	21984	21185	20865	21583	22750	22861	22838	22683	23145	265350
Tanque Verde Rd E of Pio Decimo	NE	47964	49164	50555	50406	49436	48553	46970	47589	49073	49079	47666	49798	586253
La Cholla Blvd North of Sunset Rd	NW	24650	26074	26254	26370	25698	*25446*	*25744*	25194	26042	26994	26288	26568	311322
	Average	26,563.83	27,890.17	28,009.00	27,709.33	26,898.67	26,406.00	25,981.50	26,570.33	26,762.33	27,410.67	27,030.00	27,825.33	325,057.17
	Weight	0.0817	0.0858	0.0862	0.0852	0.0828	0.0812	0.0799	0.0817	0.0823	0.0843	0.0832	0.0856	1.00

Table C3: Pima County Traffic Count Values for Year 2001

Traffic Intersection	Region	Jan	Feb	Mar	Apr	May	Jun	Jul	Aug	Sep	Oct	Nov	Dec	Total
Alvernon S of Irvington	S	18811	19719	20429	19877	19132	19574	18305	19126	18035	19112	19080	18795	229995
Ina RD E of La Canada	N	37517	38034	38342	37442	36552	35802	34881	35340	33398	34181	34953	36244	432686
Kolb Rd S of Valencia	SE	11004	11807	11816	11308	10584.5	10584.5	9861	10245	9811	10609	11110	9306	128046
Mission RD S of Wyoming Strt	SW	22601	24278	24696	24705	24653	24141	24869	25539	24987	25064	24413	24773	294719
Tanque Verde Rd E of Pio Decimo	NE	48537	51231	50501	50113	48532	46678	48187	48852	49549	50622	47813	*48902.5*	589517.5
La Cholla Blvd North of Sunset Rd	NW	25650	27956	27476	27125	26485	26489	25098	23772	20132	20137	19769	20028	290117
	Average	27,353.33	28,837.50	28,876.67	28,428.33	27,656.42	27,211.42	26,866.83	27,145.67	25,985.33	26,620.83	26,189.67	26,341.42	327,513.42
	Weight	0.0835	0.0880	0.0882	0.0868	0.0844	0.0831	0.0820	0.0829	0.0793	0.0813	0.0800	0.0804	1.00

Table C4: Pima County Traffic Count Values for Year 2002

Traffic Intersection	Region	Jan	Feb	Mar	Apr	May	Jun	Jul	Aug	Sep	Oct	Nov	Dec	Total
Alvernon S of Irvington	S	18247	19940	20141	20148	19761	19460	18403	19902	20154	20406	19895	19822	236279
Ina RD E of La Canada	N	34876	35647	36057	35596	35075	33437	31043	32812	32446	32402	32591	34566	406548
Kolb Rd S of Valencia	SE	10468	11763	11974	11512	10689	*10445.5*	10202	*11436*	12670	*10544*	*10932.5*	*10168.5*	132804.5
Mission RD S of Wyoming Strt	SW	25160	25629	24446	24536	22886	22401	21007	22777	23554	24252	24402	24342	285392
Tanque Verde Rd E of Pio Decimo	NE	47902	49043	49991	50316	49087	46976	44558	*45780*	47002	49505	47458	48007	575625
River Rd East of Shannon Rd	NW	16858	17613	18730	18591	18821	18659	18295	19526	19843	20875	*21441*	22007	231259
	Average	25,585.17	26,605.83	26,889.83	26,783.17	26,053.17	25,229.75	23,918.00	25,372.17	25,944.83	26,330.67	26,119.92	26,485.42	311,317.92
	Weight	0.0822	0.0855	0.0864	0.0860	0.0837	0.0810	0.0768	0.0815	0.0833	0.0846	0.0839	0.0851	1.00

Table C5: Pima County Traffic Count Values for Year 2003

Traffic Intersection	Region	Jan	Feb	Mar	Apr	May	Jun	Jul	Aug	Sep	Oct	Nov	Dec	Total
Alvernon S of irvington	S	*19535.5*	20976	21008	20672	20166	20487	19327	19876	20356	20346	*20022*	19698	242469.5
Ina RD E of La Canada	N	31130	33481	33183	33070	32744	31813	29967	32622	*31169*	29716	34511	35607	389013
Kolb Rd S of Valencia	SE	*10855*	*11873.25*	*12349.5*	*11849.5*	11154	11506	10401	9996	9927	10479	10755	11031	132176.25
Mission RD S of Wyoming Strt	SW	23836	24667	24534	24141	23350	22655	22145	*22494.5*	*22890.5*	*23482.5*	*23165*	22470	279830.5
Tanque Verde Rd E of Pio Decimo	NE	48642	48269	49807	50749	50693	49686	47615	48096	*46898.5*	*49708.5*	49175	49408	588747
River Rd East of Shannon Rd	NW	21944	22930	22743	22595	22673	22306	21581	23361	22869	23414	23421	*20612*	270449
	Average	25,990.42	27,032.71	27,270.75	27,179.42	26,796.67	26,408.83	25,172.67	26,074.25	25,685.00	26,191.00	26,841.50	26,471.00	317,114.21
	Weight	0.0820	0.0852	0.0860	0.0857	0.0845	0.0833	0.0794	0.0822	0.0810	0.0826	0.0846	0.0835	1.00

Table C6: Pima County Traffic Count Values for Year 2004

Traffic Intersection	Region	Jan	Feb	Mar	Apr	May	Jun	Jul	Aug	Sep	Oct	Nov	Dec	Total
Alvernon S of irvington	S	20824	21469	22010	21776	21110	23450	24328	24069	23197	24340	23642	23502	273717
Ina RD E of La Canada	N	35430	37092	37623	36888	36528	*34112.5*	*32853.5*	*34133.5*	*33359.5*	*33161*	37128	38061	426370
Kolb Rd S of Valencia	SE	11242	*11983.5*	12725	12187	11200	10985	10575	11382	11237	12340	12703	12602	141161.5
Mission RD S of Wyoming Strt	SW	23441	24111	24280	23823	23318	22530	21453	22212	22227	22713	21928	21436	273472
Tanque Verde Rd E of Pio Decimo	NE	49671	50217	51842	51378	50656	49146	46300	48863	46795	49912	48589	48870	592239
River Rd East of Shannon Rd	NW	22888	*21011.5*	*19936*	23687	22680	22346	*20975.5*	*22472*	18170	18353	18840	19217	250576
	Average	27,249.33	27,647.33	28,069.33	28,289.83	27,582.00	27,094.92	26,080.83	27,188.58	25,830.92	26,803.17	27,138.33	27,281.33	326,255.92
	Weight	0.0835	0.0847	0.0860	0.0867	0.0845	0.0830	0.0799	0.0833	0.0792	0.0822	0.0832	0.0836	1.00

Table C7: Pima County Traffic Count Values for Year 2005

Traffic Intersection	Region	Jan	Feb	Mar	Apr	May	Jun	Jul	Aug	Sep	Oct	Nov	Dec	Total
Alvernon S of irvington	S	24374	25237	25721	25627	25372	23293	21999	24436	22013	22603	22184	22236	285095
Ina RD E of La Canada	N	37667	39186	39360	38715	37927	36412	35740	*35645*	35550	36606	37007	37210	447025
Kolb Rd S of Valencia	SE	43466	45091	46107	45198	42997	41748	40497	41094	40445	42657	42111	41956	513367
Mission RD S of Wyoming Strt	SW	22634	23188	23359	23651	22739	21943	21062	21956	21763	22402	22173	21844	268714
Tanque Verde Rd E of Pio Decimo	NE	49593	49386	50516	51040	*49871*	48702	46768	*47431*	48094	*48312*	48530	47839	586082
River Rd East of Shannon Rd	NW	18849	19093	17129	16852	16998	16785	20370	21583	20391	21301	21108	22230	232689
	Average	32,763.83	33,530.17	33,698.67	33,513.83	32,650.67	31,480.50	31,072.67	32,024.17	31,376.00	32,313.50	32,185.50	32,219.17	388,828.67
	Weight	0.0843	0.0862	0.0867	0.0862	0.0840	0.0810	0.0799	0.0824	0.0807	0.0831	0.0828	0.0829	1.00

Table C8: Pima County Traffic Count Values for Year 2006

Traffic Intersection	Region	Jan	Feb	Mar	Apr	May	Jun	Jul	Aug	Sep	Oct	Nov	Dec	Total
Alvernon S of irvington	S	24150	23968	23615	23435	22854	24100	21182	21874	22551	22587	22067	*22102*	274485
Ina RD E of La Canada	N	36804	38211	37775	37700	36310	34974	33897	37399	35387	35602	36432	37027	437518
Kolb Rd S of Valencia	SE	13220	13651	13678	13108	11848	11666	11194	11623	12061	12984	13554	14151	152738
Mission RD S of Wyoming Strt	SW	*23194*	*24486.5*	23098	22973	22536	21684	20783	21707	22449	22924	23422	23861	273117.5
Tanque Verde Rd E of Pio Decimo	NE	47759	48665	49508	49260	48219	46270	43810	46353	47097	47245	46293	46187	566666
River Rd East of Shannon Rd	NW	*22022*	21814	21370	20937	20465	20163	19823	21011	20908	20712	20891	21902	252018
	Average	27,858.17	28,465.92	28,174.00	27,902.17	27,038.67	26,476.17	25,114.83	26,661.17	26,742.17	27,009.00	27,109.83	27,538.33	326,090.42
	Weight	0.0854	0.0873	0.0864	0.0856	0.0829	0.0812	0.0770	0.0818	0.0820	0.0828	0.0831	0.0844	1.00

Table C9: Pima County Traffic Count Values for Year 2007

Traffic Intersection	**Region**	**Jan**	**Feb**	**Mar**	**Apr**	**May**	**Jun**	**Jul**	**Aug**	**Sep**	**Oct**	**Nov**	**Dec**	**Total**
Alvernon S of irvington	S	22137	23127	23537	23460	22892	22822	24078	24181	24045	24328	23186	*21690.5*	279483.5
Ina RD E of La Canada	N	35821	36928	36712	36542	34232	34945	35284	36856	37004	36614	36829	37693	435460
Kolb Rd S of Valencia	SE	13829	14496	14729	14113	13034	13350	12708	13402	13990	*17015*	*14020*	*14069.75*	168755.75
Mission RD S of Wyoming Strt	SW	23754	25785	26618	25912	25325	25018	23851	*24886.5*	25922	24796	22503	22082	296452.5
Tanque Verde Rd E of Pio Decimo	NE	46080	47716	49094	48578	48016	46445	44195	46184	47343	47500	46402	*45681*	563234
Ruthrauff Rd S of Seabrooke Dr	NW	*10886*	*14272*	*14728*	19189	18884	21255	23489	24764	24545	23653	21795	20951	238411
	Average	25,417.83	27,054.00	27,569.67	27,965.67	27,063.83	27,305.83	27,267.50	28,378.92	28,808.17	28,984.33	27,455.83	27,027.88	330,299.46
	Weight	0.0770	0.0819	0.0835	0.0847	0.0819	0.0827	0.0826	0.0859	0.0872	0.0878	0.0831	0.0818	1.00

Table C10: Pima County Traffic Count Values for Year 2008

Traffic Intersection	**Region**	**Jan**	**Feb**	**Mar**	**Apr**	**May**	**Jun**	**Jul**	**Aug**	**Sep**	**Oct**	**Nov**	**Dec**	**Total**
Alvernon Wy S of Irvington Rd	S	*21860*	*22955*	*23201*	*22829*	23150	24689	24275	25643	29100	22617	21433	21279	283031
Ina RD E of La Canada	N	37162	37068	39028	37772	36958	35262	32325	*35183*	*34838*	36047	35829	36520	433992
Kolb Rd S of Valencia	SE	*14148*	15070	15134	14448	13144	12703	12252	*13242*	*13577*	*15435*	*13925*	*13929*	167004
Mission RD S of Wyoming Strt	SW	*22445*	22807	22896	22947	22075	20819	19977	21150	21433	*22134*	*21926*	*21891*	262500
Tanque Verde Rd E of Pio Decimo	NE	46239	47629	48997	47698	47444	45050	42942	44799	45159	*46374*	45519	45175	553025
River Rd E of Shannon Rd	NW	*19154*	21374	19709	19595	19045	17650	17383	18272	18095	18415	19789	21367	229848
	Average	26,834.42	27,817.17	28,160.83	27,548.17	26,969.33	26,028.83	24,859.00	26,381.33	27,033.58	26,836.99	26,403.44	26,693.45	321,566.55
	Weight	0.0834	0.0865	0.0876	0.0857	0.0839	0.0809	0.0773	0.0820	0.0841	0.0835	0.0821	0.0830	1.00

Table C11: Pima County Traffic Count Values for Year 2009

Traffic Intersection	**Region**	**Jan**	**Feb**	**Mar**	**Apr**	**May**	**Jun**	**Jul**	**Aug**	**Sep**	**Oct**	**Nov**	**Dec**	**Total**
Alvernon Wy S of Irvington	S	21582	22783	22865	22198	25007	26088	26117	34057	*25533*	*24885*	*24777*	*24764*	300656
Ina RD E of La Canada	N	35720	37166	37061	36470	35419	34114	32623	33509	32672	32368	*34814*	*34871*	416807
Kolb Rd S of Valencia	SE	14466	*14999*	15532	14625	13393	13142	12703	13081	13163	13854	*13898*	*13899*	166755
Valencia Rd E of Camino De Oeste	SW	24117	25258	25250	24715	25060	24267	23772	24691	*24285*	*24355*	*24336*	*24333*	294439
Ruthrauff Rd S of Seabrooke Dr	NW	20819	24178	25106	24668	24611	24168	22036	20797	19651	20426	*24725*	*24697*	275882
Sabino Canyon Rd S of Cloud Rd	NE	38139	39381	42242	47291	54238	40794	54665	41929	38285	51094	*42532*	*42663*	533253
	Average	25,807.17	27,294.17	28,009.33	28,327.83	29,621.33	27,095.50	28,652.67	28,010.67	25,598.13	27,830.27	27,513.68	27,537.85	331,298.60
	Weight	0.0779	0.0824	0.0845	0.0855	0.0894	0.0818	0.0865	0.0845	0.0773	0.0840	0.0830	0.0831	1.00

The figure below shows the incremental changes in Pima county population from month to month in the years 2000 and 2001. It is evident that monthly population shows significant variation over the calendar year due to the departure of college students in the summer and the arrival of vacationers during the mild winter months.

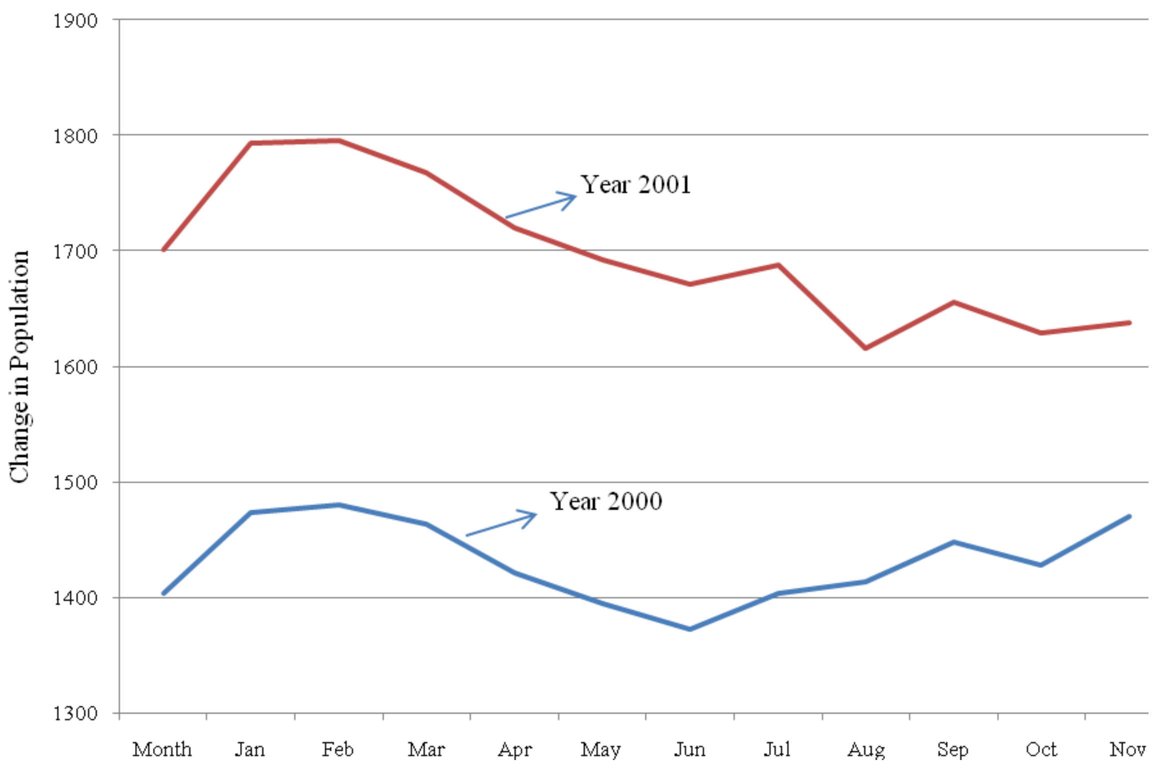

APPENDIX D Comparing 24-Hour Peak Day Load Forecasts with Actual Load

1. Trico Dry Summer (May 29, 2004)

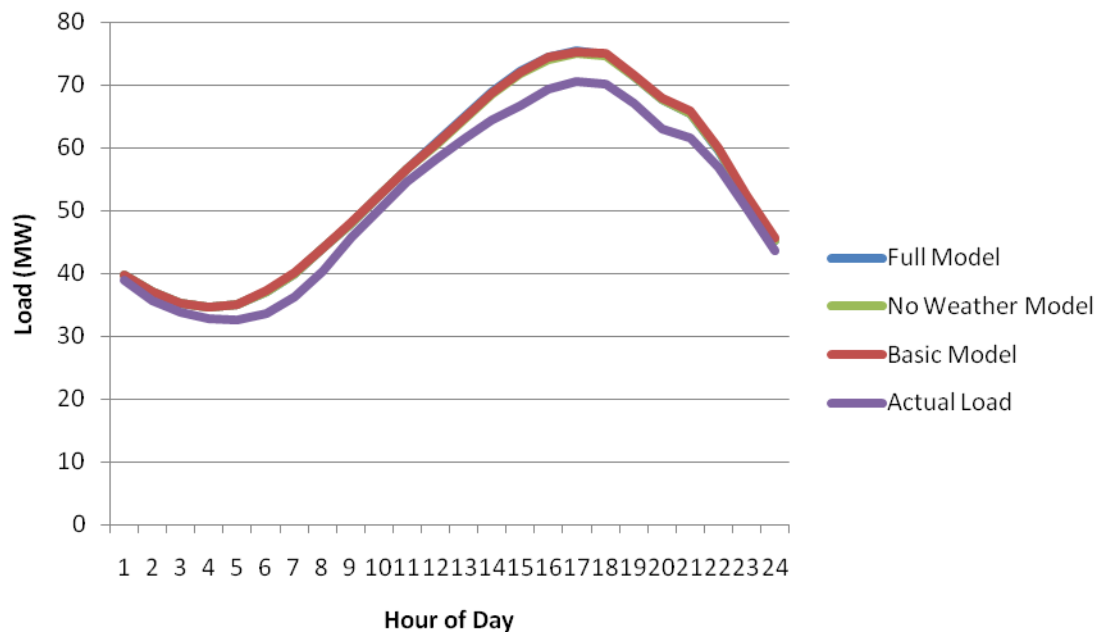

2. Trico Monsoon (August 11, 2004)

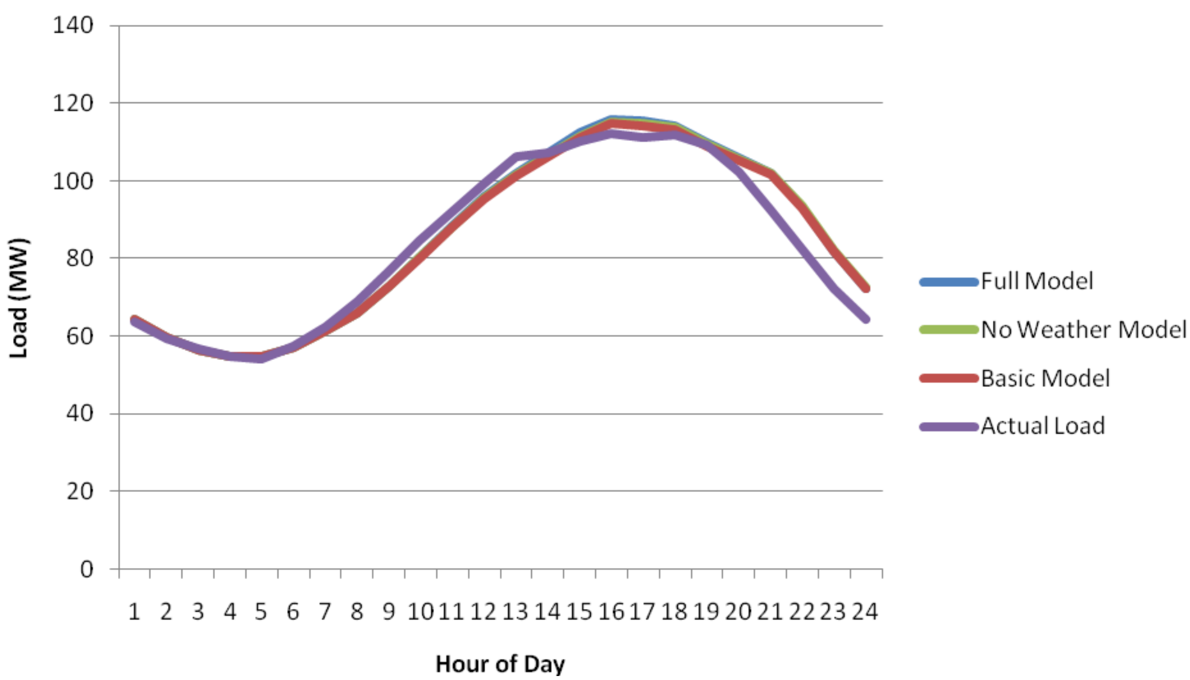

3. Graham Dry Summer (June 3, 2004)

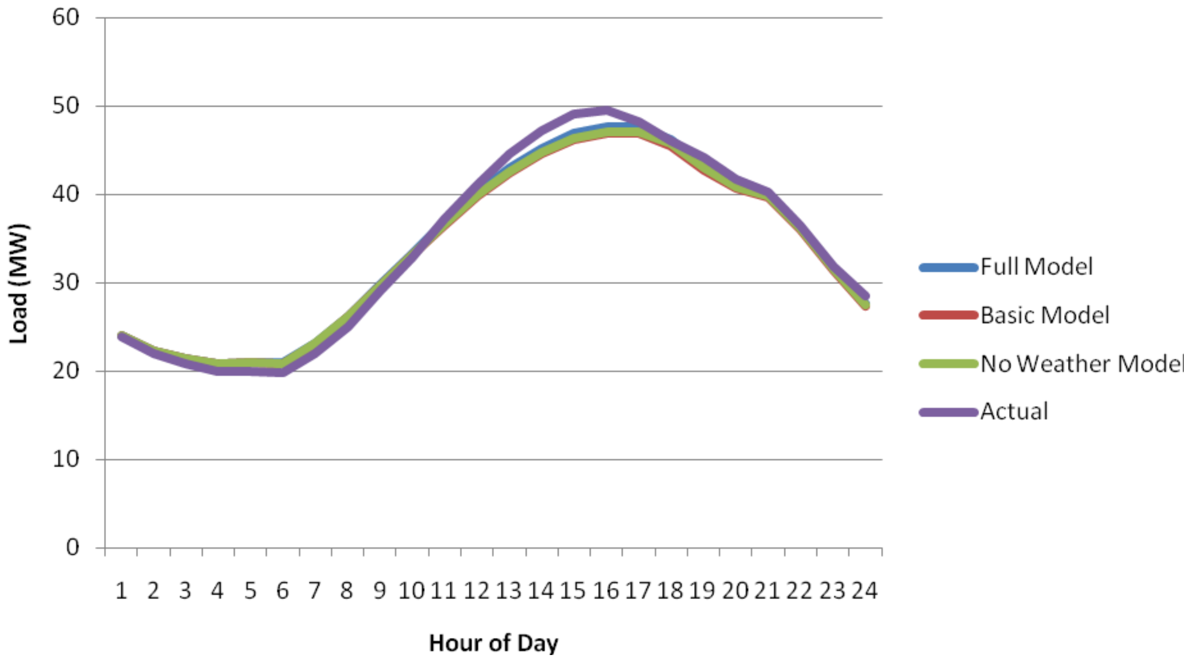

4. Graham Monsoon (July 21, 2004)

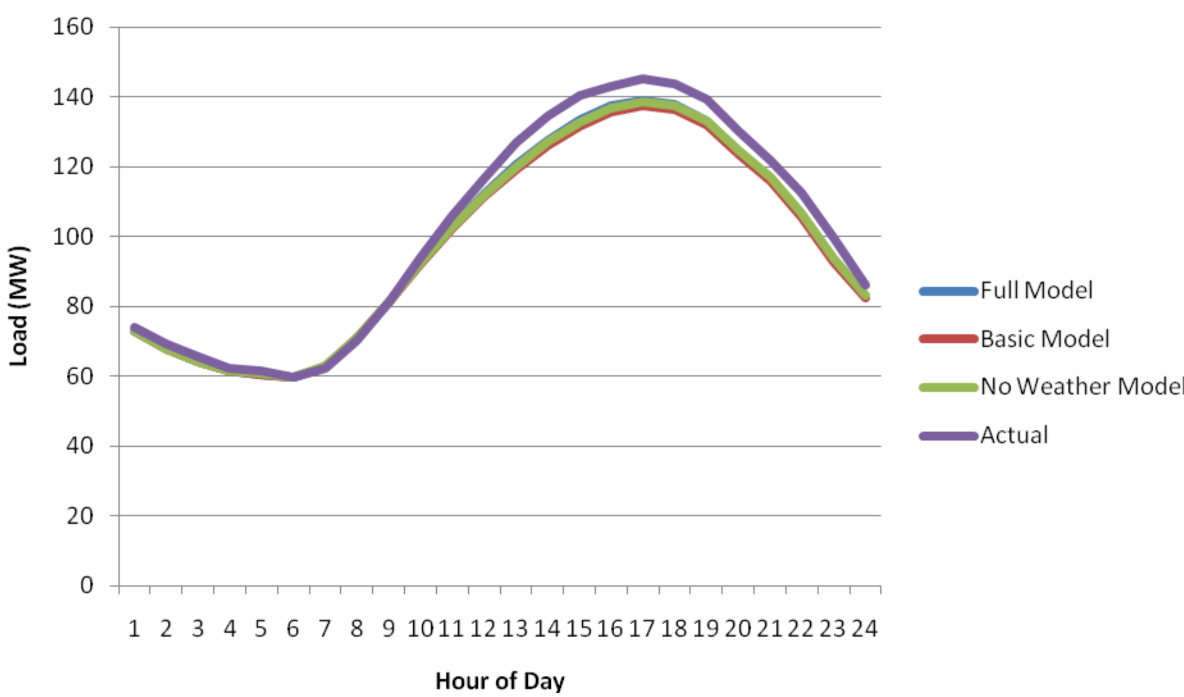

5. Mohave Dry Summer (June 24, 2004)

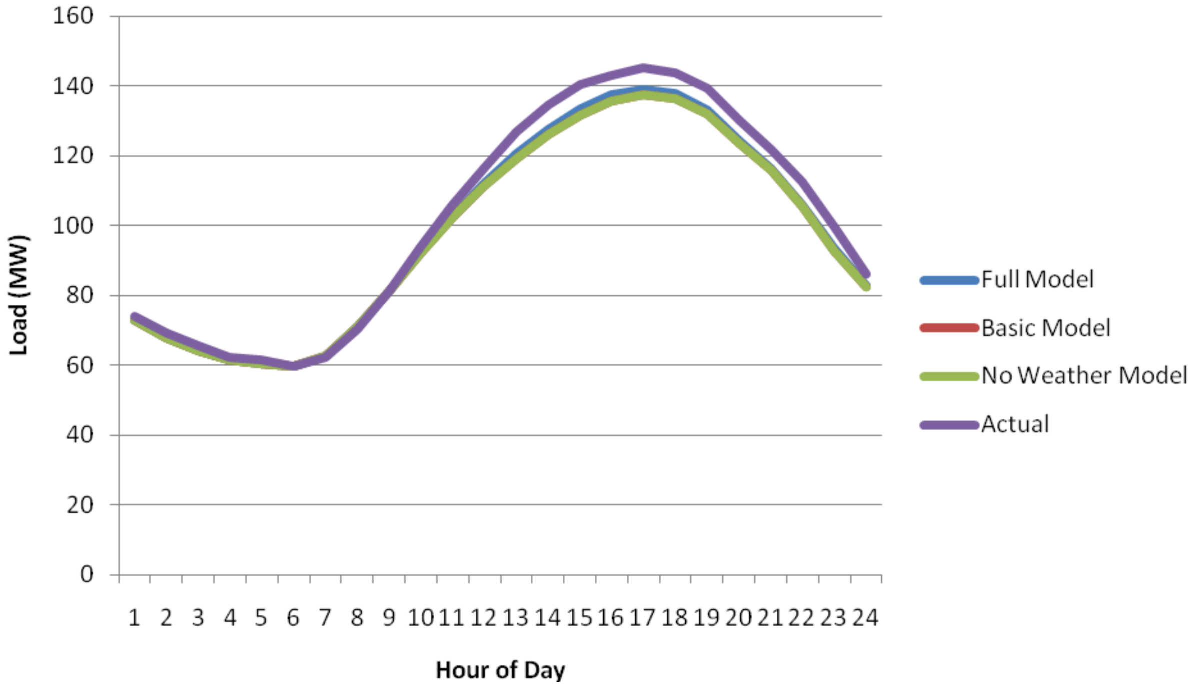

6. Mohave Monsoon (August 11. 2004)

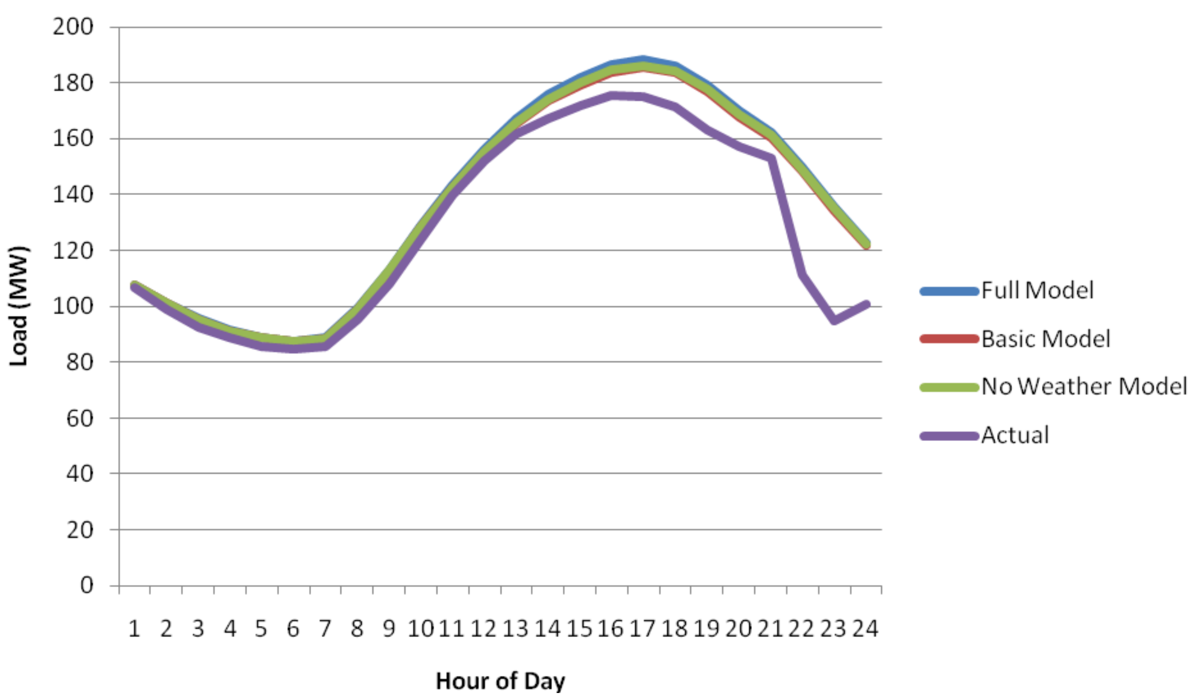

APPENDIX E Calculating Annual Cost Savings from Monthly Model 2009 Forecasts

In order to calculate annual cost savings from the use of improved forecasts from the Full model as compared to the Basic model, we follow the steps as listed below:

1. We obtain estimates of average per unit generation costs for different technologies. In our study we utilized 2009 estimates provided by Timothy Considine in his study "Powering Arizona" (2010). This estimate for scrubbed coal is $ 51.5/MW, while for conventional gas is $ 106/MW.

2. We calculate forecast errors for each month of the year 2009, whose absolute value is multiplied by the number of hours in a month, per unit generation cost and a spot market indicator to obtain losses due to forecast errors for the respective model. We apply this calculation to both the Full and Basic model forecasts for the year 2009. The spot market indicator is defined in the following manner:

$$Spot\ Market\ Indicator = \begin{cases} 1\ if\ forecast\ error \leq 0 \\ 2\ if\ forecast\ error > 0 \end{cases}$$

where $Forecast\ Error = Actual\ Load - Forecasted\ Load$

Therefore a positive forecast error implies under-production by the electric utility, necessitating its entry into the spot market (spot market indicator=2), where it pays twice as much for a unit of electricity than if it generated it (i.e., CASE B). Under this scenario we assume that the losses in the spot market are asymmetrical, depending upon whether the utility is under-producing or over-producing electricity. We incorporate this asymmetry by assuming that the loss per MW incurred by the electric utility in case of underproduction is twice the generation cost per unit of electricity

However, in absence of specific data regarding the spot market, we also assume a simple scenario where the losses per MW incurred by the electric utility in case of overproduction or underproduction are equivalent (i.e., CASE A). This means that even if the utility generates less electricity than required, it incurs a purchase price per unit of electricity in the spot market that we assume is equal to the cost of generation per unit.

3. Next, we calculate the annual cost savings using the following formula:

Annual Cost		Total losses due to		Total losses due
Savings	=	forecast errors from	-	to forecast errors
(in $)		Basic Model		in Full Model

These calculations are illustrated by Tables E1 to E4 for Case A and Tables E5 to E8 for Case B.

Table E1 : CASE A Full Model with Scrubbed Coal Technology

Month	Hours in Month (1)	Actual Load (2)	Forecast (3)	Error (4)=(2)-(3)	Spot Market Indicator (5)	Losses (6) = |(4)|x 51.5 x (1) x (5)
Jan	744	967.27	979.54	-12.28	1	470,392.88
Feb	672	962.81	976.84	-14.03	1	485,528.74
Mar	744	928.97	971.27	-42.30	1	1,620,739.31
Apr	720	966.29	1,002.88	-36.58	1	1,356,560.54
May	744	1,207.80	1,264.59	-56.79	1	2,175,860.95
Jun	720	1,285.39	1,335.60	-50.21	1	1,861,604.22
Jul	744	1,551.38	1,581.89	-30.51	1	1,169,008.29
Aug	744	1,519.35	1,535.80	-16.46	1	630,519.35
Sep	720	1,341.40	1,340.45	0.95	1	35,144.42
Oct	744	1,044.57	1,065.32	-20.75	1	794,973.79
Nov	720	934.49	984.85	-50.36	1	1,867,320.34
Dec	744	991.65	1,025.40	-33.75	1	1,293,061.46
					Total (7)	13,760,714.29

Table E2 : CASE A Basic Model with Scrubbed Coal Technology

Month	Hours in Month (1)	Actual Load (2)	Forecast (3)	Error (4)=(2)-(3)	Spot Market Indicator (5)	Losses (6) = |(4)|x 51.5 x (1) x (5)
Jan	744	967.27	999.42	-32.15	1	1,231,923.15
Feb	672	962.81	1,030.31	-67.51	1	2,336,302.41
Mar	744	928.97	1,023.75	-94.78	1	3,631,541.40
Apr	720	966.29	1,037.21	-70.91	1	2,629,418.31
May	744	1,207.80	1,077.08	130.72	1	5,008,846.07
Jun	720	1,285.39	1,258.76	26.63	1	987,589.09
Jul	744	1,551.38	1,373.64	177.74	1	6,810,308.65
Aug	744	1,519.35	1,442.72	76.62	1	2,935,918.78
Sep	720	1,341.40	1,374.30	-32.91	1	1,220,143.20
Oct	744	1,044.57	1,189.78	-145.21	1	5,563,933.74
Nov	720	934.49	1,001.04	-66.55	1	2,467,662.84
Dec	744	991.65	920.14	71.50	1	2,739,774.51
					Total (8)	37,563,362.15
					Annual Cost Savings (9)=(8)-(7)=	23,802,647.86

Table E3 : CASE A Full Model with Conventional Gas Technology

Month	Hours in Month (1)	Actual Load (2)	Forecast (3)	Error (4)=(2)-(3)	Spot Market Indicator (5)	Losses (6) = |(4)|x 106 x (1) x (5)
Jan	744	967.27	979.54	-12.28	1	968,187.29
Feb	672	962.81	976.84	-14.03	1	999,340.71
Mar	744	928.97	971.27	-42.30	1	3,335,890.62
Apr	720	966.29	1,002.88	-36.58	1	2,792,144.03
May	744	1,207.80	1,264.59	-56.79	1	4,478,471.09
Jun	720	1,285.39	1,335.60	-50.21	1	3,831,651.41
Jul	744	1,551.38	1,581.89	-30.51	1	2,406,114.14
Aug	744	1,519.35	1,535.80	-16.46	1	1,297,767.99
Sep	720	1,341.40	1,340.45	0.95	1	72,336.08
Oct	744	1,044.57	1,065.32	-20.75	1	1,636,256.73
Nov	720	934.49	984.85	-50.36	1	3,843,416.62
Dec	744	991.65	1,025.40	-33.75	1	2,661,446.88
					Total (7)	28,323,023.59

Table E4 : CASE A Basic Model with Conventional Gas Technology

Month	Hours in Month (1)	Actual Load (2)	Forecast (3)	Error (4)=(2)-(3)	Spot Market Indicator (5)	Losses (6) = |(4)|x 106 x (1) x (5)
Jan	744	967.27	999.42	-32.15	1	2,535,608.82
Feb	672	962.81	1,030.31	-67.51	1	4,808,700.11
Mar	744	928.97	1,023.75	-94.78	1	7,474,628.90
Apr	720	966.29	1,037.21	-70.91	1	5,412,006.61
May	744	1,207.80	1,077.08	130.72	1	10,309,469.59
Jun	720	1,285.39	1,258.76	26.63	1	2,032,707.65
Jul	744	1,551.38	1,373.64	177.74	1	14,017,334.31
Aug	744	1,519.35	1,442.72	76.62	1	6,042,861.95
Sep	720	1,341.40	1,374.30	-32.91	1	2,511,362.71
Oct	744	1,044.57	1,189.78	-145.21	1	11,451,980.13
Nov	720	934.49	1,001.04	-66.55	1	5,079,073.02
Dec	744	991.65	920.14	71.50	1	5,639,147.53
					Total (8)	77,314,881.33
			Annual Cost Savings (9)=(8)-(7)=			48,991,857.74

Table E5 : CASE B Full Model with Scrubbed Coal Technology

Month	Hours in Month (1)	Actual Load (2)	Forecast (3)	Error (4)=(2)-(3)	Spot Market Indicator (5)	Losses (6) = |(4)|x 51.5 x (1) x (5)
Jan	744	967.27	979.54	-12.28	1	470,392.88
Feb	672	962.81	976.84	-14.03	1	485,528.74
Mar	744	928.97	971.27	-42.30	1	1,620,739.31
Apr	720	966.29	1,002.88	-36.58	1	1,356,560.54
May	744	1,207.80	1,264.59	-56.79	1	2,175,860.95
Jun	720	1,285.39	1,335.60	-50.21	1	1,861,604.22
Jul	744	1,551.38	1,581.89	-30.51	1	1,169,008.29
Aug	744	1,519.35	1,535.80	-16.46	1	630,519.35
Sep	720	1,341.40	1,340.45	0.95	2	70,288.84
Oct	744	1,044.57	1,065.32	-20.75	1	794,973.79
Nov	720	934.49	984.85	-50.36	1	1,867,320.34
Dec	744	991.65	1,025.40	-33.75	1	1,293,061.46
					Total (7)	13,795,858.71

Table E6 : CASE B Basic Model with Scrubbed Coal Technology

Month	Hours in Month (1)	Actual Load (2)	Forecast (3)	Error (4)=(2)-(3)	Spot Market Indicator (5)	Losses (6) = |(4)|x 51.5 x (1) x (5)
Jan	744	967.27	999.42	-32.15	1	1,231,923.15
Feb	672	962.81	1,030.31	-67.51	1	2,336,302.41
Mar	744	928.97	1,023.75	-94.78	1	3,631,541.40
Apr	720	966.29	1,037.21	-70.91	1	2,629,418.31
May	744	1,207.80	1,077.08	130.72	2	10,017,692.15
Jun	720	1,285.39	1,258.76	26.63	2	1,975,178.19
Jul	744	1,551.38	1,373.64	177.74	2	13,620,617.30
Aug	744	1,519.35	1,442.72	76.62	2	5,871,837.56
Sep	720	1,341.40	1,374.30	-32.91	1	1,220,143.20
Oct	744	1,044.57	1,189.78	-145.21	1	5,563,933.74
Nov	720	934.49	1,001.04	-66.55	1	2,467,662.84
Dec	744	991.65	920.14	71.50	2	5,479,549.01
					Total (8)	56,045,799.26
			Annual Cost Savings (9)=(8)-(7)=			42,249,940.55

Table E7 : CASE B Full Model with Conventional Gas Technology

Month	Hours in Month (1)	Actual Load (2)	Forecast (3)	Error (4)=(2)-(3)	Spot Market Indicator (5)	Losses (6) = |(4)|x 106 x (1) x (5)
Jan	744	967.27	979.54	-12.28	1	968,187.29
Feb	672	962.81	976.84	-14.03	1	999,340.71
Mar	744	928.97	971.27	-42.30	1	3,335,890.62
Apr	720	966.29	1,002.88	-36.58	1	2,792,144.03
May	744	1,207.80	1,264.59	-56.79	1	4,478,471.09
Jun	720	1,285.39	1,335.60	-50.21	1	3,831,651.41
Jul	744	1,551.38	1,581.89	-30.51	1	2,406,114.14
Aug	744	1,519.35	1,535.80	-16.46	1	1,297,767.99
Sep	720	1,341.40	1,340.45	0.95	2	144,672.17
Oct	744	1,044.57	1,065.32	-20.75	1	1,636,256.73
Nov	720	934.49	984.85	-50.36	1	3,843,416.62
Dec	744	991.65	1,025.40	-33.75	1	2,661,446.88
					Total (7)	28,395,359.67

Table E8 : CASE B Basic Model with Conventional Gas Technology

Month	Hours in Month (1)	Actual Load (2)	Forecast (3)	Error (4)=(2)-(3)	Spot Market Indicator (5)	Losses (6) = |(4)|x 106 x (1) x (5)
Jan	744	967.27	999.42	-32.15	1	2,535,608.82
Feb	672	962.81	1,030.31	-67.51	1	4,808,700.11
Mar	744	928.97	1,023.75	-94.78	1	7,474,628.90
Apr	720	966.29	1,037.21	-70.91	1	5,412,006.61
May	744	1,207.80	1,077.08	130.72	2	20,618,939.18
Jun	720	1,285.39	1,258.76	26.63	2	4,065,415.30
Jul	744	1,551.38	1,373.64	177.74	2	28,034,668.62
Aug	744	1,519.35	1,442.72	76.62	2	12,085,723.91
Sep	720	1,341.40	1,374.30	-32.91	1	2,511,362.71
Oct	744	1,044.57	1,189.78	-145.21	1	11,451,980.13
Nov	720	934.49	1,001.04	-66.55	1	5,079,073.02
Dec	744	991.65	920.14	71.50	2	11,278,295.05
					Total (8)	115,356,402.36
			Annual Cost Savings (9)=(8)-(7)=			86,961,042.68

APPENDIX F Explanation of Hourly Model Dummy Variables

Variable	Description	Values
Precipdum	Precipitation dummy	=1 when precip >0 , else =0
Weekend	Weekend dummy	=1 when Saturday or Sunday, else=0
Hol	Holiday dummy	=1 when non-weekend holiday, else=0
Peakhr	Peak load hours dummy	=1 when 8 am < hours < 8 pm, else=0
Spring	Seasonal dummies	=1 when January or February, else =0
Drysummer		=1 when May or June, else =0
Monssummer		=1 when July or August, else =0
Fall		=1 when September or October or November, else =0

APPENDIX G Service Areas of AEPCO Cooperatives

The map below shows the approximate service areas of Trico,, GCEC and MEC in Arizona.

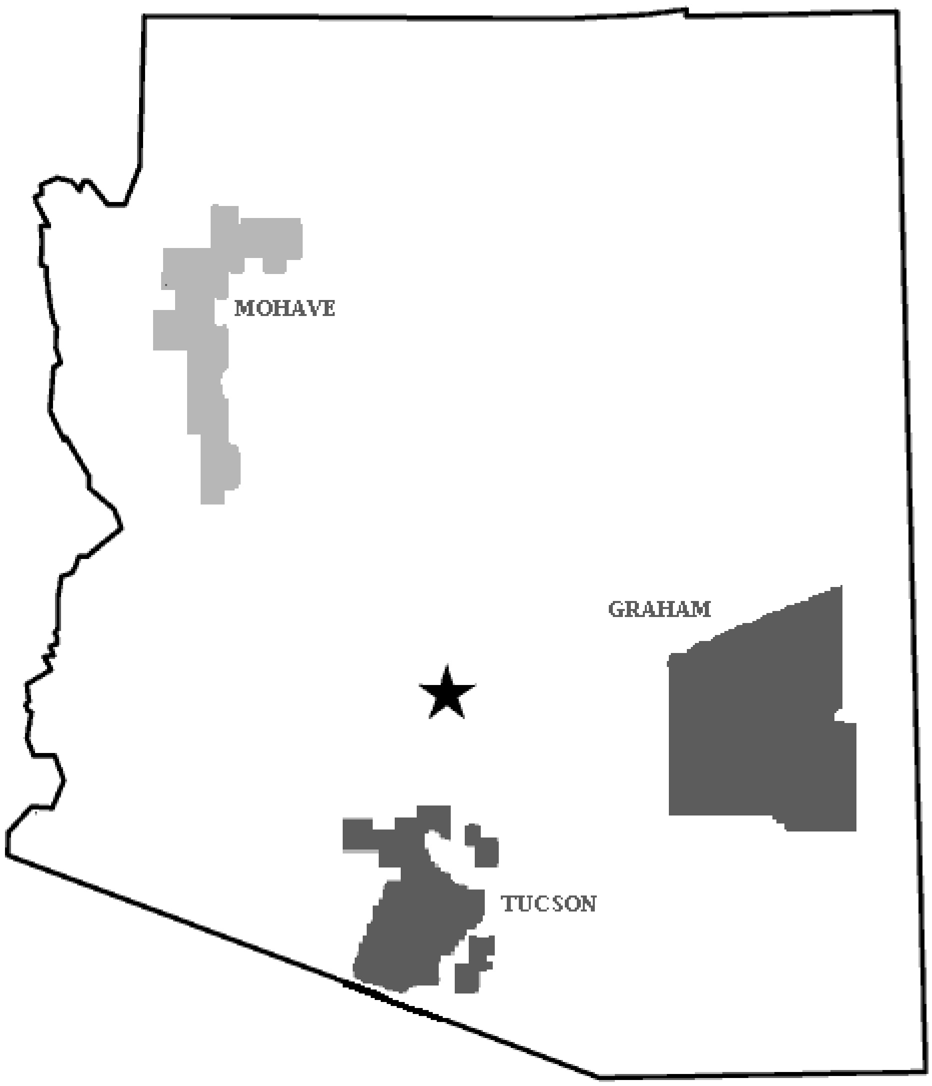

APPENDIX H Major Copper Mines Production Data

For our monthly model, we used copper mine production data in lieu of actual electricity consumed by the three major copper mines (Sierrita, Silver Bell and Mission Complex) in the TEP service area. Annual measures for these 3 mines were available for the years 2000 to 2007 using the Arizona Department of Mines and Mineral Resources Mining Update reports from 2002 to 2007. These reports also provided information regarding activities which disrupted or altered the normal monthly production at these mines. Therefore, based on this information we were able to generate monthly estimates for each of the copper mines, using not just interpolation, but also adjusting monthly averages based on reports of strikes and shutdowns. The monthly copper mining estimates from 2000 to 2007 are shown in Table H1.

Table H1: Monthly Total TEP Copper Mine Production Estimates (2000-2007) in metric tons

Month	2000	2001	2002	2003	2004	2005	2006	2007
Jan	17,913.83	15,971.28	12,688.69	9,501.13	9,693.88	9,962.21	11,492.82	12,018.14
Feb	17,913.83	15,971.28	12,688.69	9,501.13	9,693.88	9,962.21	11,492.82	12,018.14
Mar	17,913.83	15,971.28	12,688.69	9,501.13	9,693.88	9,962.21	11,492.82	12,018.14
Apr	17,913.83	15,971.28	12,688.69	9,501.13	9,693.88	9,962.21	11,492.82	12,018.14
May	17,913.83	15,971.28	12,688.69	9,501.13	9,693.88	9,962.21	11,492.82	12,018.14
Jun	17,913.83	15,971.28	12,688.69	9,501.13	9,693.88	9,962.21	11,492.82	12,018.14
Jul	17,913.83	15,971.28	7,460.32	9,501.13	9,693.88	7,796.67	11,492.82	12,018.14
Aug	17,913.83	15,971.28	7,460.32	9,501.13	9,693.88	7,796.67	11,492.82	12,018.14
Sep	17,913.83	15,971.28	7,460.32	9,501.13	9,693.88	7,796.67	11,492.82	12,018.14
Oct	17,913.83	15,971.28	7,460.32	9,501.13	9,693.88	7,796.67	11,492.82	12,018.14
Nov	17,913.83	15,971.28	7,460.32	9,501.13	9,693.88	9,962.21	11,492.82	12,018.14
Dec	17,913.83	15,971.28	12,688.69	9,501.13	9,693.88	9,962.21	11,492.82	12,018.14

As is evident, from the change in monthly production numbers, adjustments for strikes and shutdowns were made for the years 2002 and 2005. Data on shutdowns and strikes from the AZDMMR mining updates resulted in estimates of zero production at specific mines in specific months (See Tables H2 and H3).

Table H2: Monthly Total TEP Copper Mine Production Estimates (2002) in metric tons

Month	Mission	SilverBell	Sierrita	Monthly Total
Jan	5,228.38	1,700.68	5,759.64	12,688.69
Feb	5,228.38	1,700.68	5,759.64	12,688.69
Mar	5,228.38	1,700.68	5,759.64	12,688.69
Apr	5,228.38	1,700.68	5,759.64	12,688.69
May	5,228.38	1,700.68	5,759.64	12,688.69
Jun	5,228.38	1,700.68	5,759.64	12,688.69
Jul	0.00	1,700.68	5,759.64	7,460.32
Aug	0.00	1,700.68	5,759.64	7,460.32
Sep	0.00	1,700.68	5,759.64	7,460.32
Oct	0.00	1,700.68	5,759.64	7,460.32
Nov	0.00	1,700.68	5,759.64	7,460.32
Dec	5,228.38	1,700.68	5,759.64	12,688.69

Table H3: Monthly Total TEP Copper Mine Production Estimates (2005) in metric tons

Month	Mission	SilverBell	Sierrita	Monthly Total
Jan	1,802.72	2,165.53	5,993.95	9,962.21
Feb	1,802.72	2,165.53	5,993.95	9,962.21
Mar	1,802.72	2,165.53	5,993.95	9,962.21
Apr	1,802.72	2,165.53	5,993.95	9,962.21
May	1,802.72	2,165.53	5,993.95	9,962.21
Jun	1,802.72	2,165.53	5,993.95	9,962.21
Jul	1,802.72	0.00	5,993.95	7,796.67
Aug	1,802.72	0.00	5,993.95	7,796.67
Sep	1,802.72	0.00	5,993.95	7,796.67
Oct	1,802.72	0.00	5,993.95	7,796.67
Nov	1,802.72	2,165.53	5,993.95	9,962.21
Dec	1,802.72	2,165.53	5,993.95	9,962.21

For the years 2008 and 2009, copper mine production data for these 3 mines was no longer available as it had been for prior years. Therefore we utilized a different approach to obtain monthly estimates for these two years.

First, using data of total copper mine production by these 3 mines from 2000 to 2007, we estimated the annual percentage share of these 3 mines in the total annual copper mine production of the United States and Arizona. Next, we averaged this percentage share to obtain average percentage share of these 3 mines for years 2008 and 2009. This process is illustrated by Table H4.

Table H4: Estimating 2008 & 2009 National and State Share of TEP Copper Mine Production (in cubic million pounds)

Year	Sierritta	Mission	Silver Bell	Total of 3 Mines	Arizona Copper Mine Production	% Share of Arizona	US Copper Mine Production	% of US Copper Mine Production
2000	245.00	189.00	40.00	474.00	2,062.00	22.99	3,197.25	14.83
2001	241.80	138.90	41.90	422.60	1,959.80	21.56	2,954.70	14.30
2002	152.40	80.70	45.00	278.10	1,706.80	16.29	2,513.70	11.06
2003	151.20	51.60	48.60	251.40	1,640.60	15.32	2,469.60	10.18
2004	155.00	54.00	47.50	256.50	1,602.10	16.01	2,557.80	10.03
2005	158.60	38.20	47.70	244.50	1,526.20	16.02	2,513.70	9.73
2006	161.60	95.60	46.90	304.10	1,569.80	19.37	2,646.00	11.49
2007	150.00	121.30	46.70	318.00	1,619.70	19.63	2,579.85	12.33
2008					1,843.38	18.40*	2,888.55	11.74*
2009					1,567.76	18.40*	2,601.90	11.74*

*Estimated percentage based on average of 2000-2007

Finally using available 2008 and 2009 estimates of annual U.S. copper mine production and annual Arizona copper mine production, we determine annual total estimates for these 3 mines. This is shown by Table H5.

Table H5: Calculating Annual TEP Copper Mine Production (in cubic million pounds)

Year	Arizona Copper Mine Production	% Share of Arizona	Estimated Total of 3 Mines	US Copper Mine Production	% of US Copper Mine Production	Estimated Total of 3 Mines
2008	1,843.38	18.40	339.19	2,888.55	11.74	339.21
2009	1,567.76	18.40	288.47	2,601.90	11.74	305.54

Since estimates based on U.S. copper mine production were found to be more consistent with reality, we used only the following measures as annual estimates of total copper mine production for the 3 mines included in our study. Interpolation was used to obtain monthly estimates from these annual estimates.

APPENDIX I Marginal Effects for Hourly Load Forecasting Models

A. Temperature for Trico

	Sustained Shock			Initial Shock		
Time Period (t)	Before Shock	After Shock	Marginal Effect	Before Shock	After Shock	Marginal Effect
0	51.96982813	51.96920386	-0.000624273	51.96982813	51.96920386	-0.000624273
1	51.966363	51.96479753	-0.001565472	51.966363	51.96542175	-0.000941251
2	51.9628981	51.96028223	-0.002615870	51.9628981	51.96184757	-0.001050534
3	51.95943343	51.95573803	-0.003695406	51.95943343	51.95835367	-0.001079766
4	51.955969	51.95118839	-0.004780611	51.955969	51.95488347	-0.001085528
5	51.95250479	51.9466386	-0.005866186	51.95250479	51.9514188	-0.001085994
6	51.94904081	51.94208943	-0.006951385	51.94904081	51.9479551	-0.001085713
7	51.94557707	51.9375408	-0.008036265	51.94557707	51.94449158	-0.001085489
8	51.94211356	51.93299264	-0.009120919	51.94211356	51.9410282	-0.001085358
9	51.93865027	51.92844488	-0.010205388	51.93865027	51.93756501	-0.001085268
10	51.93518722	51.92389754	-0.011289686	51.93518722	51.93410203	-0.001085191
11	51.9317244	51.91935058	-0.012373816	51.9317244	51.93063928	-0.001085118
12	51.92826181	51.91480403	-0.013457778	51.92826181	51.92717676	-0.001085046
13	51.92479945	51.91025788	-0.014541573	51.92479945	51.92371448	-0.001084974
14	51.92133732	51.90571212	-0.015625202	51.92133732	51.92025242	-0.001084901
15	51.91787543	51.90116676	-0.016708662	51.91787543	51.9167906	-0.001084829
16	51.91441376	51.8966218	-0.017791956	51.91441376	51.913329	-0.001084757
17	51.91095232	51.89207724	-0.018875083	51.91095232	51.90986764	-0.001084684
18	51.90749112	51.88753308	-0.019958042	51.90749112	51.90640651	-0.001084612
19	51.90403014	51.88298931	-0.021040834	51.90403014	51.9029456	-0.001084540
20	51.9005694	51.87844594	-0.022123459	51.9005694	51.89948493	-0.001084468
21	51.89710889	51.87390297	-0.023205917	51.89710889	51.89602449	-0.001084395
22	51.89364861	51.8693604	-0.024288208	51.89364861	51.89256428	-0.001084323
23	51.89018855	51.86481822	-0.025370331	51.89018855	51.8891043	-0.001084251
24	51.88326914	51.8561957	-0.027073440	51.88326914	51.88156182	-0.001707327
25	51.87635066	51.84725832	-0.029092337	51.87635066	51.87432709	-0.002023563
26	51.86943309	51.83821339	-0.031219701	51.86943309	51.86730065	-0.002132439
27	51.86251645	51.82914081	-0.033375638	51.86251645	51.86035505	-0.002161401
28	51.85560073	51.820064	-0.035536729	51.85560073	51.85343379	-0.002166936
29	51.84868593	51.81098824	-0.037697690	51.84868593	51.84651874	-0.002167185
30	51.84177205	51.80191428	-0.039857775	51.84177205	51.83960537	-0.002166687
31	51.8348591	51.79284206	-0.042017042	51.8348591	51.83269285	-0.002166248
32	51.82794707	51.78377148	-0.044175583	51.82794707	51.82578117	-0.002165900
33	51.82103595	51.77470251	-0.046333440	51.82103595	51.81887036	-0.002165593

34	51.81412577	51.76563514	-0.048490626	51.81412577	51.81196046	-0.002165300
35	51.8072165	51.75656935	-0.050647145	51.8072165	51.80505149	-0.002165011
36	51.80030815	51.74750515	-0.052802997	51.80030815	51.79814343	-0.002164722
37	51.79340073	51.73844254	-0.054958183	51.79340073	51.79123629	-0.002164434
38	51.78649422	51.72938152	-0.057112704	51.78649422	51.78433008	-0.002164145
39	51.77958864	51.72032208	-0.059266558	51.77958864	51.77742478	-0.002163857
40	51.77268398	51.71126423	-0.061419747	51.77268398	51.77052041	-0.002163568
41	51.76578023	51.70220796	-0.063572270	51.76578023	51.76361696	-0.002163280
42	51.75887741	51.69315329	-0.065724127	51.75887741	51.75671442	-0.002162991
43	51.75197551	51.68410019	-0.067875320	51.75197551	51.74981281	-0.002162703
44	51.74507453	51.67504869	-0.070025847	51.74507453	51.74291212	-0.002162414
45	51.73817447	51.66599876	-0.072175709	51.73817447	51.73601235	-0.002162126
46	51.73127533	51.65695043	-0.074324907	51.73127533	51.7291135	-0.002161838
47	51.72437711	51.64790367	-0.076473439	51.72437711	51.72221556	-0.002161549
48	51.71403151	51.63479519	-0.079236322	51.71403151	51.71124922	-0.002782292

B. Wind Speed for Trico

	Sustained Shock			Initial Shock		
Time Period (t)	Before Shock	After Shock	Marginal Effect	Before Shock	After Shock	Marginal Effect
0	51.96982813	51.95939364	-0.010434494	51.96982813	51.95939364	-0.010434494
1	51.966363	51.94020046	-0.026162544	51.966363	51.9506311	-0.015731905
2	51.9628981	51.919188	-0.043710103	51.9628981	51.94533996	-0.017558143
3	51.95943343	51.8976948	-0.061738637	51.95943343	51.9413868	-0.018046629
4	51.955969	51.87611311	-0.079855883	51.955969	51.93782608	-0.018142919
5	51.95250479	51.85453142	-0.097973372	51.95250479	51.93435408	-0.018150711
6	51.94904081	51.83296219	-0.116078625	51.94904081	51.93089481	-0.018146006
7	51.94557707	51.81140444	-0.134172625	51.94557707	51.92743479	-0.018142277
8	51.94211356	51.78985665	-0.152256901	51.94211356	51.92397348	-0.018140077
9	51.93865027	51.76831812	-0.170332153	51.93865027	51.9205117	-0.018138573
10	51.93518722	51.74678861	-0.188398611	51.93518722	51.91704992	-0.018137296
11	51.9317244	51.72526806	-0.206456337	51.9317244	51.91358832	-0.018136077
12	51.92826181	51.70375647	-0.224505344	51.92826181	51.91012694	-0.018134868
13	51.92479945	51.68225381	-0.242545636	51.92479945	51.90666579	-0.018133660
14	51.92133732	51.66076011	-0.260577218	51.92133732	51.90320487	-0.018132452
15	51.91787543	51.63927533	-0.278600091	51.91787543	51.89974418	-0.018131243
16	51.91441376	51.6177995	-0.296614260	51.91441376	51.89628372	-0.018130034
17	51.91095232	51.59633259	-0.314619729	51.91095232	51.8928235	-0.018128825
18	51.90749112	51.57487462	-0.332616501	51.90749112	51.8893635	-0.018127616
19	51.90403014	51.55342556	-0.350604579	51.90403014	51.88590374	-0.018126408
20	51.9005694	51.53198543	-0.368583968	51.9005694	51.8824442	-0.018125199

21	51.89710889	51.51055422	-0.386554671	51.89710889	51.8789849	-0.018123991
22	51.89364861	51.48913191	-0.404516693	51.89364861	51.87552582	-0.018122782
23	51.89018855	51.46771852	-0.422470035	51.89018855	51.87206698	-0.018121574
24	51.88326914	51.43255511	-0.450714032	51.88326914	51.85473651	-0.028532634
25	51.87635066	51.39217457	-0.484176081	51.87635066	51.84253474	-0.033815912
26	51.86943309	51.3500194	-0.519413695	51.86943309	51.83379832	-0.035634766
27	51.86251645	51.30741511	-0.555101332	51.86251645	51.82639786	-0.036118587
28	51.85560073	51.26474995	-0.590850775	51.85560073	51.81938968	-0.036211042
29	51.84868593	51.22211139	-0.626574538	51.84868593	51.81247074	-0.036215193
30	51.84177205	51.17951174	-0.662260316	51.84177205	51.80556517	-0.036206878
31	51.8348591	51.13694999	-0.697909106	51.8348591	51.79865956	-0.036199537
32	51.82794707	51.09442462	-0.733522449	51.82794707	51.79175334	-0.036193722
33	51.82103595	51.05193489	-0.769101060	51.82103595	51.78484735	-0.036188602
34	51.81412577	51.00948057	-0.804645192	51.81412577	51.77794206	-0.036183709
35	51.8072165	50.96706157	-0.840154930	51.8072165	51.77103762	-0.036178874
36	51.80030815	50.92467784	-0.875630316	51.80030815	51.7641341	-0.036174050
37	51.79340073	50.88232935	-0.911071378	51.79340073	51.7572315	-0.036169228
38	51.78649422	50.84001608	-0.946478145	51.78649422	51.75032982	-0.036164405
39	51.77958864	50.79773799	-0.981850645	51.77958864	51.74342906	-0.036159583
40	51.77268398	50.75549507	-1.017188909	51.77268398	51.73652922	-0.036154761
41	51.76578023	50.71328727	-1.052492964	51.76578023	51.72963029	-0.036149940
42	51.75887741	50.67111457	-1.087762840	51.75887741	51.72273229	-0.036145120
43	51.75197551	50.62897695	-1.122998567	51.75197551	51.71583521	-0.036140300
44	51.74507453	50.58687436	-1.158200172	51.74507453	51.70893905	-0.036135481
45	51.73817447	50.54480679	-1.193367686	51.73817447	51.70204381	-0.036130662
46	51.73127533	50.5027742	-1.228501136	51.73127533	51.69514949	-0.036125844
47	51.72437711	50.46077656	-1.263600553	51.72437711	51.68825609	-0.036121027
48	51.71403151	50.40532973	-1.308701781	51.71403151	51.66754182	-0.046489686

C. Solar Radiation for Trico

	Sustained Shock			Initial Shock		
Time Period (t)	Before Shock	After Shock	Marginal Effect	Before Shock	After Shock	Marginal Effect
0	51.96982813	51.978066	0.008237871	51.96982813	51.978066	0.008237871
1	51.966363	51.98702352	0.020660518	51.966363	51.97878423	0.012421227
2	51.9628981	51.99742634	0.034528234	51.9628981	51.97676168	0.013863582
3	51.95943343	52.00821824	0.048784802	51.95943343	51.97368284	0.014249402
4	51.955969	52.01908945	0.063120454	51.955969	51.97029445	0.014325455
5	51.95250479	52.02997006	0.077465267	51.95250479	51.9668364	0.014331610
6	51.94904081	52.04085017	0.091809360	51.94904081	51.96336871	0.014327894
7	51.94557707	52.05173057	0.106153503	51.94557707	51.95990202	0.014324949

8	51.94211356	52.06261246	0.120498907	51.94211356	51.95643677	0.014323212
9	51.93865027	52.0734964	0.134846122	51.93865027	51.9529723	0.014322024
10	51.93518722	52.08438255	0.149195328	51.93518722	51.94950824	0.014321016
11	51.9317244	52.09527097	0.163546571	51.9317244	51.94604445	0.014320053
12	51.92826181	52.10616167	0.177899860	51.92826181	51.94258091	0.014319099
13	51.92479945	52.11705465	0.192255195	51.92479945	51.9391176	0.014318145
14	51.92133732	52.1279499	0.206612577	51.92133732	51.93565451	0.014317190
15	51.91787543	52.13884743	0.220972006	51.91787543	51.93219166	0.014316236
16	51.91441376	52.14974724	0.235333482	51.91441376	51.92872904	0.014315281
17	51.91095232	52.16064933	0.249697007	51.91095232	51.92526665	0.014314327
18	51.90749112	52.1715537	0.264062579	51.90749112	51.92180449	0.014313373
19	51.90403014	52.18246034	0.278430201	51.90403014	51.91834256	0.014312418
20	51.9005694	52.19336927	0.292799872	51.9005694	51.91488086	0.014311464
21	51.89710889	52.20428048	0.307171592	51.89710889	51.9114194	0.014310510
22	51.89364861	52.21519397	0.321545363	51.89364861	51.90795816	0.014309556
23	51.89018855	52.22610974	0.335921185	51.89018855	51.90449716	0.014308601
24	51.88326914	52.24182452	0.358555374	51.88326914	51.90580225	0.022533111
25	51.87635066	52.26175071	0.385400052	51.87635066	51.90305857	0.026707917
26	51.86943309	52.28313619	0.413703097	51.86943309	51.89757843	0.028145340
27	51.86251645	52.30491963	0.442403180	51.86251645	51.89104416	0.028527716
28	51.85560073	52.32678967	0.471188948	51.85560073	51.88420151	0.028600788
29	51.84868593	52.34867603	0.499990100	51.84868593	51.87729	0.028604071
30	51.84177205	52.37056876	0.528796703	51.84177205	51.87036955	0.028597502
31	51.8348591	52.39246863	0.557609533	51.8348591	51.8634508	0.028591703
32	51.82794707	52.41437688	0.586429810	51.82794707	51.85653417	0.028587109
33	51.82103595	52.43629405	0.615258092	51.82103595	51.84961902	0.028583065
34	51.81412577	52.45822033	0.644094563	51.81412577	51.84270497	0.028579200
35	51.8072165	52.48015577	0.672939274	51.8072165	51.83579188	0.028575382
36	51.80030815	52.50210039	0.701792235	51.80030815	51.82887972	0.028571572
37	51.79340073	52.52405418	0.730653453	51.79340073	51.82196849	0.028567762
38	51.78649422	52.54601715	0.759522929	51.78649422	51.81505818	0.028563953
39	51.77958864	52.56798931	0.788400669	51.77958864	51.80814878	0.028560145
40	51.77268398	52.58997065	0.817286675	51.77268398	51.80124031	0.028556336
41	51.76578023	52.61196119	0.846180953	51.76578023	51.79433276	0.028552528
42	51.75887741	52.63396092	0.875083505	51.75887741	51.78742613	0.028548721
43	51.75197551	52.65596985	0.903994336	51.75197551	51.78052043	0.028544914
44	51.74507453	52.67798798	0.932913449	51.74507453	51.77361564	0.028541108
45	51.73817447	52.70001532	0.961840850	51.73817447	51.76671177	0.028537302
46	51.73127533	52.72205187	0.990776541	51.73127533	51.75980883	0.028533496
47	51.72437711	52.74409764	1.019720526	51.72437711	51.7529068	0.028529692
48	51.71403151	52.77099794	1.056966429	51.71403151	51.75075734	0.036725830

D. Relative Humidity for Trico

	Sustained Shock			Initial Shock		
Time Period (t)	Before Shock	After Shock	Marginal Effect	Before Shock	After Shock	Marginal Effect
0	51.96982813	51.96970413	-0.000124007	51.96982813	51.96970413	-0.000124007
1	51.966363	51.96605203	-0.000310971	51.966363	51.96617603	-0.000186973
2	51.9628981	51.96237847	-0.000519630	51.9628981	51.96268942	-0.000208681
3	51.95943343	51.95869935	-0.000734082	51.95943343	51.95921895	-0.000214488
4	51.955969	51.95501933	-0.000949662	51.955969	51.95575336	-0.000215633
5	51.95250479	51.95133947	-0.001165320	51.95250479	51.95228906	-0.000215725
6	51.94904081	51.94765991	-0.001380907	51.94904081	51.94882514	-0.000215669
7	51.94557707	51.94398064	-0.001596434	51.94557707	51.94536144	-0.000215625
8	51.94211356	51.94030164	-0.001811920	51.94211356	51.94189796	-0.000215599
9	51.93865027	51.9366229	-0.002027372	51.93865027	51.93843469	-0.000215581
10	51.93518722	51.93294443	-0.002242794	51.93518722	51.93497166	-0.000215566
11	51.9317244	51.92926621	-0.002458187	51.9317244	51.93150885	-0.000215551
12	51.92826181	51.92558826	-0.002673549	51.92826181	51.92804627	-0.000215537
13	51.92479945	51.92191057	-0.002888883	51.92479945	51.92458393	-0.000215523
14	51.92133732	51.91823314	-0.003104186	51.92133732	51.92112181	-0.000215508
15	51.91787543	51.91455597	-0.003319460	51.91787543	51.91765993	-0.000215494
16	51.91441376	51.91087905	-0.003534704	51.91441376	51.91419828	-0.000215479
17	51.91095232	51.9072024	-0.003749919	51.91095232	51.91073686	-0.000215465
18	51.90749112	51.90352601	-0.003965104	51.90749112	51.90727567	-0.000215451
19	51.90403014	51.89984988	-0.004180260	51.90403014	51.90381471	-0.000215436
20	51.9005694	51.89617401	-0.004395385	51.9005694	51.90035398	-0.000215422
21	51.89710889	51.89249841	-0.004610482	51.89710889	51.89689348	-0.000215408
22	51.89364861	51.88882306	-0.004825548	51.89364861	51.89343321	-0.000215393
23	51.89018855	51.88514797	-0.005040585	51.89018855	51.88997317	-0.000215379
24	51.88326914	51.87789011	-0.005379031	51.88326914	51.88292999	-0.000339150
25	51.87635066	51.87057041	-0.005780241	51.87635066	51.87594869	-0.000401970
26	51.86943309	51.86323007	-0.006203021	51.86943309	51.86900949	-0.000423598
27	51.86251645	51.85588495	-0.006631493	51.86251645	51.8620871	-0.000429351
28	51.85560073	51.84853972	-0.007061005	51.85560073	51.85517028	-0.000430450
29	51.84868593	51.84119542	-0.007490504	51.84868593	51.84825543	-0.000430500
30	51.84177205	51.83385221	-0.007919844	51.84177205	51.84134165	-0.000430401
31	51.8348591	51.82651006	-0.008349036	51.8348591	51.83442878	-0.000430314
32	51.82794707	51.81916897	-0.008778098	51.82794707	51.82751682	-0.000430245
33	51.82103595	51.81182892	-0.009207038	51.82103595	51.82060577	-0.000430184
34	51.81412577	51.80448991	-0.009635859	51.81412577	51.81369564	-0.000430125
35	51.8072165	51.79715194	-0.010064562	51.8072165	51.80678643	-0.000430068
36	51.80030815	51.789815	-0.010493148	51.80030815	51.79987814	-0.000430011
37	51.79340073	51.78247911	-0.010921615	51.79340073	51.79297077	-0.000429953

38	51.78649422	51.77514426	-0.011349964	51.78649422	51.78606433	-0.000429896
39	51.77958864	51.76781044	-0.011778195	51.77958864	51.7791588	-0.000429839
40	51.77268398	51.76047767	-0.012206308	51.77268398	51.77225419	-0.000429781
41	51.76578023	51.75314593	-0.012634303	51.76578023	51.76535051	-0.000429724
42	51.75887741	51.74581523	-0.013062180	51.75887741	51.75844775	-0.000429667
43	51.75197551	51.73848557	-0.013489939	51.75197551	51.7515459	-0.000429609
44	51.74507453	51.73115695	-0.013917580	51.74507453	51.74464498	-0.000429552
45	51.73817447	51.72382937	-0.014345104	51.73817447	51.73774498	-0.000429495
46	51.73127533	51.71650282	-0.014772510	51.73127533	51.7308459	-0.000429438
47	51.72437711	51.70917732	-0.015199797	51.72437711	51.72394773	-0.000429380
48	51.71403151	51.69828222	-0.015749285	51.71403151	51.71347882	-0.000552690

E. Temperature for Graham

	Sustained Shock			Initial Shock		
Time Period (t)	Before Shock	After Shock	Marginal Effect	Before Shock	After Shock	Marginal Effect
0	18.46234771	18.46233048	-0.000017230	18.46234771	18.46233048	-0.000017230
1	18.47094156	18.47090693	-0.000034638	18.47094156	18.47092416	-0.000017401
2	18.47953942	18.47948842	-0.000050992	18.47953942	18.47952308	-0.000016337
3	18.48814127	18.48807393	-0.000067340	18.48814127	18.48812494	-0.000016325
4	18.49674713	18.49666336	-0.000083770	18.49674713	18.49673073	-0.000016399
5	18.50535699	18.50525677	-0.000100217	18.50535699	18.50534058	-0.000016408
6	18.51397086	18.51385419	-0.000116675	18.51397086	18.51395445	-0.000016412
7	18.52258874	18.5224556	-0.000133148	18.52258874	18.52257232	-0.000016419
8	18.53121064	18.531061	-0.000149637	18.53121064	18.53119421	-0.000016427
9	18.53983654	18.5396704	-0.000166142	18.53983654	18.53982011	-0.000016435
10	18.54846646	18.5482838	-0.000182661	18.54846646	18.54845002	-0.000016442
11	18.5571004	18.55690121	-0.000199196	18.5571004	18.55708395	-0.000016450
12	18.56573836	18.56552261	-0.000215746	18.56573836	18.5657219	-0.000016458
13	18.57438034	18.57414803	-0.000232312	18.57438034	18.57436387	-0.000016465
14	18.58302634	18.58277744	-0.000248893	18.58302634	18.58300986	-0.000016473
15	18.59167636	18.59141087	-0.000265489	18.59167636	18.59165988	-0.000016481
16	18.60033041	18.60004831	-0.000282101	18.60033041	18.60031393	-0.000016488
17	18.60898849	18.60868977	-0.000298728	18.60898849	18.608972	-0.000016496
18	18.6176506	18.61733523	-0.000315370	18.6176506	18.6176341	-0.000016504
19	18.62631675	18.62598472	-0.000332028	18.62631675	18.62630023	-0.000016511
20	18.63498692	18.63463822	-0.000348701	18.63498692	18.6349704	-0.000016519
21	18.64366113	18.64329574	-0.000365390	18.64366113	18.64364461	-0.000016527
22	18.65233938	18.65195729	-0.000382094	18.65233938	18.65232285	-0.000016534

23	18.66102167	18.66062286	-0.000398814	18.66102167	18.66100513	-0.000016542
24	18.67839838	18.6779652	-0.000433173	18.67839838	18.67836439	-0.000033989
25	18.69579126	18.6953235	-0.000467761	18.69579126	18.69575708	-0.000034185
26	18.71320034	18.71269901	-0.000501328	18.71320034	18.71316721	-0.000033132
27	18.73062563	18.7300907	-0.000534937	18.73062563	18.73059249	-0.000033142
28	18.74806715	18.74749848	-0.000568674	18.74806715	18.74803391	-0.000033241
29	18.76552491	18.76492243	-0.000602477	18.76552491	18.76549164	-0.000033274
30	18.78299892	18.78236259	-0.000636337	18.78299892	18.78296562	-0.000033300
31	18.80048921	18.79981895	-0.000670260	18.80048921	18.80045588	-0.000033331
32	18.81799578	18.81729154	-0.000704245	18.81799578	18.81796242	-0.000033363
33	18.83551866	18.83478036	-0.000738293	18.83551866	18.83548526	-0.000033394
34	18.85305785	18.85228545	-0.000772404	18.85305785	18.85302442	-0.000033425
35	18.87061337	18.86980679	-0.000806578	18.87061337	18.87057992	-0.000033456
36	18.88818524	18.88734443	-0.000840814	18.88818524	18.88815176	-0.000033487
37	18.90577348	18.90489836	-0.000875114	18.90577348	18.90573996	-0.000033518
38	18.92337809	18.92246861	-0.000909477	18.92337809	18.92334454	-0.000033549
39	18.94099909	18.94005519	-0.000943903	18.94099909	18.94096551	-0.000033581
40	18.9586365	18.95765811	-0.000978392	18.9586365	18.95860289	-0.000033612
41	18.97629034	18.9752774	-0.001012944	18.97629034	18.9762567	-0.000033643
42	18.99396062	18.99291306	-0.001047560	18.99396062	18.99392694	-0.000033675
43	19.01164734	19.0105651	-0.001082240	19.01164734	19.01161364	-0.000033706
44	19.02935054	19.02823356	-0.001116983	19.02935054	19.02931681	-0.000033737
45	19.04707023	19.04591844	-0.001151790	19.04707023	19.04703646	-0.000033769
46	19.06480641	19.06361975	-0.001186660	19.06480641	19.06477261	-0.000033800
47	19.08255911	19.08133751	-0.001221595	19.08255911	19.08252528	-0.000033832
48	19.10921916	19.10794415	-0.001275010	19.10921916	19.10916744	-0.000051712

F. Relative Humidity for Graham

	Sustained Shock			Initial Shock		
Time Period (t)	Before Shock	After Shock	Marginal Effect	Before Shock	After Shock	Marginal Effect
0	18.46234771	18.46235123	0.000003515	18.46234771	18.46235123	0.000003515
1	18.47094156	18.47094863	0.000007067	18.47094156	18.47094511	0.000003550
2	18.47953942	18.47954982	0.000010403	18.47953942	18.47954275	0.000003333
3	18.48814127	18.48815501	0.000013738	18.48814127	18.4881446	0.000003330
4	18.49674713	18.49676422	0.000017090	18.49674713	18.49675047	0.000003346
5	18.50535699	18.50537744	0.000020446	18.50535699	18.50536034	0.000003347
6	18.51397086	18.51399467	0.000023803	18.51397086	18.51397421	0.000003348
7	18.52258874	18.52261591	0.000027164	18.52258874	18.52259209	0.000003350

8	18.53121064	18.53124116	0.000030528	18.53121064	18.53121399	0.000003351
9	18.53983654	18.53987044	0.000033895	18.53983654	18.5398399	0.000003353
10	18.54846646	18.54850373	0.000037265	18.54846646	18.54846982	0.000003354
11	18.5571004	18.55714104	0.000040639	18.5571004	18.55710376	0.000003356
12	18.56573836	18.56578237	0.000044015	18.56573836	18.56574172	0.000003358
13	18.57438034	18.57442773	0.000047395	18.57438034	18.5743837	0.000003359
14	18.58302634	18.58307711	0.000050778	18.58302634	18.5830297	0.000003361
15	18.59167636	18.59173053	0.000054164	18.59167636	18.59167972	0.000003362
16	18.60033041	18.60038797	0.000057553	18.60033041	18.60033378	0.000003364
17	18.60898849	18.60904944	0.000060945	18.60898849	18.60899186	0.000003365
18	18.6176506	18.61771494	0.000064340	18.6176506	18.61765397	0.000003367
19	18.62631675	18.62638448	0.000067739	18.62631675	18.62632011	0.000003369
20	18.63498692	18.63505806	0.000071140	18.63498692	18.63499029	0.000003370
21	18.64366113	18.64373568	0.000074545	18.64366113	18.6436645	0.000003372
22	18.65233938	18.65241734	0.000077953	18.65233938	18.65234276	0.000003373
23	18.66102167	18.66110304	0.000081364	18.66102167	18.66102505	0.000003375
24	18.67839838	18.67848675	0.000088374	18.67839838	18.67840531	0.000006934
25	18.69579126	18.69588669	0.000095431	18.69579126	18.69579823	0.000006974
26	18.71320034	18.71330262	0.000102279	18.71320034	18.7132071	0.000006759
27	18.73062563	18.73073477	0.000109136	18.73062563	18.73063239	0.000006761
28	18.74806715	18.74818317	0.000116019	18.74806715	18.74807393	0.000006782
29	18.76552491	18.76564782	0.000122915	18.76552491	18.7655317	0.000006788
30	18.78299892	18.78312875	0.000129823	18.78299892	18.78300572	0.000006794
31	18.80048921	18.80062595	0.000136744	18.80048921	18.80049601	0.000006800
32	18.81799578	18.81813946	0.000143678	18.81799578	18.81800259	0.000006806
33	18.83551866	18.83566928	0.000150625	18.83551866	18.83552547	0.000006813
34	18.85305785	18.85321543	0.000157584	18.85305785	18.85306467	0.000006819
35	18.87061337	18.87077793	0.000164556	18.87061337	18.8706202	0.000006825
36	18.88818524	18.88835679	0.000171541	18.88818524	18.88819208	0.000006832
37	18.90577348	18.90595202	0.000178539	18.90577348	18.90578032	0.000006838
38	18.92337809	18.92356364	0.000185550	18.92337809	18.92338493	0.000006845
39	18.94099909	18.94119167	0.000192574	18.94099909	18.94100594	0.000006851
40	18.9586365	18.95883612	0.000199611	18.9586365	18.95864336	0.000006857
41	18.97629034	18.976497	0.000206660	18.97629034	18.9762972	0.000006864
42	18.99396062	18.99417434	0.000213723	18.99396062	18.99396749	0.000006870
43	19.01164734	19.01186814	0.000220798	19.01164734	19.01165422	0.000006876
44	19.02935054	19.02957843	0.000227887	19.02935054	19.02935743	0.000006883
45	19.04707023	19.04730521	0.000234988	19.04707023	19.04707712	0.000006889
46	19.06480641	19.06504851	0.000242103	19.06480641	19.0648133	0.000006896
47	19.08255911	19.08280834	0.000249230	19.08255911	19.08256601	0.000006902
48	19.10921916	19.10947929	0.000260129	19.10921916	19.10922971	0.000010550

G. Solar Radiation for Graham

	Sustained Shock			Initial Shock		
Time Period (t)	Before Shock	After Shock	Marginal Effect	Before Shock	After Shock	Marginal Effect
0	18.46234771	18.46406405	0.001716340	18.46234771	18.46406405	0.001716340
1	18.47094156	18.47439222	0.003450659	18.47094156	18.47267492	0.001733359
2	18.47953942	18.48461941	0.005079993	18.47953942	18.48116684	0.001627424
3	18.48814127	18.49485024	0.006708967	18.48814127	18.48976743	0.001626163
4	18.49674713	18.50509336	0.008346231	18.49674713	18.49838068	0.001633548
5	18.50535699	18.51534234	0.009985351	18.50535699	18.50699149	0.001634497
6	18.51397086	18.52559659	0.011625728	18.51397086	18.51560571	0.001634847
7	18.52258874	18.5358565	0.013267759	18.52258874	18.52422434	0.001635592
8	18.53121064	18.54612212	0.014911486	18.53121064	18.53284702	0.001636379
9	18.53983654	18.55639343	0.016556886	18.53983654	18.54147368	0.001637142
10	18.54846646	18.56667042	0.018203958	18.54846646	18.55010437	0.001637902
11	18.5571004	18.57695311	0.019852705	18.5571004	18.55873907	0.001638665
12	18.56573836	18.58724149	0.021503127	18.56573836	18.56737779	0.001639428
13	18.57438034	18.59753556	0.023155227	18.57438034	18.57602053	0.001640191
14	18.58302634	18.60783534	0.024809005	18.58302634	18.58466729	0.001640954
15	18.59167636	18.61814083	0.026464463	18.59167636	18.59331808	0.001641718
16	18.60033041	18.62845202	0.028121602	18.60033041	18.6019729	0.001642482
17	18.60898849	18.63876892	0.029780423	18.60898849	18.61063174	0.001643247
18	18.6176506	18.64909153	0.031440928	18.6176506	18.61929462	0.001644012
19	18.62631675	18.65941986	0.033103117	18.62631675	18.62796152	0.001644777
20	18.63498692	18.66975391	0.034766993	18.63498692	18.63663246	0.001645543
21	18.64366113	18.68009369	0.036432557	18.64366113	18.64530744	0.001646308
22	18.65233938	18.69043919	0.038099809	18.65233938	18.65398646	0.001647075
23	18.66102167	18.70079042	0.039768751	18.66102167	18.66266951	0.001647841
24	18.67839838	18.72159733	0.043198952	18.67839838	18.68178433	0.003385954
25	18.69579126	18.74244384	0.046652580	18.69579126	18.69919679	0.003405526
26	18.71320034	18.7632052	0.050004855	18.71320034	18.71650094	0.003300596
27	18.73062563	18.7839875	0.053361865	18.73062563	18.73392726	0.003301624
28	18.74806715	18.80479956	0.056732406	18.74806715	18.75137857	0.003311418
29	18.76552491	18.82563487	0.060109957	18.76552491	18.7688396	0.003314692
30	18.78299892	18.84649284	0.063493918	18.78299892	18.78631629	0.003317362
31	18.80048921	18.86737391	0.066884701	18.80048921	18.80380965	0.003320435
32	18.81799578	18.88827814	0.070282360	18.81799578	18.82131934	0.003323553
33	18.83551866	18.90920554	0.073686878	18.83551866	18.83884531	0.003326649
34	18.85305785	18.93015611	0.077098265	18.85305785	18.85638759	0.003329745
35	18.87061337	18.95112991	0.080516532	18.87061337	18.87394622	0.003332846
36	18.88818524	18.97212693	0.083941690	18.88818524	18.89152119	0.003335949
37	18.90577348	18.99314723	0.087373750	18.90577348	18.90911253	0.003339055

38	18.92337809	19.01419081	0.090812721	18.92337809	18.92672025	0.003342165
39	18.94099909	19.03525771	0.094258614	18.94099909	18.94434437	0.003345277
40	18.9586365	19.05634795	0.097711440	18.9586365	18.9619849	0.003348392
41	18.97629034	19.07746155	0.101171210	18.97629034	18.97964185	0.003351510
42	18.99396062	19.09859855	0.104637934	18.99396062	18.99731525	0.003354631
43	19.01164734	19.11975897	0.108111623	19.01164734	19.0150051	0.003357754
44	19.02935054	19.14094283	0.111592287	19.02935054	19.03271142	0.003360881
45	19.04707023	19.16215016	0.115079937	19.04707023	19.05043424	0.003364011
46	19.06480641	19.18338099	0.118574584	19.06480641	19.06817355	0.003367143
47	19.08255911	19.20463535	0.122076238	19.08255911	19.08592939	0.003370279
48	19.10921916	19.23665068	0.127431523	19.10921916	19.11437093	0.005151777

H. Temperature for Mohave

	Sustained Shock			Initial Shock		
Time Period (t)	Before Shock	After Shock	Marginal Effect	Before Shock	After Shock	Marginal Effect
0	68.21617315	68.21469534	-0.001477810	68.21617315	68.21469534	-0.001477810
1	68.21105236	68.20739488	-0.003657483	68.21105236	68.20739488	-0.003657483
2	68.20593196	68.19988159	-0.006050368	68.20593196	68.19988159	-0.006050368
3	68.20081194	68.19232464	-0.008487298	68.20081194	68.19232464	-0.008487298
4	68.19569231	68.18476474	-0.010927570	68.19569231	68.18476474	-0.010927570
5	68.19057306	68.17720748	-0.013365580	68.19057306	68.17720748	-0.013365580
6	68.1854542	68.16965223	-0.015801970	68.1854542	68.16965223	-0.015801970
7	68.18033572	68.16209822	-0.018237498	68.18033572	68.16209822	-0.018237498
8	68.17521762	68.15454515	-0.020672475	68.17521762	68.15454515	-0.020672475
9	68.17009991	68.14699293	-0.023106985	68.17009991	68.14699293	-0.023106985
10	68.16498258	68.13944154	-0.025541044	68.16498258	68.13944154	-0.025541044
11	68.15986564	68.13189099	-0.027974653	68.15986564	68.13189099	-0.027974653
12	68.15474908	68.12434127	-0.030407809	68.15474908	68.12434127	-0.030407809
13	68.14963291	68.1167924	-0.032840513	68.14963291	68.1167924	-0.032840513
14	68.14451712	68.10924435	-0.035272764	68.14451712	68.10924435	-0.035272764
15	68.13940171	68.10169715	-0.037704564	68.13940171	68.10169715	-0.037704564
16	68.13428669	68.09415078	-0.040135910	68.13428669	68.09415078	-0.040135910
17	68.12917205	68.08660524	-0.042566805	68.12917205	68.08660524	-0.042566805
18	68.1240578	68.07906055	-0.044997248	68.1240578	68.07906055	-0.044997248
19	68.11894392	68.07151669	-0.047427238	68.11894392	68.07151669	-0.047427238
20	68.11383044	68.06397366	-0.049856776	68.11383044	68.06397366	-0.049856776
21	68.10871733	68.05643147	-0.052285863	68.10871733	68.05643147	-0.052285863
22	68.10360462	68.04889012	-0.054714497	68.10360462	68.04889012	-0.054714497

23	68.09849228	68.0413496	-0.057142679	68.09849228	68.0413496	-0.057142679
24	68.08826876	68.02722907	-0.061039687	68.08826876	68.02722907	-0.061039687
25	68.07804678	68.01241137	-0.065635409	68.07804678	68.01241137	-0.065635409
26	68.06782633	67.99738391	-0.070442412	68.06782633	67.99738391	-0.070442412
27	68.05760741	67.98231543	-0.075291981	68.05760741	67.98231543	-0.075291981
28	68.04739003	67.9672465	-0.080143528	68.04739003	67.9672465	-0.080143528
29	68.03717418	67.95218271	-0.084991466	68.03717418	67.95218271	-0.084991466
30	68.02695987	67.93712343	-0.089836436	68.02695987	67.93712343	-0.089836436
31	68.01674709	67.92206789	-0.094679196	68.01674709	67.92206789	-0.094679196
32	68.00653584	67.90701578	-0.099520054	68.00653584	67.90701578	-0.099520054
33	67.99632612	67.89196703	-0.104359095	67.99632612	67.89196703	-0.104359095
34	67.98611794	67.87692161	-0.109196335	67.98611794	67.87692161	-0.109196335
35	67.97591129	67.86187952	-0.114031776	67.97591129	67.86187952	-0.114031776
36	67.96570618	67.84684076	-0.118865416	67.96570618	67.84684076	-0.118865416
37	67.95550259	67.83180534	-0.123697256	67.95550259	67.83180534	-0.123697256
38	67.94530054	67.81677324	-0.128527296	67.94530054	67.81677324	-0.128527296
39	67.93510002	67.80174448	-0.133355536	67.93510002	67.80174448	-0.133355536
40	67.92490103	67.78671905	-0.138181977	67.92490103	67.78671905	-0.138181977
41	67.91470357	67.77169695	-0.143006620	67.91470357	67.77169695	-0.143006620
42	67.90450764	67.75667818	-0.147829464	67.90450764	67.75667818	-0.147829464
43	67.89431325	67.74166273	-0.152650511	67.89431325	67.74166273	-0.152650511
44	67.88412038	67.72665062	-0.157469760	67.88412038	67.72665062	-0.157469760
45	67.87392904	67.71164183	-0.162287213	67.87392904	67.71164183	-0.162287213
46	67.86373924	67.69663637	-0.167102870	67.86373924	67.69663637	-0.167102870
47	67.85355096	67.68163423	-0.171916732	67.85355096	67.68163423	-0.171916732
48	67.83827141	67.66009009	-0.178181327	67.83827141	67.66009009	-0.178181327

I. Relative Humidity for Mohave

	Sustained Shock			Initial Shock		
Time Period (t)	Before Shock	After Shock	Marginal Effect	Before Shock	After Shock	Marginal Effect
0	68.21617315	68.21561821	-0.000554932	68.21617315	68.21561821	-0.000554932
1	68.21105236	68.20967893	-0.001373434	68.21105236	68.21023381	-0.000818550
2	68.20593196	68.20365994	-0.002272019	68.20593196	68.20503325	-0.000898707
3	68.20081194	68.19762478	-0.003187165	68.20081194	68.1998966	-0.000915346
4	68.19569231	68.19158872	-0.004103586	68.19569231	68.19477561	-0.000916703
5	68.19057306	68.18555388	-0.005019178	68.19057306	68.18965711	-0.000915955
6	68.1854542	68.17952002	-0.005934181	68.1854542	68.18453875	-0.000915448
7	68.18033572	68.17348684	-0.006848882	68.18033572	68.17942049	-0.000915226

8	68.17521762	68.16745423	-0.007763397	68.17521762	68.1743025	-0.000915120
9	68.17009991	68.16142216	-0.008677756	68.17009991	68.16918487	-0.000915046
10	68.16498258	68.15539062	-0.009591966	68.16498258	68.16406761	-0.000914978
11	68.15986564	68.14935961	-0.010506027	68.15986564	68.15895073	-0.000914910
12	68.15474908	68.14332914	-0.011419940	68.15474908	68.15383424	-0.000914842
13	68.14963291	68.13729921	-0.012333702	68.14963291	68.14871814	-0.000914773
14	68.14451712	68.1312698	-0.013247315	68.14451712	68.14360241	-0.000914704
15	68.13940171	68.12524093	-0.014160779	68.13940171	68.13848708	-0.000914636
16	68.13428669	68.1192126	-0.015074093	68.13428669	68.13337212	-0.000914567
17	68.12917205	68.11318479	-0.015987257	68.12917205	68.12825755	-0.000914498
18	68.1240578	68.10715752	-0.016900273	68.1240578	68.12314337	-0.000914430
19	68.11894392	68.10113079	-0.017813138	68.11894392	68.11802956	-0.000914361
20	68.11383044	68.09510458	-0.018725855	68.11383044	68.11291614	-0.000914293
21	68.10871733	68.08907891	-0.019638421	68.10871733	68.10780311	-0.000914224
22	68.10360462	68.08305378	-0.020550839	68.10360462	68.10269046	-0.000914155
23	68.09849228	68.07702917	-0.021463107	68.09849228	68.09757819	-0.000914087
24	68.08826876	68.0653415	-0.022927256	68.08826876	68.08680093	-0.001467833
25	68.07804678	68.05339279	-0.024653986	68.07804678	68.07631602	-0.001730755
26	68.06782633	68.04136615	-0.026460179	68.06782633	68.06601578	-0.001810550
27	68.05760741	68.02932496	-0.028282447	68.05760741	68.05578046	-0.001826950
28	68.04739003	68.01728449	-0.030105539	68.04739003	68.04556193	-0.001828098
29	68.03717418	68.00524682	-0.031927357	68.03717418	68.03534703	-0.001827146
30	68.02695987	67.99321173	-0.033748141	68.02695987	68.02513343	-0.001826434
31	68.01674709	67.98117891	-0.035568176	68.01674709	68.01492108	-0.001826007
32	68.00653584	67.96914826	-0.037387577	68.00653584	68.00471014	-0.001825696
33	67.99632612	67.95711975	-0.039206378	67.99632612	67.99450071	-0.001825417
34	67.98611794	67.94509336	-0.041024583	67.98611794	67.9842928	-0.001825143
35	67.97591129	67.9330691	-0.042842192	67.97591129	67.97408642	-0.001824870
36	67.96570618	67.92104697	-0.044659207	67.96570618	67.96388158	-0.001824596
37	67.95550259	67.90902697	-0.046475626	67.95550259	67.95367827	-0.001824322
38	67.94530054	67.89700909	-0.048291450	67.94530054	67.94347649	-0.001824049
39	67.93510002	67.88499334	-0.050106678	67.93510002	67.93327624	-0.001823775
40	67.92490103	67.87297972	-0.051921312	67.92490103	67.92307753	-0.001823501
41	67.91470357	67.86096822	-0.053735350	67.91470357	67.91288034	-0.001823227
42	67.90450764	67.84895885	-0.055548794	67.90450764	67.90268469	-0.001822953
43	67.89431325	67.8369516	-0.057361643	67.89431325	67.89249057	-0.001822680
44	67.88412038	67.82494648	-0.059173898	67.88412038	67.88229797	-0.001822406
45	67.87392904	67.81294348	-0.060985559	67.87392904	67.87210691	-0.001822132
46	67.86373924	67.80094261	-0.062796625	67.86373924	67.86191738	-0.001821859
47	67.85355096	67.78894386	-0.064607097	67.85355096	67.85172937	-0.001821585
48	67.83827141	67.77130811	-0.066963307	67.83827141	67.83589839	-0.002373018

J. Solar Radiation for Mohave

	Sustained Shock			Initial Shock		
Time Period (t)	Before Shock	After Shock	Marginal Effect	Before Shock	After Shock	Marginal Effect
0	68.21617315	68.22927873	0.013105586	68.21617315	68.22927873	0.013105586
1	68.21105236	68.24349294	0.032440583	68.21105236	68.23038463	0.019332267
2	68.20593196	68.25960588	0.053673921	68.20593196	68.22715764	0.021225679
3	68.20081194	68.27611759	0.075305652	68.20081194	68.22243069	0.021618747
4	68.19569231	68.29266701	0.096974701	68.19569231	68.21734311	0.021650796
5	68.19057306	68.30920437	0.118631310	68.19057306	68.21220619	0.021633126
6	68.1854542	68.32573536	0.140281165	68.1854542	68.20707534	0.021621146
7	68.18033572	68.34226673	0.161931011	68.18033572	68.20195162	0.021615905
8	68.17521762	68.35880121	0.183583592	68.17521762	68.19683103	0.021613404
9	68.17009991	68.37533958	0.205239665	68.17009991	68.19171157	0.021611658
10	68.16498258	68.39188195	0.226899368	68.16498258	68.18659263	0.021610048
11	68.15986564	68.40842835	0.248562705	68.15986564	68.18147408	0.021608442
12	68.15474908	68.42497875	0.270229668	68.15474908	68.17635591	0.021606827
13	68.14963291	68.44153316	0.291900252	68.14963291	68.17123811	0.021605207
14	68.14451712	68.45809158	0.313574458	68.14451712	68.1661207	0.021603585
15	68.13940171	68.474654	0.335252286	68.13940171	68.16100367	0.021601963
16	68.13428669	68.49122043	0.356933737	68.13428669	68.15588703	0.021600342
17	68.12917205	68.50779086	0.378618812	68.12917205	68.15077077	0.021598720
18	68.1240578	68.52436531	0.400307513	68.1240578	68.14565489	0.021597099
19	68.11894392	68.54094376	0.421999839	68.11894392	68.1405394	0.021595478
20	68.11383044	68.55752623	0.443695792	68.11383044	68.13542429	0.021593857
21	68.10871733	68.57411271	0.465395373	68.10871733	68.13030957	0.021592236
22	68.10360462	68.5907032	0.487098583	68.10360462	68.12519523	0.021590615
23	68.09849228	68.6072977	0.508805423	68.09849228	68.12008127	0.021588994
24	68.08826876	68.63192776	0.543658997	68.08826876	68.12293967	0.034670913
25	68.07804678	68.66283379	0.584787015	68.07804678	68.11892997	0.040883200
26	68.06782633	68.69566162	0.627835291	68.06782633	68.11059501	0.042768688
27	68.05760741	68.72890273	0.671295319	68.05760741	68.10076363	0.043156225
28	68.04739003	68.76219387	0.714803838	68.04739003	68.09057338	0.043183355
29	68.03717418	68.79548495	0.758310767	68.03717418	68.08033504	0.043160859
30	68.02695987	68.8287817	0.801821830	68.02695987	68.07010391	0.043144043
31	68.01674709	68.86209091	0.845343822	68.01674709	68.05988104	0.043133956
32	68.00653584	68.89541535	0.888879513	68.00653584	68.04966244	0.043126604
33	67.99632612	68.9287558	0.932429673	67.99632612	68.03944613	0.043120006
34	67.98611794	68.96211239	0.975994447	67.98611794	68.02923149	0.043113545
35	67.97591129	68.99548514	1.019573847	67.97591129	68.01901838	0.043107088
36	67.96570618	69.02887405	1.063167872	67.96570618	68.0088068	0.043100623
37	67.95550259	69.06227912	1.106776524	67.95550259	67.99859675	0.043094155

38	67.94530054	69.09570035	1.150399810	67.94530054	67.98838822	0.043087685
39	67.93510002	69.12913776	1.194037739	67.93510002	67.97818123	0.043081217
40	67.92490103	69.16259135	1.237690317	67.92490103	67.96797578	0.043074749
41	67.91470357	69.19606112	1.281357553	67.91470357	67.95777185	0.043068282
42	67.90450764	69.2295471	1.325039455	67.90450764	67.94756946	0.043061816
43	67.89431325	69.26304928	1.368736032	67.89431325	67.9373686	0.043055351
44	67.88412038	69.29656767	1.412447290	67.88412038	67.92716927	0.043048888
45	67.87392904	69.33010228	1.456173239	67.87392904	67.91697147	0.043042425
46	67.86373924	69.36365312	1.499913886	67.86373924	67.9067752	0.043035963
47	67.85355096	69.3972202	1.543669240	67.85355096	67.89658046	0.043029502
48	67.83827141	69.43892949	1.600658081	67.83827141	67.89433247	0.056061061

APPENDIX J Marginal Effects for Monthly Load Forecasting Model

A. Temperature

	Sustained Shock			Initial Shock		
Time Period (t)	Before Shock	After Shock	Marginal Effect	Before Shock	After Shock	Marginal Effect
0	641.276067	655.664187	14.388120000	641.276067	655.664187	14.388120000
1	641.276067	649.1032042	7.827137280	641.276067	634.7150842	-6.560982720
2	641.276067	652.0950124	10.818945400	641.276067	644.2678751	2.991808120
3	641.276067	653.4357144	12.159647457	641.276067	642.616769	1.340702057
4	641.276067	651.5908895	10.314822568	641.276067	639.4312421	-1.844824889
5	641.276067	652.9945896	11.718522644	641.276067	642.679767	1.403700076
6	641.276067	652.6065544	11.330487396	641.276067	640.8880317	-0.388035248
7	641.276067	652.4366713	11.160604390	641.276067	641.1061839	-0.169883006
8	641.276067	652.7780336	11.501966655	641.276067	641.6174292	0.341362265
9	641.276067	652.5494218	11.273354836	641.276067	641.0474551	-0.228611820
10	641.276067	652.6217308	11.345663820	641.276067	641.3483759	0.072308985
11	641.276067	652.652934	11.376867029	641.276067	641.3072702	0.031203209
12	641.276067	649.20013	7.924063024	641.276067	637.8232629	-3.452804005
13	641.276067	652.3365946	11.060527661	641.276067	644.4125316	3.136464637
14	641.276067	650.2061662	8.930099273	641.276067	639.1456386	-2.130428388
15	641.276067	650.2121087	8.936041780	641.276067	641.2820095	0.005942506
16	641.276067	651.234433	9.958366023	641.276067	642.2983912	1.022324243
17	641.276067	650.0364594	8.760392413	641.276067	640.0780933	-1.197973610
18	641.276067	650.6754288	9.399361889	641.276067	641.9150364	0.638969476
19	641.276067	650.6163481	9.340281155	641.276067	641.2169862	-0.059080734
20	641.276067	650.3375084	9.061441436	641.276067	640.9972272	-0.278839719
21	641.276067	650.638738	9.362670999	641.276067	641.5772965	0.301229562
22	641.276067	650.4732052	9.197138220	641.276067	641.1105342	-0.165532779
23	641.276067	650.4889023	9.212835343	641.276067	641.2917641	0.015697123
24	641.276067	651.3532373	10.077170358	641.276067	642.140402	0.864335015
25	641.276067	650.1877747	8.911707774	641.276067	640.1106044	-1.165462584
26	641.276067	651.2249578	9.948890871	641.276067	642.3132501	1.037183097
27	641.276067	650.9130949	9.637027930	641.276067	640.964204	-0.311862941
28	641.276067	650.5949289	9.318861944	641.276067	640.957901	-0.318165986
29	641.276067	651.2177248	9.941657828	641.276067	641.8988628	0.622795884
30	641.276067	650.7243028	9.448235876	641.276067	640.782645	-0.493421952
31	641.276067	650.9034311	9.627364134	641.276067	641.4551952	0.179128258
32	641.276067	651.0046404	9.728573448	641.276067	641.3772763	0.101209314
33	641.276067	650.7946355	9.518568497	641.276067	641.066062	-0.210004951

34	641.276067	650.9631396	9.687072603	641.276067	641.4445711	0.168504106
35	641.276067	650.9016245	9.625557560	641.276067	641.2145519	-0.061515042
36	641.276067	650.6862114	9.410144425	641.276067	641.0606538	-0.215413135
37	641.276067	651.0911677	9.815100757	641.276067	641.6810233	0.404956331
38	641.276067	650.6501676	9.374100631	641.276067	640.8350668	-0.441000126
39	641.276067	650.8843656	9.608298673	641.276067	641.510265	0.234198042
40	641.276067	650.9287903	9.652723329	641.276067	641.3204916	0.044424656
41	641.276067	650.6786448	9.402577833	641.276067	641.0259215	-0.250145495
42	641.276067	650.9531879	9.677120992	641.276067	641.5506101	0.274543158
43	641.276067	650.7940738	9.518006878	641.276067	641.1169528	-0.159114114
44	641.276067	650.7957171	9.519650163	641.276067	641.2777102	0.001643285
45	641.276067	650.8961431	9.620076107	641.276067	641.3764929	0.100425944
46	641.276067	650.7806684	9.504601454	641.276067	641.1605923	-0.115474653
47	641.276067	650.8481513	9.572084383	641.276067	641.3435499	0.067482929
48	641.276067	650.8870967	9.611029745	641.276067	641.3150123	0.038945362

B. Precipitation

	Sustained Shock			Initial Shock		
Time Period (t)	Before Shock	After Shock	Marginal Effect	Before Shock	After Shock	Marginal Effect
0	641.276067	825.666067	184.390000000	641.276067	825.666067	184.390000000
1	641.276067	741.584227	100.308160000	641.276067	557.194227	-84.081840000
2	641.276067	779.925546	138.649479040	641.276067	679.617386	38.341319040
3	641.276067	797.1072245	155.831157558	641.276067	658.4577455	17.181678518
4	641.276067	773.4649932	132.188926234	641.276067	617.6338356	-23.642231324
5	641.276067	791.4540187	150.177951697	641.276067	659.2650924	17.989025463
6	641.276067	786.4811786	145.205111647	641.276067	636.3032269	-4.972840050
7	641.276067	784.3040542	143.027987221	641.276067	639.0989425	-2.177124426
8	641.276067	788.6787597	147.402692746	641.276067	645.6507725	4.374705525
9	641.276067	785.7490001	144.472933097	641.276067	638.3463073	-2.929759649
10	641.276067	786.6756711	145.399604105	641.276067	642.202738	0.926671008
11	641.276067	787.0755537	145.799486764	641.276067	641.6759496	0.399882659
12	641.276067	742.8263724	101.550305458	641.276067	597.0268856	-44.249181307
13	641.276067	783.0215275	141.745460523	641.276067	681.471222	40.195155065
14	641.276067	755.7191634	114.443096460	641.276067	613.9737029	-27.302364063
15	641.276067	755.7953192	114.519252257	641.276067	641.3522228	0.076155797
16	641.276067	768.8968479	127.620780958	641.276067	654.3775957	13.101528701
17	641.276067	753.5442964	112.268229417	641.276067	625.9235154	-15.352551541

18	641.276067	761.7329674	120.456900461	641.276067	649.464738	8.188671044
19	641.276067	760.9758222	119.699755226	641.276067	640.5189217	-0.757145236
20	641.276067	757.4023702	116.126303259	641.276067	637.702615	-3.573451966
21	641.276067	761.2627577	119.986690789	641.276067	645.1364545	3.860387530
22	641.276067	759.1413834	117.865316414	641.276067	639.1546926	-2.121374376
23	641.276067	759.3425488	118.066481852	641.276067	641.4772324	0.201165438
24	641.276067	770.419377	129.143310056	641.276067	652.3528952	11.076828204
25	641.276067	755.4834684	114.207401417	641.276067	626.3401583	-14.935908639
26	641.276067	768.7754197	127.499352778	641.276067	654.5680183	13.291951361
27	641.276067	764.7787608	123.502693891	641.276067	637.2794081	-3.996658886
28	641.276067	760.7013257	119.425258746	641.276067	637.1986318	-4.077435146
29	641.276067	768.6827251	127.406658192	641.276067	649.2574664	7.981399446
30	641.276067	762.3593088	121.083241807	641.276067	634.9526506	-6.323416384
31	641.276067	764.6549151	123.378848147	641.276067	643.5716733	2.295606340
32	641.276067	765.9519564	124.675889416	641.276067	642.5731082	1.297041269
33	641.276067	763.2606518	121.984584860	641.276067	638.5847624	-2.691304556
34	641.276067	765.420105	124.144038082	641.276067	643.4355202	2.159453222
35	641.276067	764.6317631	123.355696128	641.276067	640.487725	-0.788341954
36	641.276067	761.8711503	120.595083346	641.276067	638.5154542	-2.760612782
37	641.276067	767.0608414	125.784774419	641.276067	646.465758	5.189691073
38	641.276067	761.4092334	120.133166481	641.276067	635.624459	-5.651607938
39	641.276067	764.410583	123.134515995	641.276067	644.2774165	3.001349514
40	641.276067	764.9799042	123.703837233	641.276067	641.8453882	0.569321238
41	641.276067	761.7741811	120.498114187	641.276067	638.0703439	-3.205723046
42	641.276067	765.2925708	124.016503871	641.276067	644.7944566	3.518389684
43	641.276067	763.2534544	121.977387472	641.276067	639.2369506	-2.039116399
44	641.276067	763.2745138	121.998446878	641.276067	641.2971264	0.021059406
45	641.276067	764.5615159	123.285448925	641.276067	642.563069	1.287002047
46	641.276067	763.0816581	121.805591148	641.276067	639.7962092	-1.479857777
47	641.276067	763.9464811	122.670414163	641.276067	642.14089	0.864823016
48	641.276067	764.4455828	123.169515870	641.276067	641.7751687	0.499101706

C. Wind Speed

	Sustained Shock			Initial Shock		
Time Period (t)	Before Shock	After Shock	Marginal Effect	Before Shock	After Shock	Marginal Effect
0	641.276067	628.370447	-12.905620000	641.276067	628.370447	-12.905620000
1	641.276067	634.2554097	-7.020657280	641.276067	647.1610297	5.884962720
2	641.276067	631.5718667	-9.704200280	641.276067	638.592524	-2.683543000
3	641.276067	630.3693057	-10.906761232	641.276067	640.073506	-1.202560952
4	641.276067	632.0240465	-9.252020447	641.276067	642.9308077	1.654740785

5	641.276067	630.7649786	-10.511088329	641.276067	640.0169991	-1.259067882
6	641.276067	631.1130321	-10.163034834	641.276067	641.6241205	0.348053495
7	641.276067	631.265411	-10.010655960	641.276067	641.4284458	0.152378874
8	641.276067	630.9592215	-10.316845488	641.276067	640.9698774	-0.306189528
9	641.276067	631.1642779	-10.111789006	641.276067	641.4811234	0.205056482
10	641.276067	631.0994194	-10.176647534	641.276067	641.2112084	-0.064858528
11	641.276067	631.0714313	-10.204635676	641.276067	641.2480788	-0.027988143
12	641.276067	634.1684708	-7.107596145	641.276067	644.3731065	3.097039532
13	641.276067	631.3551762	-9.920890776	641.276067	638.4627723	-2.813294632
14	641.276067	633.2660929	-8.009974047	641.276067	643.1869837	1.910916729
15	641.276067	633.2607627	-8.015304259	641.276067	641.2707367	-0.005330212
16	641.276067	632.3437751	-8.932291898	641.276067	640.3590793	-0.916987639
17	641.276067	633.4183138	-7.857753170	641.276067	642.3506057	1.074538729
18	641.276067	632.8451814	-8.430885535	641.276067	640.7029346	-0.573132365
19	641.276067	632.8981747	-8.377892267	641.276067	641.3290602	0.052993268
20	641.276067	633.1482838	-8.127783187	641.276067	641.526176	0.250109079
21	641.276067	632.8780918	-8.397975142	641.276067	641.005875	-0.270191955
22	641.276067	633.0265687	-8.249498264	641.276067	641.4245438	0.148476878
23	641.276067	633.0124889	-8.263578011	641.276067	641.2619872	-0.014079748
24	641.276067	632.2372119	-9.038855063	641.276067	640.5007899	-0.775277052
25	641.276067	633.2825894	-7.993477541	641.276067	642.3214445	1.045377522
26	641.276067	632.3522739	-8.923793032	641.276067	640.3457515	-0.930315491
27	641.276067	632.6320036	-8.644063324	641.276067	641.5557967	0.279729708
28	641.276067	632.9173869	-8.358680014	641.276067	641.5614503	0.285383310
29	641.276067	632.3587617	-8.917305256	641.276067	640.7174417	-0.558625242
30	641.276067	632.8013432	-8.474723722	641.276067	641.7186485	0.442581533
31	641.276067	632.6406717	-8.635395250	641.276067	641.1153954	-0.160671528
32	641.276067	632.5498906	-8.726176322	641.276067	641.1852859	-0.090781071
33	641.276067	632.7382574	-8.537809524	641.276067	641.4644338	0.188366798
34	641.276067	632.5871154	-8.688951574	641.276067	641.1249249	-0.151142051
35	641.276067	632.6422921	-8.633774820	641.276067	641.3312437	0.055176754
36	641.276067	632.8355099	-8.440557078	641.276067	641.4692847	0.193217742
37	641.276067	632.4722788	-8.803788169	641.276067	640.9128359	-0.363231091
38	641.276067	632.8678398	-8.408227106	641.276067	641.671628	0.395561063
39	641.276067	632.6577727	-8.618294226	641.276067	641.0659998	-0.210067120
40	641.276067	632.6179254	-8.658141525	641.276067	641.2362197	-0.039847299
41	641.276067	632.8422968	-8.433770120	641.276067	641.5004384	0.224371405
42	641.276067	632.5960416	-8.680025341	641.276067	641.0298117	-0.246255221
43	641.276067	632.7387612	-8.537305772	641.276067	641.4187865	0.142719569
44	641.276067	632.7372872	-8.538779739	641.276067	641.274593	-0.001473967
45	641.276067	632.6472088	-8.628858156	641.276067	641.1859885	-0.090078417
46	641.276067	632.7507854	-8.525281595	641.276067	641.3796435	0.103576561
47	641.276067	632.6902556	-8.585811326	641.276067	641.2155372	-0.060529732

48	641.276067	632.6553231	-8.620743898	641.276067	641.2411344	-0.034932572

D. Per Capita Income

	Sustained Shock			Initial Shock		
Time Period (t)	Before Shock	After Shock	Marginal Effect	Before Shock	After Shock	Marginal Effect
0	641.276067	641.298067	0.022000000	641.276067	641.298067	0.022000000
1	641.276067	641.288035	0.011968000	641.276067	641.266035	-0.010032000
2	641.276067	641.2926095	0.016542592	641.276067	641.2806415	0.004574592
3	641.276067	641.2946595	0.018592578	641.276067	641.2781169	0.002049986
4	641.276067	641.2918387	0.015771768	641.276067	641.2732461	-0.002820810
5	641.276067	641.293985	0.017918081	641.276067	641.2782133	0.002146312
6	641.276067	641.2933917	0.017324760	641.276067	641.2754736	-0.000593321
7	641.276067	641.293132	0.017065002	641.276067	641.2758072	-0.000259758
8	641.276067	641.2936539	0.017586958	641.276067	641.2765889	0.000521956
9	641.276067	641.2933044	0.017237402	641.276067	641.2757174	-0.000349556
10	641.276067	641.2934149	0.017347965	641.276067	641.2761775	0.000110563
11	641.276067	641.2934626	0.017395676	641.276067	641.2761147	0.000047711
12	641.276067	641.2881832	0.012116203	641.276067	641.2707875	-0.005279473
13	641.276067	641.2929789	0.016911981	641.276067	641.2808627	0.004795777
14	641.276067	641.2897214	0.013654472	641.276067	641.2728094	-0.003257509
15	641.276067	641.2897305	0.013663558	641.276067	641.276076	0.000009086
16	641.276067	641.2912937	0.015226732	641.276067	641.2776301	0.001563174
17	641.276067	641.2894619	0.013394984	641.276067	641.2742352	-0.001831749
18	641.276067	641.2904389	0.014371993	641.276067	641.277044	0.000977009
19	641.276067	641.2903486	0.014281656	641.276067	641.2759766	-0.000090337
20	641.276067	641.2899223	0.013855299	641.276067	641.2756406	-0.000426357
21	641.276067	641.2903828	0.014315891	641.276067	641.2765275	0.000460592
22	641.276067	641.2901297	0.014062785	641.276067	641.2758138	-0.000253106
23	641.276067	641.2901537	0.014086787	641.276067	641.276091	0.000024002
24	641.276067	641.2914753	0.015408389	641.276067	641.2773886	0.001321602
25	641.276067	641.2896933	0.013626351	641.276067	641.2742849	-0.001782038
26	641.276067	641.2912792	0.015212244	641.276067	641.2776528	0.001585894
27	641.276067	641.2908023	0.014735394	641.276067	641.2755901	-0.000476851
28	641.276067	641.2903159	0.014248906	641.276067	641.2755805	-0.000486488
29	641.276067	641.2912681	0.015201185	641.276067	641.2770192	0.000952279
30	641.276067	641.2905137	0.014446723	641.276067	641.2753125	-0.000754462
31	641.276067	641.2907876	0.014720617	641.276067	641.2763408	0.000273894
32	641.276067	641.2909423	0.014875371	641.276067	641.2762217	0.000154753

33	641.276067	641.2906212	0.014554265	641.276067	641.2757458	-0.000321106
34	641.276067	641.2908789	0.014811914	641.276067	641.2763246	0.000257649
35	641.276067	641.2907848	0.014717855	641.276067	641.2759729	-0.000094059
36	641.276067	641.2904554	0.014388480	641.276067	641.2757376	-0.000329375
37	641.276067	641.2910746	0.015007674	641.276067	641.2766861	0.000619194
38	641.276067	641.2904003	0.014333368	641.276067	641.2753926	-0.000674306
39	641.276067	641.2907584	0.014691466	641.276067	641.2764251	0.000358098
40	641.276067	641.2908263	0.014759393	641.276067	641.2761349	0.000067927
41	641.276067	641.2904439	0.014376910	641.276067	641.2756845	-0.000382482
42	641.276067	641.2908637	0.014796698	641.276067	641.2764867	0.000419787
43	641.276067	641.2906204	0.014553406	641.276067	641.2758237	-0.000243292
44	641.276067	641.2906229	0.014555919	641.276067	641.2760695	0.000002513
45	641.276067	641.2907764	0.014709474	641.276067	641.2762205	0.000153555
46	641.276067	641.2905999	0.014532909	641.276067	641.2758904	-0.000176565
47	641.276067	641.290703	0.014636093	641.276067	641.2761701	0.000103184
48	641.276067	641.2907626	0.014695642	641.276067	641.2761265	0.000059549

E. Change in Population

	Sustained Shock			Initial Shock		
Time Period (t)	Before Shock	After Shock	Marginal Effect	Before Shock	After Shock	Marginal Effect
0	641.276067	641.283067	0.007000000	641.276067	641.283067	0.007000000
1	641.276067	641.279875	0.003808000	641.276067	641.272875	-0.003192000
2	641.276067	641.2813305	0.005263552	641.276067	641.2775225	0.001455552
3	641.276067	641.2819828	0.005915820	641.276067	641.2767192	0.000652268
4	641.276067	641.2810852	0.005018290	641.276067	641.2751694	-0.000897530
5	641.276067	641.2817682	0.005701208	641.276067	641.2767499	0.000682918
6	641.276067	641.2815794	0.005512424	641.276067	641.2758782	-0.000188784
7	641.276067	641.2814967	0.005429773	641.276067	641.2759843	-0.000082650
8	641.276067	641.2816628	0.005595850	641.276067	641.276233	0.000166077
9	641.276067	641.2815516	0.005484628	641.276067	641.2759557	-0.000111223
10	641.276067	641.2815868	0.005519807	641.276067	641.2761021	0.000035179
11	641.276067	641.2816019	0.005534988	641.276067	641.2760821	0.000015181
12	641.276067	641.2799221	0.003855156	641.276067	641.2743871	-0.001679832
13	641.276067	641.281448	0.005381085	641.276067	641.2775929	0.001525929
14	641.276067	641.2804116	0.004344605	641.276067	641.2750305	-0.001036480
15	641.276067	641.2804145	0.004347496	641.276067	641.2760698	0.000002891
16	641.276067	641.2809118	0.004844869	641.276067	641.2765643	0.000497374
17	641.276067	641.280329	0.004262040	641.276067	641.2754841	-0.000582829

18	641.276067	641.2806399	0.004572907	641.276067	641.2763778	0.000310867
19	641.276067	641.2806111	0.004544163	641.276067	641.2760382	-0.000028744
20	641.276067	641.2804755	0.004408504	641.276067	641.2759313	-0.000135659
21	641.276067	641.280622	0.004555056	641.276067	641.2762135	0.000146552
22	641.276067	641.2805415	0.004474523	641.276067	641.2759864	-0.000080534
23	641.276067	641.2805491	0.004482159	641.276067	641.2760746	0.000007637
24	641.276067	641.2809696	0.004902669	641.276067	641.2764875	0.000420510
25	641.276067	641.2804026	0.004335657	641.276067	641.2754999	-0.000567012
26	641.276067	641.2809072	0.004840260	641.276067	641.2765716	0.000504603
27	641.276067	641.2807555	0.004688534	641.276067	641.2759152	-0.000151725
28	641.276067	641.2806007	0.004533743	641.276067	641.2759122	-0.000154792
29	641.276067	641.2809037	0.004836741	641.276067	641.27637	0.000302998
30	641.276067	641.2806636	0.004596685	641.276067	641.2758269	-0.000240056
31	641.276067	641.2807508	0.004683833	641.276067	641.2761541	0.000087148
32	641.276067	641.2808	0.004733072	641.276067	641.2761162	0.000049240
33	641.276067	641.2806979	0.004630902	641.276067	641.2759648	-0.000102170
34	641.276067	641.2807798	0.004712882	641.276067	641.2761489	0.000081979
35	641.276067	641.2807499	0.004682954	641.276067	641.276037	-0.000029928
36	641.276067	641.2806451	0.004578153	641.276067	641.2759622	-0.000104801
37	641.276067	641.2808421	0.004775169	641.276067	641.276264	0.000197016
38	641.276067	641.2806276	0.004560617	641.276067	641.2758524	-0.000214552
39	641.276067	641.2807415	0.004674557	641.276067	641.2761809	0.000113940
40	641.276067	641.2807631	0.004696170	641.276067	641.2760886	0.000021613
41	641.276067	641.2806414	0.004574471	641.276067	641.2759453	-0.000121699
42	641.276067	641.280775	0.004708040	641.276067	641.2762005	0.000133569
43	641.276067	641.2806976	0.004630629	641.276067	641.2759895	-0.000077411
44	641.276067	641.2806984	0.004631429	641.276067	641.2760678	0.000000799
45	641.276067	641.2807472	0.004680287	641.276067	641.2761158	0.000048858
46	641.276067	641.2806911	0.004624107	641.276067	641.2760108	-0.000056180
47	641.276067	641.2807239	0.004656939	641.276067	641.2760998	0.000032831
48	641.276067	641.2807428	0.004675886	641.276067	641.2760859	0.000018947

F. Copper Mine Production

	Sustained Shock			Initial Shock		
Time Period (t)	Before Shock	After Shock	Marginal Effect	Before Shock	After Shock	Marginal Effect
0	641.276067	641.280067	0.004000000	641.276067	641.280067	0.004000000
1	641.276067	641.278243	0.002176000	641.276067	641.274243	-0.001824000
2	641.276067	641.2790747	0.003007744	641.276067	641.2768987	0.000831744

3	641.276067	641.2794474	0.003380469	641.276067	641.2764397	0.000372725
4	641.276067	641.2789345	0.002867594	641.276067	641.2755541	-0.000512874
5	641.276067	641.2793248	0.003257833	641.276067	641.2764572	0.000390239
6	641.276067	641.2792169	0.003149956	641.276067	641.2759591	-0.000107877
7	641.276067	641.2791697	0.003102728	641.276067	641.2760197	-0.000047229
8	641.276067	641.2792646	0.003197629	641.276067	641.2761619	0.000094901
9	641.276067	641.279201	0.003134073	641.276067	641.2760034	-0.000063556
10	641.276067	641.2792211	0.003154175	641.276067	641.2760871	0.000020102
11	641.276067	641.2792298	0.003162850	641.276067	641.2760756	0.000008675
12	641.276067	641.2782699	0.002202946	641.276067	641.2751071	-0.000959904
13	641.276067	641.2791419	0.003074906	641.276067	641.2769389	0.000871960
14	641.276067	641.2785496	0.002482631	641.276067	641.2754747	-0.000592274
15	641.276067	641.2785512	0.002484283	641.276067	641.2760686	0.000001652
16	641.276067	641.2788355	0.002768497	641.276067	641.2763512	0.000284213
17	641.276067	641.2785024	0.002435452	641.276067	641.2757339	-0.000333045
18	641.276067	641.27868	0.002613090	641.276067	641.2762446	0.000177638
19	641.276067	641.2786636	0.002596665	641.276067	641.2760505	-0.000016425
20	641.276067	641.2785861	0.002519145	641.276067	641.2759894	-0.000077519
21	641.276067	641.2786698	0.002602889	641.276067	641.2761507	0.000083744
22	641.276067	641.2786238	0.002556870	641.276067	641.2760209	-0.000046019
23	641.276067	641.2786282	0.002561234	641.276067	641.2760713	0.000004364
24	641.276067	641.2788685	0.002801525	641.276067	641.2763072	0.000240291
25	641.276067	641.2785445	0.002477518	641.276067	641.2757429	-0.000324007
26	641.276067	641.2788328	0.002765863	641.276067	641.2763553	0.000288344
27	641.276067	641.2787461	0.002679163	641.276067	641.2759803	-0.000086700
28	641.276067	641.2786577	0.002590710	641.276067	641.2759785	-0.000088452
29	641.276067	641.2788308	0.002763852	641.276067	641.2762401	0.000173142
30	641.276067	641.2786936	0.002626677	641.276067	641.2759298	-0.000137175
31	641.276067	641.2787434	0.002676476	641.276067	641.2761168	0.000049799
32	641.276067	641.2787716	0.002704613	641.276067	641.2760951	0.000028137
33	641.276067	641.2787132	0.002646230	641.276067	641.2760086	-0.000058383
34	641.276067	641.27876	0.002693075	641.276067	641.2761138	0.000046845
35	641.276067	641.2787429	0.002675974	641.276067	641.2760499	-0.000017102
36	641.276067	641.278683	0.002616087	641.276067	641.2760071	-0.000059886
37	641.276067	641.2787956	0.002728668	641.276067	641.2761795	0.000112581
38	641.276067	641.278673	0.002606067	641.276067	641.2759444	-0.000122601
39	641.276067	641.2787381	0.002671176	641.276067	641.2761321	0.000065109
40	641.276067	641.2787505	0.002683526	641.276067	641.2760793	0.000012350
41	641.276067	641.2786809	0.002613984	641.276067	641.2759974	-0.000069542
42	641.276067	641.2787573	0.002690309	641.276067	641.2761433	0.000076325
43	641.276067	641.278713	0.002646074	641.276067	641.2760227	-0.000044235
44	641.276067	641.2787135	0.002646531	641.276067	641.2760674	0.000000457
45	641.276067	641.2787414	0.002674450	641.276067	641.2760949	0.000027919

46	641.276067	641.2787093	0.002642347	641.276067	641.2760349	-0.000032103
47	641.276067	641.2787281	0.002661108	641.276067	641.2760857	0.000018761
48	641.276067	641.2787389	0.002671935	641.276067	641.2760778	0.000010827

References

Acclimatise (Firm), and International Business Machines Corporation. "Carbon Disclosure Project Report 2008 FTSE 350: Building Business Resilience to Inevitable Climate Change." *Carbon Disclosure Project*. 2009.

Alfares, H. K., and M.Nazeeruddin. "Electric Load Forecasting: Literature Survey and Classification of Methods." *International Journal of Systems Science* 33.1 (2002): 23.

Al-Saba, T., and I. El-Amin. "Artificial Neural Networks as Applied to Long-Term Demand Forecasting." *Artificial Intelligence in Engineering*. 13.2 (1999): 189.

Al-Zayer, J., and A.A. Al-Ibrahim. “Modeling the impact of the temperature on electricity consumption in Eastern province of Saudi Arabia.” *Journal of Forecasting*. 15 (1996): 97–106.

Amato, A.D., M. Ruth, P. Kirshen and J. Horwitz. “Regional Energy Demand Response to Climate Change: Methodology and Application to the Commonwealth of Massachusetts.” *Climate Change* 71 (2005): 175–201.

Backlund P, A. Janetos and D. Schimel. “The Effects of Climate Change on Agriculture, Land Resources, Water Resources, and Biodiversity.” Synthesis and Assessment Product 4.3, U.S. Climate Change Science Program, Washington, DC, 2008.

Batty, M. "Monitoring an Exponential Smoothing Forecasting System." *Operational Research Quarterly* 20 (1969): 319-325.

Bessec M. and J. Fouquau. “The Non-linear Link between Electricity Consumption and Temperature in Europe: a Threshold Panel Approach.” *Energy Economics* 30 (2008): 2705–2721.

Box, G.E.P., G. M. Jenkins and G.C. Reinsel, eds. *Time Series Analysis: Forecasting and Control*, 4th edition. New York: John Wiley and Sons, 2008.

Chen, C. S., Y. M. Tzeng, and J. C. Hwang. "The Application of Artificial Neural Networks to Substation Load Forecasting." *Electric Power Systems Research*. 38.2 (1996): 153.

Considine, T. and D. McLaren. “ Powering Arizona, Choices and Trade-Offs for Electricity Policy: A Study Assessing Arizona’s Energy Future.” Draft Report, The Communications Institute, Los Angeles, CA, 2008.

Contaxi, E., C. Delkis, S. Kavatza and C. Vournas. "The Effect of Humidity in a Weather-Sensitive Peak Load Forecasting Model." *Power Systems Conference and Exposition 2006. IEEE PES*, (2006):1528-1534

Dominguez, F., J. Canon, and J. Valdes. "IPCC-AR4 Climate Simulations for the Southwestern US: The Importance of Future ENSO Projections." *Climatic Change* 99.3 (2010): 499-514.

Electric Power Research Institute. “Climate Change Impacts and the Electric Sector.” Technical Report 1013189, EPRI, Palo Alto, CA, December 2006.

Enders, W. *Applied Econometric Time Series*, 2nd edition. Hoboken, NJ: John Wiley & Sons, 2004.

Engle, R.F., C.W.J. Granger, J. Rice and A.Weiss. “Semiparametric Estimates of the Relation between Weather and Electricity Sales.” *Journal of the American Statistical Association* 81 (1986): 310–320.

Feinberg E. and D. Genethliou, “Load forecasting.” In *Applied Mathematics for Restructured Electric Power Systems: Optimization, Control, and Computational Intelligence, eds.,* J. Chow, F. Wu and J. Momoh, pp. 269–285. Springer, 2005.

Feinberg, E."Peak Load Forecasting." Presented at the Advanced Energy 2009 Conference, Hauppage, NY, 19 Nov. 2009.

Glennon, R. *Unquenchable: America’s Water Crisis and What To Do About It*, 1st edition. Washington, DC: Island Press, 2009.

Goldstein, R. and W. Smith. “Water & Sustainability (Volume 4): U.S. Electricity Consumption for Water Supply & Treatment - the Next Half Century.” Topical Report 1006787, Electric Power Research Institute, Palo Alto, CA, March 2002.

Hagan, M.T. and S. H. Behr. “The Times Series Approach to Short Term Load Forecasting.” *IEEE Transactions on Power Systems* Vol. PWRS-2, No.3 (August 1987): 785-790.

Henley, A. and J. Peirson. “Non-linearities in Electricity Demand and Temperature: Parametric versus Non-parametric Methods.” *Oxford Bulletin of Economics and Statistics* 59.1(1997): 149–162.

Hutson, S. S., N. L. Barber, J. F. Kenny, K. S. Linsey, D. S. Lumia, and M. A. Maupin. "Estimated use of Water in the United States in 2000." U.S. Geological Survey, Reston, VA, 2004.

Islam, S. M., S. M. Al-Alawi, and K. A. Ellithy. "Forecasting Monthly Electric Load and Energy for a Fast Growing Utility using an Artificial Neural Network." *Electric Power Systems Research*. 34.1 (1995): 1-9.

Kalekar P. S. "Time-series forecasting using Holt-Winters Exponential Smoothing." Seminar Paper, Kanwal Rekhi School of Information Technology, Bombay, India, 2004.

Kermanshahi, B. and H. Iwamiya. "Up to Year 2020 Load Forecasting using Neural Nets." *International Journal of Electrical Power and Energy Systems* 24.9 (2002): 789-97.

Lam, J. C. "Climatic and Economic Influences on Residential Electricity Consumption." *Energy Conversion and Management.* 39.7 (1998): 623-629.

Lam, J. C., C. L. Tsang, and D. H. Li. "Long Term Ambient Temperature Analysis and Energy use Implications in Hong Kong." *Energy Conversion and Management.* 45.3 (2004): 315-27.

Leamer, E. E. *Specification Searches: Ad Hoc Inference from Non-Experimental Data*. New York: Wiley, 1978.

Lenart, M., "Global Warming in the Southwest: An Overview," in *Global Warming in the Southwest: Projections, Observations, and Impacts*, eds., Melanie Lenart, pp. 2–5, Climate Assessment for the Southwest, 2007.

Mirasgedis, S., Y. Sarafidis, E. Georgopoulou, D.P. Lalas, M. Moschovits, F. Karagiannis and D. Papakonstantinou**.** "Models for Mid-Term Electricity Demand Forecasting Incorporating Weather Influences." *Energy* 31.2-3 (2006): 208-227.

Moral-Carcedo, J. and J. Vicéns-Otero. “Modeling the Non-linear Response of Spanish Electricity Demand to Temperature Variations.” *Energy Economics* 27 (2005): 477–494.

Murphy, A. H. “What is a good forecast? An essay on the nature of goodness in weather forecasting”. *Weather Forecasting* 8 (1993): 281–293.

Niemuth, N.J. “Arizona Mining Update – 2002 and 2003.” Circular No. 108, Arizona Department of Mines and Mineral Resources, Phoenix, AZ, November 2004.

Niemuth, N.J. “Arizona 2004 Mining Review.” Arizona Department of Mines and Mineral Resources, Phoenix, AZ, 2005.

Niemuth, N.J. “Arizona Mining Update – 2005.” Circular No. 118, Arizona Department of Mines and Mineral Resources, Phoenix, AZ, July 2006.

Niemuth, N.J. “Arizona Mining Update – 2006.” Circular No. 125, Arizona Department of Mines and Mineral Resources, Phoenix, AZ, May 2007.

Niemuth, N.J. “Arizona Mining Update – 2007.” Circular No. 129, Arizona Department of Mines and Mineral Resources, Phoenix, AZ, June 2008.

Paatero, J.V. and P. D. Lund. “A Model for Generating Household Electricity Load Profiles.” *International Journal of Energy Research* 30.5 (2006): 273–290.

Pappas, S. Sp, L. Ekonomou, D.Ch. Karamousantas, G.E. Chatzarakis, S.K. Katsikas and P. Liatsis**.**" Electricity Demand Loads Modeling using AutoRegressive Moving Average (ARMA) Models." *Energy* 33.9 (2008): 1353-60.

Pardo, A., V. Meneu, and E. Valor. "Temperature and Seasonality Influences on Spanish Electricity Load." *Energy Economics*. 24.1 (2002): 55-70.

Petridis, V., A. Kehagias , L. Petrou , A. Bakirtzis , N. Maslaris , S. Kiartzis and H. Panagiotou. "A Bayesian Multiple Models Combination Method for Time Series Prediction." *Journal of Intelligent & Robotic Systems* 31.1 (2001): 69-89.

Phillips, K.A. , N.J. Niemuth and D. Bain. “Arizona Mining Update – 2000 and 2001.” Circular No. 100, Arizona Department of Mines and Mineral Resources, Phoenix, AZ, November 2002.

Psiloglou, B. E., C. Giannakopoulos, S. Majithia and M. Petrakis. "Factors Affecting Electricity Demand in Athens, Greece and London, UK: A Comparative Assessment." *Energy* 34.11 (2009): 1855-1863.

Ranjan, M., and V. K. Jain. "Modelling of Electrical Energy Consumption in Delhi." *Energy* 24.4 (1999): 351-361.

Ringwood, J. V., D. Bofelli, and F. T. Murray. "Forecasting Electricity Demand on Short, Medium and Long Time Scales using Neural Networks." *Journal of Intelligent and Robotic Systems* 31.1/3 (2001): 129-147.

Robinson, P. J. "Modeling Utility Load and Temperature Relationships for use with Long-Lead Forecasts." *Journal of Applied Meteorology* 36.5 (1997): 591-598.

Sailor, D. J., and J. R. Muñoz. "Sensitivity of Electricity and Natural Gas Consumption to Climate in the U.S.A. - Methodology and Results for Eight States." *Energy* 22.10 (1997): 987-998.

Sailor, D.J. "Relating Residential and Commercial Sector Electricity Loads to Climate — Evaluating State Level Sensitivities and Vulnerabilities." *Energy* 26 (2001): 645–657.

Srinivasan, D. and M. A. Lee. "Survey of Hybrid Fuzzy Neural Approaches to Electric Load Forecasting." *Systems, Man and Cybernetics, 1995. Intelligent Systems for the 21st Century., IEEE International Conference on* 5 (October 1995): 4004-4008.

Tanimoto, P. M. "Forecasting the Impact of Climate Change for Electric Power Management in the Southwest." Master's thesis, Department Of Agricultural And Resource Economics, University Of Arizona, 2008.

Thompson, G. D. and C. A. Cathers. "Forecasting Short-Term Electricity Load Profiles." Technical Report, University of Arizona, Tucson, December 2005.

Tzafestas, S. and E. Tzafestas. "Computational Intelligence Techniques for Short-Term Electric Load Forecasting." *Journal of Intelligent and Robotic Systems* 31.1/3 (2001): 7-68.

U.S. Department of Energy. *Energy Demands on Water Resources: Report to Congress on the Interdependency of Energy and Water.* Technical Report, USDOE, Washington, DC, December 2006.

U.S. Energy Information Administration, *Electric Power Annual 2009.* DOE/EIA-0348, Washington, DC, November 2010.

U.S. Global Change Research Program. *Global Climate Change Impacts in the United States.* Cambridge University Press, 2009.

Weron, R. *Modeling and Forecasting Electricity Loads and Prices: A Statistical Approach*. West Sussex, England: John Wiley & Sons, 2006.

Willis, H. L. *Spatial Electric Load Forecasting*, 2nd edition. New York, NY: Marcel Dekker, Inc., 2002.

Wilson, T. "A Climate Contingency Roadmap: The U.S. Electric Sector and Climate Change" Technical Update 1009311, Electric Power Research Institute, Palo Alto, CA, December 2003.